1972

Elastic and plastic behaviour of frozen sand.

John S. Lucente
University of Windsor

ELASTIC AND PLASTIC BEHAVIOUR OF FROZEN SAND.

by

John S. Lucente

A Thesis
Submitted to the Faculty of Graduate Studies through the
Department of Civil Engineering in Partial Fulfillment
of the Requirements for the Degree of
Master of Applied Science at the
University of Windsor

Windsor, Ontario
1972

CONTENTS

		Page
ABSTRACT		iii
ACKNOWLEDGEMENTS		iv
LIST OF FIGURES		v
LIST OF TABLES		vii
CHAPTER		
I.	INTRODUCTION	1
II.	REVIEW OF LITERATURE	3
III.	EXPERIMENTAL PROGRAMME	14
	a) Outline of Experiments	14
	b) Apparatus	15
	c) Preparation of Samples	18
	d) Reliability of Experiments	21
IV.	DISCUSSION OF TEST RESULTS	26
	a) Tests with Various Loading Rates	26
	b) Tests Separating the Elastic and Plastic Components	27
	c) Derivation of Formula for Plastic Component.	29
V.	CONCLUSIONS AND RECOMMENDATIONS	38
	a) Conclusions	38
	b) Recommendations for Further Work	39
APPENDIX A.	NOMENCLATURE	41
APPENDIX B.	TOTAL STRESS-STRAIN CURVES FOR VARIOUS Si, T and t	43
APPENDIX C.	TABLES OF 'A' and 'm' FOR VARIOUS t	61

CONTENTS con'd

		Page
APPENDIX D.	TOTAL, ELASTIC AND PLASTIC STRAINS VS. STRESS.....	65
APPENDIX E.	TABLE FOR 'A' AND 'm' FOR PLASTIC CURVES TABLE FOR 'n' AND 'C' FOR VARIOUS T.....	78
APPENDIX F.	COMPARISON OF EXPERIMENTAL DATA TO THE EMPIRICAL EQUATION.....	81
BIBLIOGRAPHY.....		94

ABSTRACT

The stress-strain behaviour of frozen sand was investigated by hydraulically applying radial stress (to 200 p.s.i.) to a cylindrical sample. The strain was measured on strain gauges imbedded in the sample. Variables considered were time, ice saturation (25%-100%), and temperature (0^{o}F-25^{o}F).

Experiments were also designed to separate the elastic and plastic components of strain. From these was found a method of determining the modulus of elasticity as a function of ice saturation and temperature, and independent of the plastic strain. Also, an expression was derived to describe the plastic behaviour. Using these two expressions, a general parabolic equation was developed to describe the frozen sand's stress-strain behaviour. This equation was in reasonable agreement with experimental data.

ACKNOWLEDGEMENTS

The author wishes to express his gratitude to his advisor Dr. J.T. Laba for his guidance.

The author is also indebted to Dr. C. MacInnis for the proofreading and for offering helpful suggestions and criticism in the preparation of this work.

The author would also like to thank Mr. Omar ElZein for his assistance.

LIST OF FIGURES

		Page
FIGURE 1.	Moduli of Elasticity.....	4
FIGURE 2.	Hyperbolic Stress-Strain Curve (Kondner)....	5
FIGURE 3.	Transformed Curve (Kondner).....	5
FIGURE 4.	Stress-Strain Curve (Makhlouf & Stewart)....	7
FIGURE 5.	Typical Stress-Strain Curve (Goughour & Andersland).....	7
FIGURE 6.	Stress-Strain Curves for Clay (Akili).....	9
FIGURE 7.	Strain - A Function of Stress and Temperature.....	11
FIGURE 8.	Mechanical Model (Vialov).....	11
FIGURE 9.	Steel Cylinder with Rubber Diaghragm.....	16
FIGURE 10.	Equipment Displayed with Freezer.....	17
FIGURE 11.	Preparation of Strain Gauges.....	17
FIGURE 12.	Grain Size Distribution Curve.....	19
FIGURE 13.	Placing of Strain Gauges.....	20
FIGURE 14.	Completed Sample in Freezer Compartment.....	20
FIGURE 15.	Maihak Transmitter & Receiver.....	22
FIGURE 16.	Comparison of Maihak & Strain Gauge Curves.	24
FIGURE 17.	Comparison of Cyclic Loading with Virgin Curve.....	25
FIGURE 18.	Modulus of Elasticity vs. Ice Saturation....	28
FIGURE 19.	Typical Log-Log Plots of Plastic Stress-Strain Curves.....	30
FIGURE 20.	Determination of 'm' as a Function of the Ice Saturation.....	31
FIGURE 21.	Determination of 'A' as a Function of the Ice Saturation.....	33

LIST OF FIGURES con'd

		Page
FIGURE 22.	Determination of 'C' as a Function of Temperature.....	34
FIGURE 23.	Determination of 'n' as a Function of Temperature.....	35
FIGURES 24 to 39.	Total Stress-Strain Curves for Various S_i, T and t.....	44-59
FIGURE 40.	Special Case at $30^{\circ}F$.....	60
FIGURES 41 to 52.	Total Strain, Plastic Strain and Elastic Strain vs. Stress for Various S_i and T at t = 5 min. and tr = 5 min.....	66-77
FIGURES 53 to 64.	Comparison of Experimental Data to the Curves from the Impirical Equation.....	82-93

LIST OF TABLES

		Page
TABLE I.	'A' and 'm' for t = 1 min.....	62
TABLE II.	'A' and 'm' for t = 5 min.....	63
TABLE III.	'A' and 'm' for t = 10 min.....	64
TABLE IV.	'A' and 'm' for plastic curves.....	79
TABLE V.	'n' and 'C' for various temperatures.....	80

CHAPTER I

INTRODUCTION

The concept of the modulus of elasticity has been very useful in studying materials such as metals, concrete, wood, plastics, etc. However, it has not been used very much in the case of soils. Solutions to problems of settlement, consolidation, bearing capacity, etc., are determined from data obtained from soil samples. Recently, more research has been conducted in the area of the dynamic properties of soils such as their time dependency and their behaviour under different loading conditions. From these investigations a need has arisen for theories involving the concept of modulus of elasticity. Consequently, studies of the stress-strain behaviour of frozen soils (as well as soils in general) is necessary.

The stress-strain behaviour of any type of soil depends on density, water content, structure, drainage conditions, loading conditions, duration of loading, etc.[1]. In the case of frozen sands, important factors affecting its behaviour are the ice saturation of the sample, the temperature, the time or duration of the loading, and the porosity.

For a sample with a high ice saturation, its behaviour will tend to approximate that of ice. On the other hand, the behaviour of a sample with a low ice saturation will depend more on the interparticle action of the sand. At the present time, little is known about the interactions between sand grains and ice. This could only be explained by a microscopic study. In the present study only the macroscopic behaviour of the sand-ice system is considered and no attempt is made to describe the microscopic actions.

The behaviour of frozen sand is time dependent[2]. To study this aspect a series of tests was performed with different times of application of loads, that is, different loading rates. In these tests, the plastic and elastic components of strain were not separated.

Another series of experiments was conducted in order to separate the elastic strain and plastic strain. The elastic strain is that which is totally reversible or recoverable when the stress is removed. When this strain is plotted against the applied stress it should approximate a linear relationship.

The plastic strain, on the other hand, is not recovered when the stress is removed. This is the permanent deformation due to the consolidation of the sample. It is therefore important to differentiate between these two distinct types of strain.

CHAPTER II

REVIEW OF LITERATURE

Most of the experimentation to date which has been performed to provide information on the stress-strain behaviour of frozen soils, has been carried out in a triaxial cell which was usually immersed in a cold temperature bath of ethylene glycol.

Some theories developed from studies of unfrozen sand have been considered and attempts have been made to extend these same theories to describe the behaviour of frozen sand. As in other materials, such as concrete, it is important to arrive at some measure of elasticity. Since there is no linear portion to the stress-strain curves of these materials, the elastic modulus must be expressed as an initial tanget modulus (E_i), a final modulus after unloading (E_f), a secant modulus (E_s), a tangent modulus (E_t), or some sort of average modulus (Fig. 1).

Kondner[3,4] proposed a hyperbolic equation which was

$$(\sigma_1 - \sigma_3) = \frac{\varepsilon}{a + b\varepsilon} \qquad (1)$$

where $(\sigma_1 - \sigma_3)$ is the stress difference; 'ε' the axial strain; 'a' and 'b' constants which can be determined

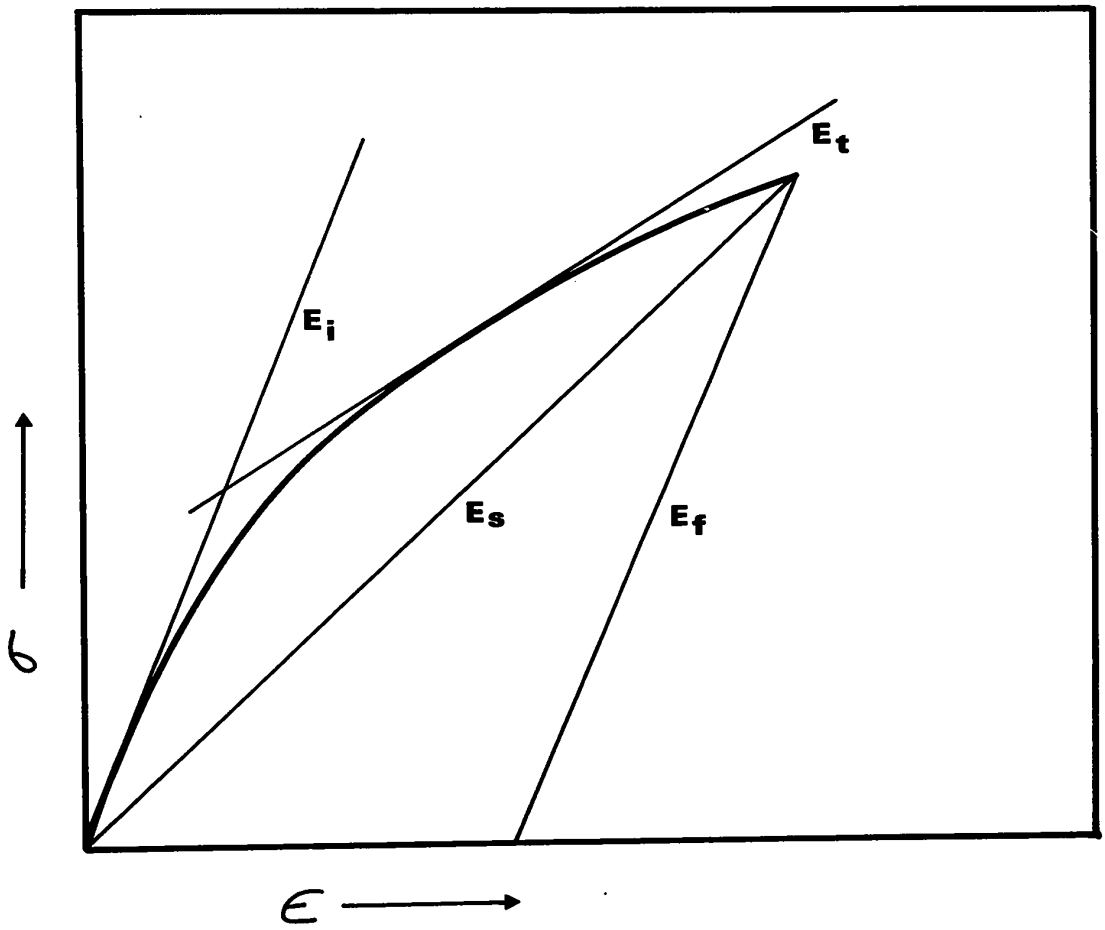

FIG. 1. - Moduli of Elasticity

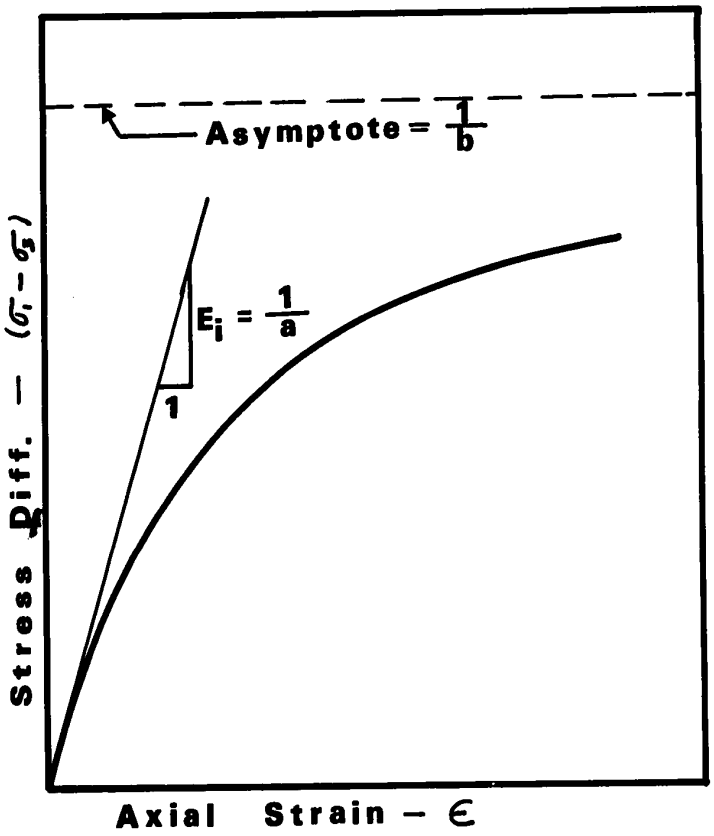

FIG. 2. - Hyperbolic Stress-Strain Curve (Kondner)

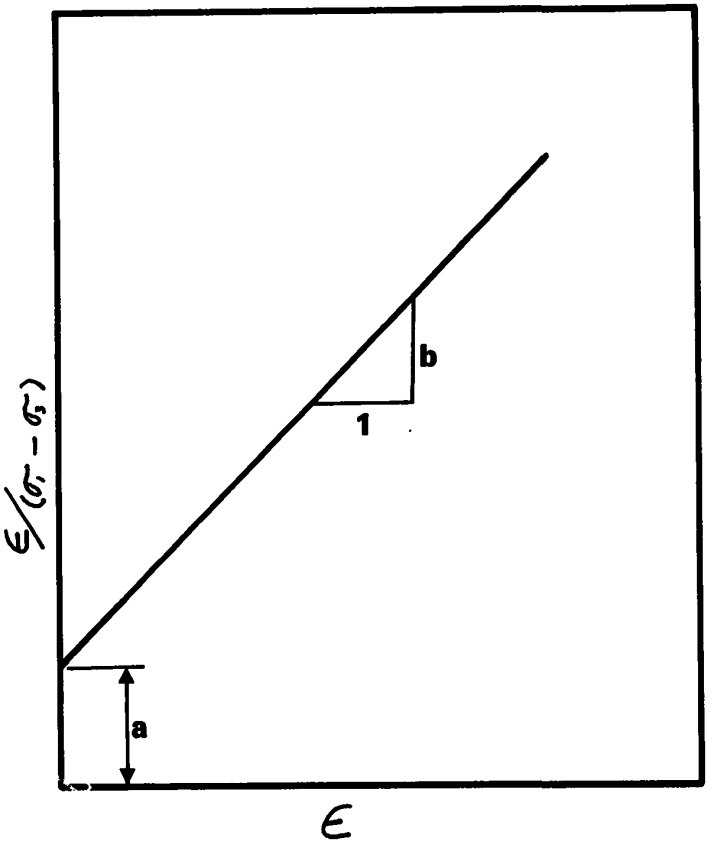

FIG. 3. - Transformed Curve (Kondner)

experimentally. As can be seen in Fig. 2, 'a' is the reciprocal of the initial tangent modulus (E_i) and 'b' is the reciprocal of the asymptotic value of stress difference which the curve approaches at infinite strain. When the stress-strain is plotted on transformed axes as in Fig. 3, it can be seen by rewriting Eqn. (1) as

$$\frac{\varepsilon}{\sigma_1 - \sigma_3} = a + b\varepsilon \qquad (2)$$

that 'a' is the intercept and 'b' the slope of the straight line. This theory was also later ratified experimentally by Duncan and Chang[1] for dense and loose silica sand.

Makhlouf and Stewart[5] investigated the modulus of elasticity of dry Ottawa sand. The shape of the stress-strain curve obtained can be seen in Fig. 4, which also shows successive loading and unloading cycles. An important characteristic shown is that in spite of the cycled loads the main curve is still the same as the virgin curve (without cycling). Therefore, the modulus of elasticity for values of deviator stress greater than those which have been cycled is unaffected by the previous cycling.

The elastic moduli were determined from the slopes of the reloading curves and were found to vary with the range of the deviator stress, confining pressure and relative density of the sample.

Goughour and Andersland[6] investigated the mechanical properties of sand-ice systems, with the

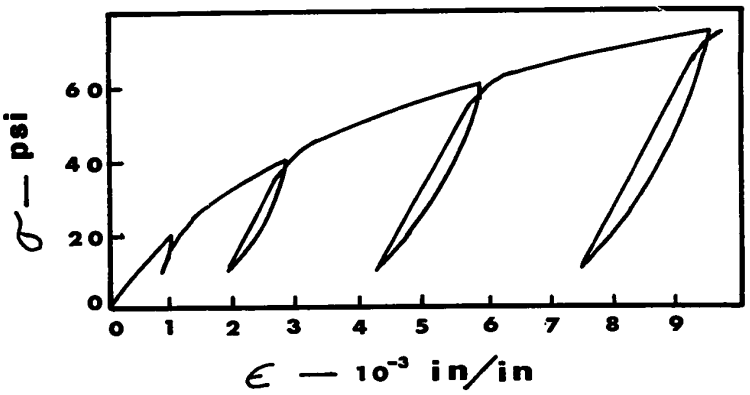

FIG. 4. - Stress-Strain Curve
Loading & Unloading Cycles
(Makhlouf and Stewart)

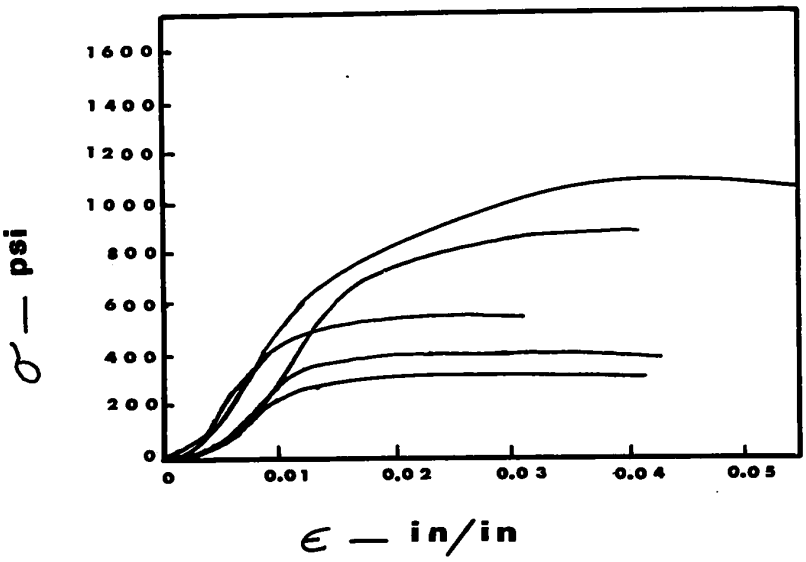

-FIG. 5. - Typical Stress-Strain Curves
(Goughour and Andersland)

triaxial cell. These tests were conducted under constant axial strain. The resulting curves can be seen in Fig. 5, showing typical stress-strain curves. Stresses are high due to the unusually high ice content in the samples. Rather than frozen sand, these are sand-ice systems, better described as sand particles dispersed through an ice matrix. Samples vary from 0% sand to about 60% sand by volume. This means that the ice saturation is well above 100%. Therefore, it is more a study of ice with sand as an impurity, rather than of a frozen sand with realistic ice saturations.

Akili[7] conducted tests on frozen clay in a triaxial cell. As can be seen in Fig. 6, the curves exhibit a linear relationship in the initial portion, with a very steep slope (high modulus of elasticity) and then flatten out very quickly.

Ladanyi[8] has used common methods applied in certain engineering theories of creep of metals and applied them to frozen soils. Using also concepts and data from frozen soils literature, he has developed a proposed theory of creep with the main purpose of solving bearing capacity problems of buried footings. While it is aimed at a study of creep, his discussion of elastic and plastic strain is of interest. He gives the strain as the sum of the instantaneous strain and the creep strain. The creep strain becomes important for time intervals longer than 24 hours. Therefore, the instantaneous strain ε_i is the 'total' strain ε_T for the experiments which are presented in Chapter IV of this thesis.

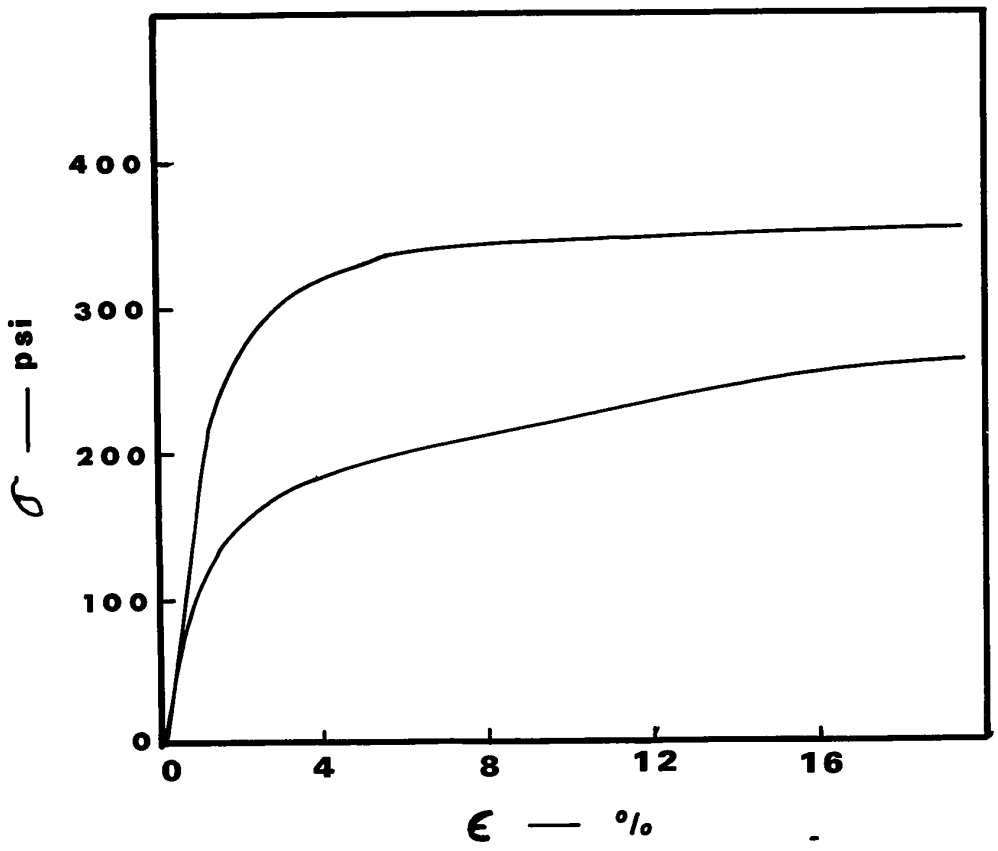

FIG. 6. - Stress-Strain Curves for Clay at -5°C
Various Strain Rates (Akili)

This ε_T is a function of stress and temperature as can be seen in Fig. 7. Also, this total strain can be divided into plastic strain ε_{PL} and elastic strain ε_{EL} where

$$\varepsilon_T = \varepsilon_{PL} + \varepsilon_{EL} \tag{3}$$

The elastic strain can be expressed as

$$\varepsilon_{EL} = \sigma/E \tag{4}$$

and the plastic portion can be expressed as a pure power function such as

$$\varepsilon_{PL} = \left(\frac{\sigma}{\sigma_k}\right)^k \tag{5}$$

where 'σ_k' is a constant and 'k' the exponent (usually greater than one). This equation becomes linear when plotted on log-log paper as can be seen from the equation

$$\log\varepsilon_{PL} = k(\log\sigma - \log\sigma_k) \tag{6}$$

A mechanical model, as shown in Fig. 8, was proposed by Vialov[9] to illustrate the behaviour of frozen soil. He describes the action as consisting of three types of deformations. The first is completely elastic and recoverable and is represented by a spring (A). The second includes recoverable and residual components and is represented

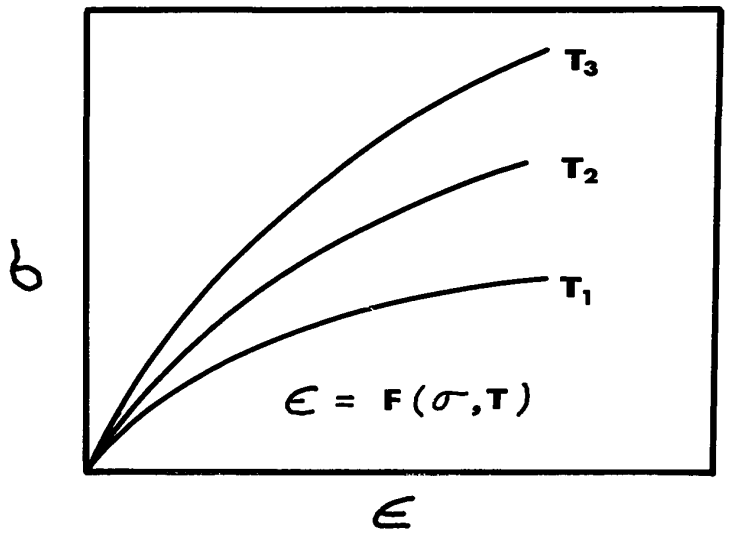

FIG. 7. - Strain - A Function of Stress and Temperature

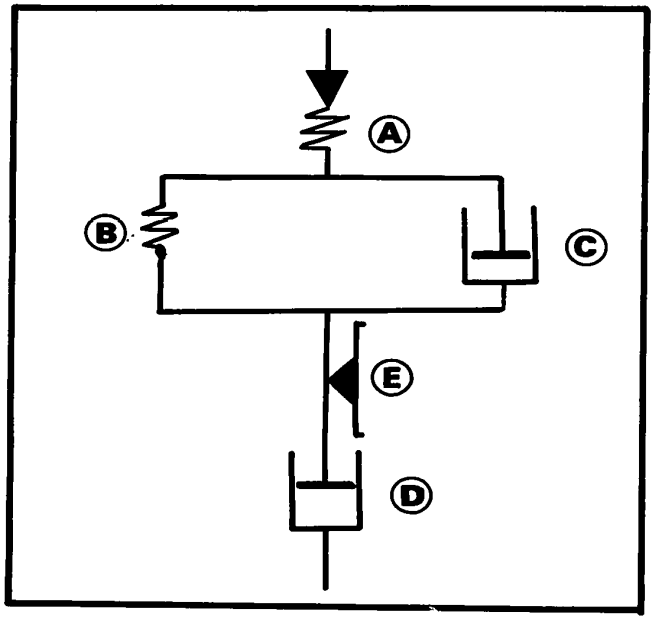

FIG. 8. - Mechanical Model (Vialov)

by a spring and dashpot is parallel (B,C). The other type is completely residual and represented by a dashpot (D) with a braking element (E) as the plastic qualities. However, this model is only qualitative and gives no quantitative information.

Stress-strain curves for different times of load duration as in Fig. 7 are all similar in shape and Vialov describes them with a power law

$$\sigma = A_t \, \varepsilon^m \tag{7}$$

where A_t is the modulus of total deformation and $m < 1$ is the strengthening factor which is independent of time and temperature.

Despite the studies reviewed in this chapter, little is still known about the behaviour of frozen sand. There is a need for more specific, detailed work. Previous work has been general, dealing with both clays, sands, and ice. Many theories which may be applicable have, so far, only been tested on unfrozen soil.

Also, almost all the research conducted to date has been performed on the triaxial cell. Unfortunately, this introduces the added parameter of confining pressure which greatly influences the stress-strain relationship. This makes analysis of results very difficult.

In addition, very few researchers have attempted to separate the plastic and elastic strains. This would not be

easy to do on a triaxial cell with a controlled strain rate which most studies have employed. A more meaningful analysis could be performed if tests were conducted on equipment independent of confining pressure and with a controlled stress rate. Also, in this way the plastic strain and elastic strain could be separated. As a result of this literature study, the experimental program proposed in Chapter III has been designed to obtain still needed information pertaining to the modulus of elasticity and the stress-strain relationship of frozen sands.

CHAPTER III

EXPERIMENTAL PROGRAMME

a) Outline of Experiments

Two types of experiments were conducted. The first type was designed to obtain a stress-strain curve for the soil and the second was designed to differentiate between the elastic and plastic components of the first curve.

1. Tests Involving Total Strain at Various Loading Rates

In the first set 20 p.s.i. stress increments were applied at different loading rates of 1 minute, 5 minutes and 10 minutes. The corresponding strain was recorded for each stress (i.e. 20 p.s.i., 40 p.s.i., 60 p.s.i....). When plotted this resulted in an elastic-plastic curve. Four different ice saturations were used (25%, 50%, 75%, 100%) at different temperatures of $0^{\circ}F$, $10^{\circ}F$, $20^{\circ}F$ and $25^{\circ}F$. This resulted in 48 different curves for 48 samples (Fig. 24-39, Appendix B). In addition, one experiment was conducted at $30^{\circ}F$ with a loading rate of 1 p.s.i. per minute (Fig. 40).

2. Tests Involving Separation of Elastic and Plastic Strains

In the second set, the procedure was similar to the first with the exception that the stress was dropped to zero and the sample was allowed to relax for 5 minutes after

every stress increment. Two strain readings were taken for every load increment: one with the sample stressed (ε_T, total strain) and one with the sample relaxed (ε_{PL}, plastic strain). A loading rate of 20 p.s.i. per 5 minutes was used. Four different ice saturations were used (25%, 50%, 75%, 100%) at different temperatures of 0^oF, 10^oF and 20^oF (Fig. 41-52, Appendix D). At 25^oF results for this type of experiment were found to be unreliable since only a few readings could be taken before the sample failed.

b) Apparatus

The equipment used to hold the sample and apply the radial pressure is the one devised by Willmot (1956) which he used for studies on ice. This is shown in Fig. (9). It consists of an outer steel cylinder and an inner rubber diaphragm with a space between the two where the oil can enter under pressure. The pressure is applied by a hand operated hydraulic pump (Fig. 10). A 6" pressure gauge with a range of 200 p.s.i. was fitted at the hydraulic pump so as to remain outside the freezer during tests. All stress readings were obtained from this gauge.

To measure the strain, a STRAINSERT, 8-channel Transtrain Indicator (Model TN8C) was used, as shown at the centre in Fig. 10. The strain gauges used were BLH, SR-4 type A-9. These are paper bonded, resistance strain gauges. To increase the bond between the gauge and the sand specimen a coating of sand was applied to each gauge using Eastman 910 Adhesive Cement to bond the sand particles to the paper (Fig. 11).

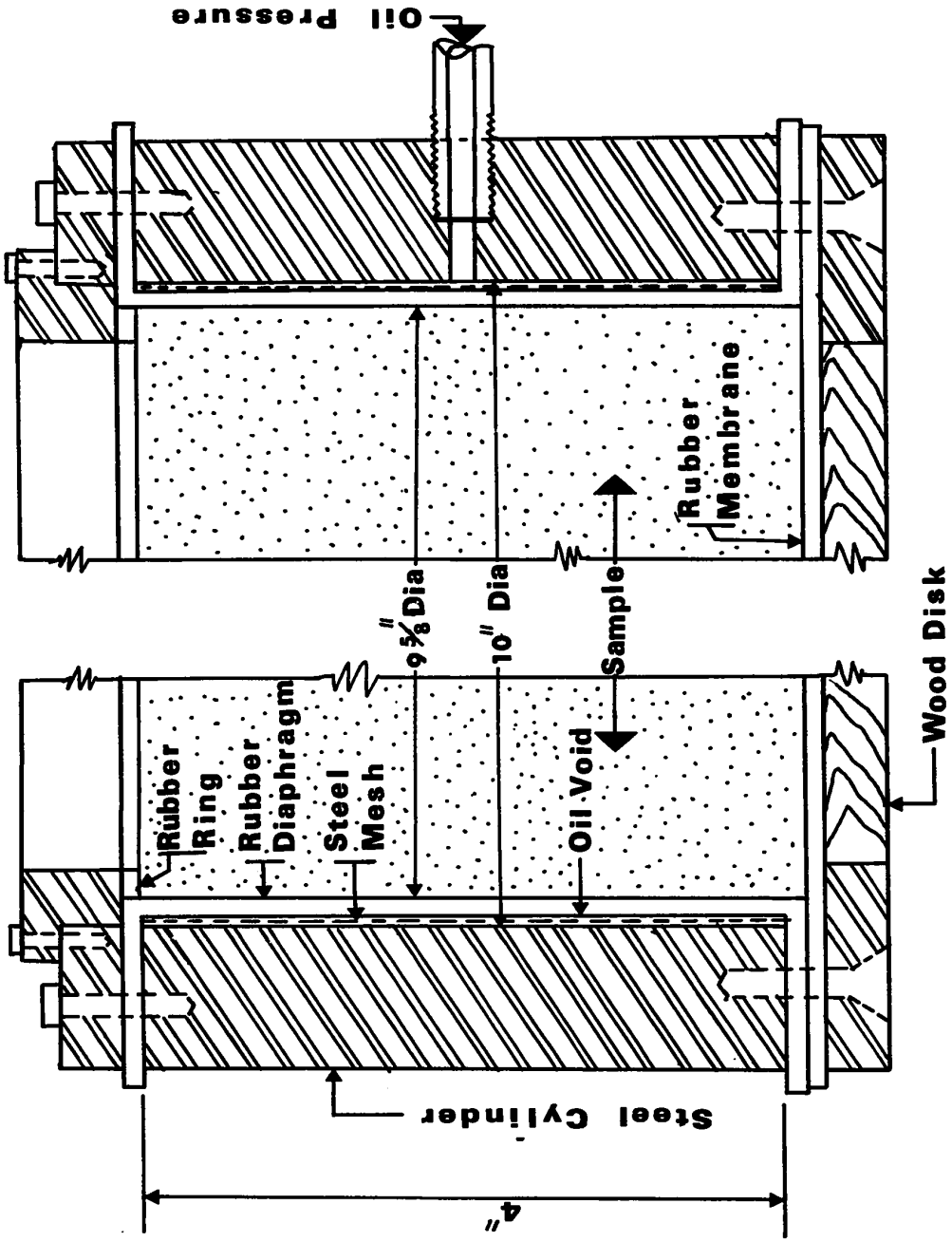

FIG. 9. - Steel Cylinder with Rubber Diaphragm

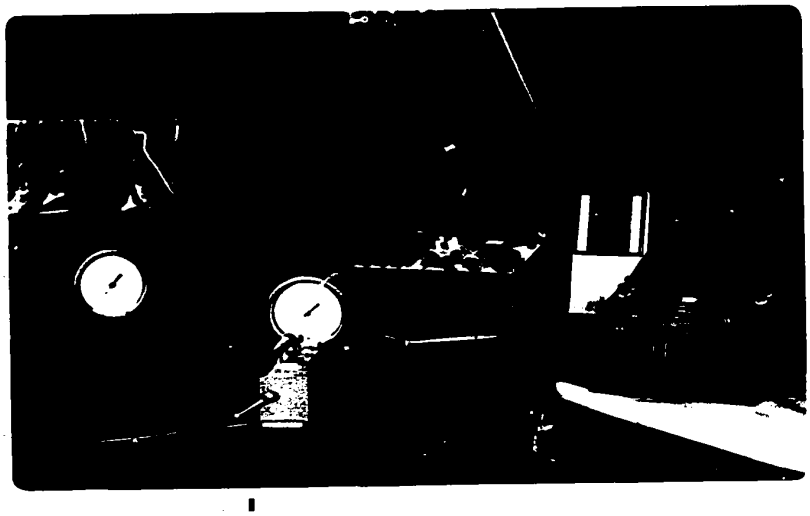

FIG. 10. - Equipment Displayed with Freezer

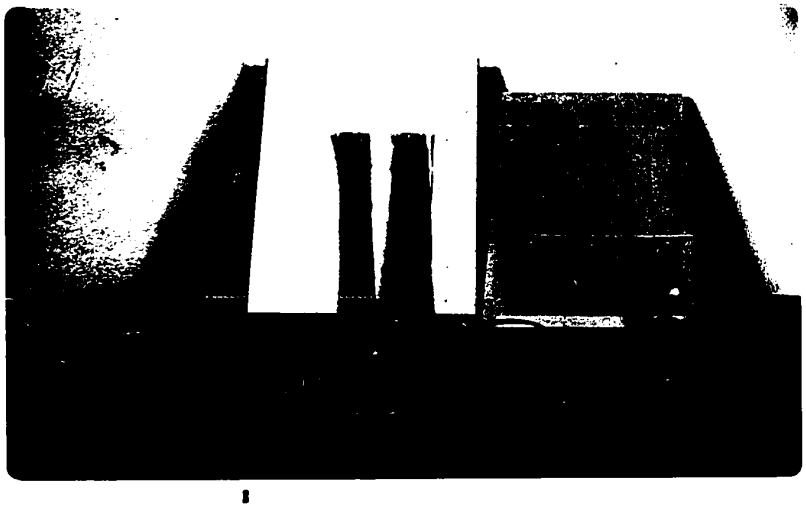

FIG. 11. - Preparation of Strain Gauges

The freezer used was a V.E. chest type freezer with a through-the-lid fan (Fig. 10). Mounts inside the freezer were used to protect the sample from any vibrations from the freezer.

c) Preparation of Samples

The soil used was Ottawa sand. A grain size distribution curve for this sand is shown in Fig. 12.

A known weight of pre-cooled dry sand was mixed thoroughly with the required amount of water required to give the desired ice saturation when frozen. This soil was then placed in the hollow core of the apparatus and was uniformly compacted to form a 9 5/8" diameter and 4" thick sample of a certain void ratio.

While this was being filled, two strain gauges were placed halfway through the sample, horizontally and at right angles at the specimen's centroidal axis (Fig. 13). Although only one gauge was recorded, the second gauge acted as an emergency spare, so that if one malfunctioned, the experiment could be conducted on the other without preparing and freezing a new sample. To balance the bridge, a dummy gauge was also placed in a sand box inside the freezer along with the sample (Fig. 14). The sample was then covered with a loosely fitting plexiglas disc to avoid moisture loss at the top surface.

The temperature of the sample was taken using four copper constantan thermocouples at three different depths:

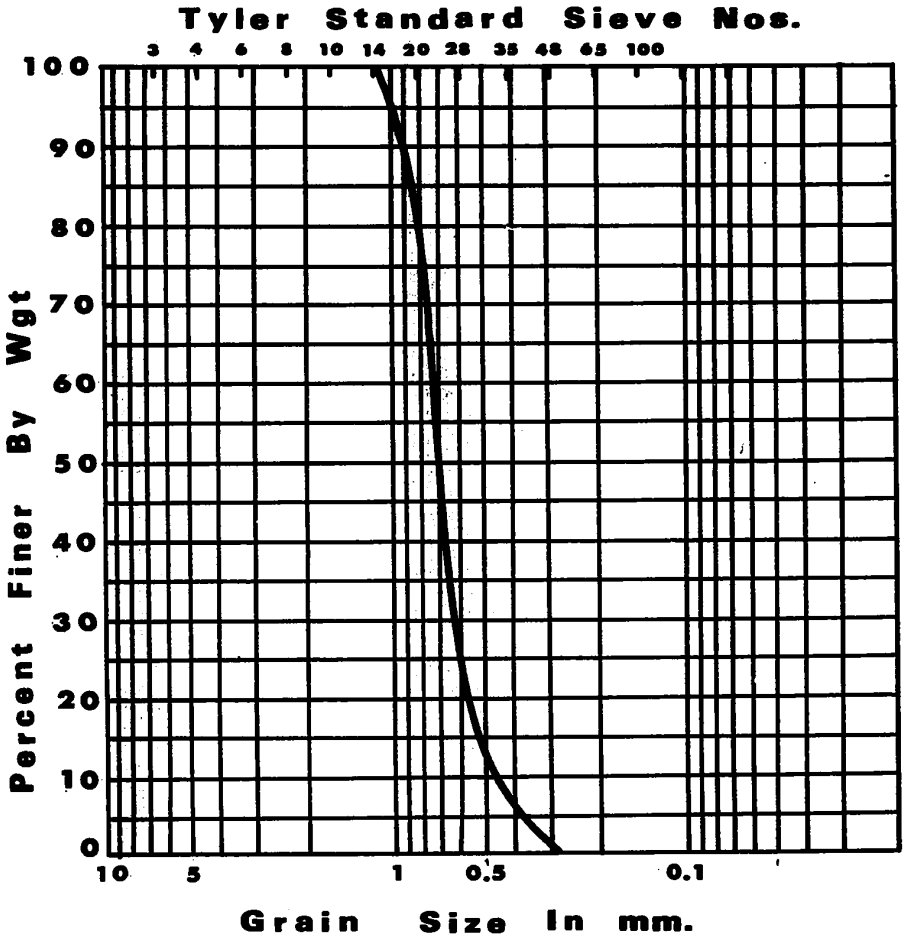

FIG. 12. - Grain Size Distribution Curve

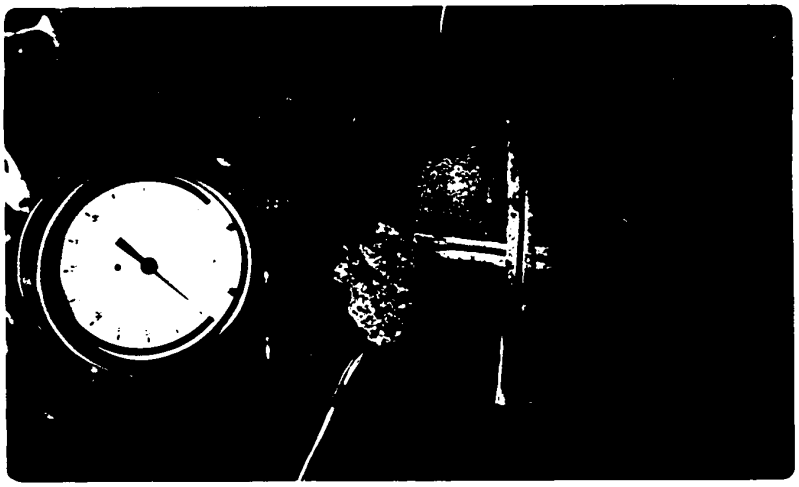

FIG. 13. - Placing of Strain Gauges

FIG. 14. - Completed Sample in Freezer Compartment.

1. ¼" below top surface, at centre;
2. 2" below top surface, at centre;
3. 2" below top surface, 1" from edge;
4. ¼" from bottom, at centre.

In addition, another thermocouple was used to measure the air temperature inside the freezer and another one to measure the temperature in the vicinity of the dummy gauge. A sample with thermocouples in place can be seen in Fig. 14. They were all, in turn, connected to a temperature potentiometer by way of a multi-polar switch (Fig. 10). Before being tested, the frozen sample was allowed to remain at a constant temperature long enough to ensure a constant, uniform temperature throughout the sample before being tested (i.e. all thermocouple readings were equal and constant).

d) Reliability of Experiments

1. Strain Gauge Reliability

The validity of this work depends upon the reliability of the bond between the sand-ice system and the strain gauges. To check this, one experiment was performed using the strain gauge and a Maihak device simultaneously (Fig. 15). A Maihak transmitter MDS53 and receiver MDS3 were used. This method is independent of any bond with the sample but relies only on the direct soil pressure on the measuring device. It operated on the principle of attaining the coincidence in frequency of vibration between a stretched

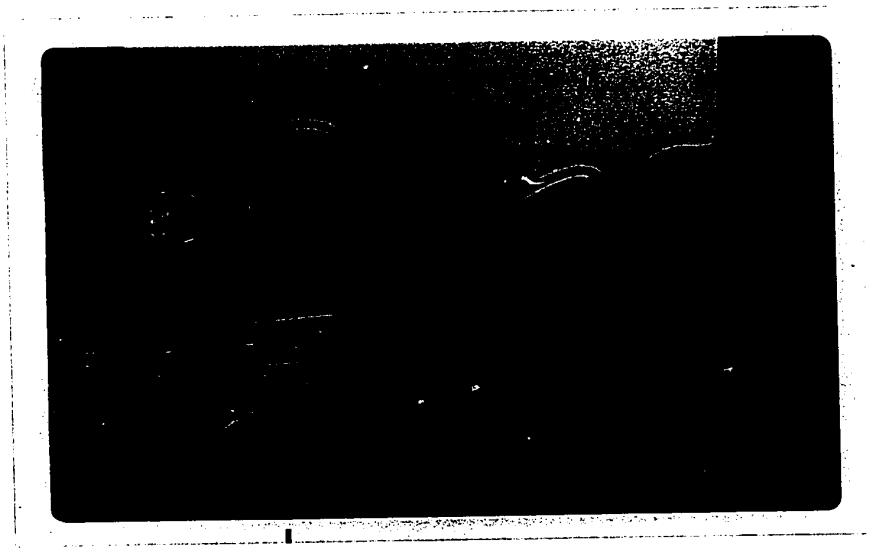

FIG. 15. - Maihak Transmitter & Receiver

measuring wire in the transmitter and a standard wire in the receiver.

The resulting curves (Fig. 16) were almost identical, thereby verifying the reliability of the paper strain gauges. In fact, this also proved that they were superior to the Maihak device since they were much easier and quicker to take readings than the Maihak where the frequencies had to be balanced before a reading could be taken. Some experiments would have been impossible with the Maihak unit.

2. Affect of Unloading Cycles on Virgin Curve

It was also important to prove that the curve was unaffected by releasing the stress at each load increment in order to separate the plastic and elastic portions. Two identical samples were tested - one with unloading after each increment was applied and one without unloading (virgin curve).

Arbitrarily, the temperature was 10°F and the saturation 50%. Rate of stress was 10 p.s.i. per 3 min. up to 100 p.s.i. and 25 p.s.i. per 3 min. from 100 p.s.i. to 200 p.s.i. The two curves (Fig. 17) were close enough to conclude that this type of loading did not affect significantly the virgin curve.

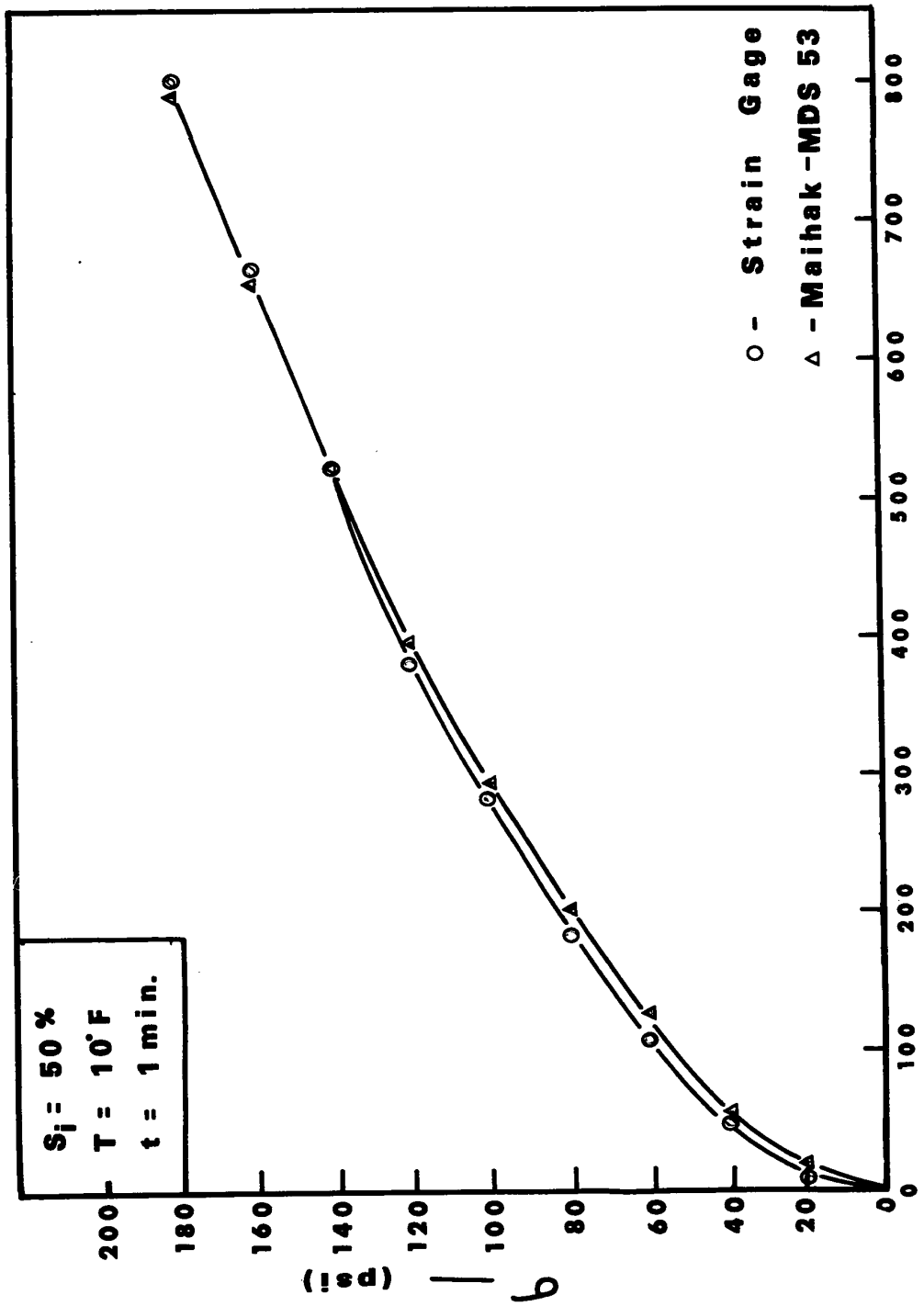
S_i = 50 %
T = 10°F
t = 1 min.
○ - Strain Gage
△ - Maihak-MDS 53
σ — (psi)
ε — (microin./in.)
0
100
200
300
400
500
600
700
800
20
40
60
80
100
120
140
160
180
200

FIG. 16.

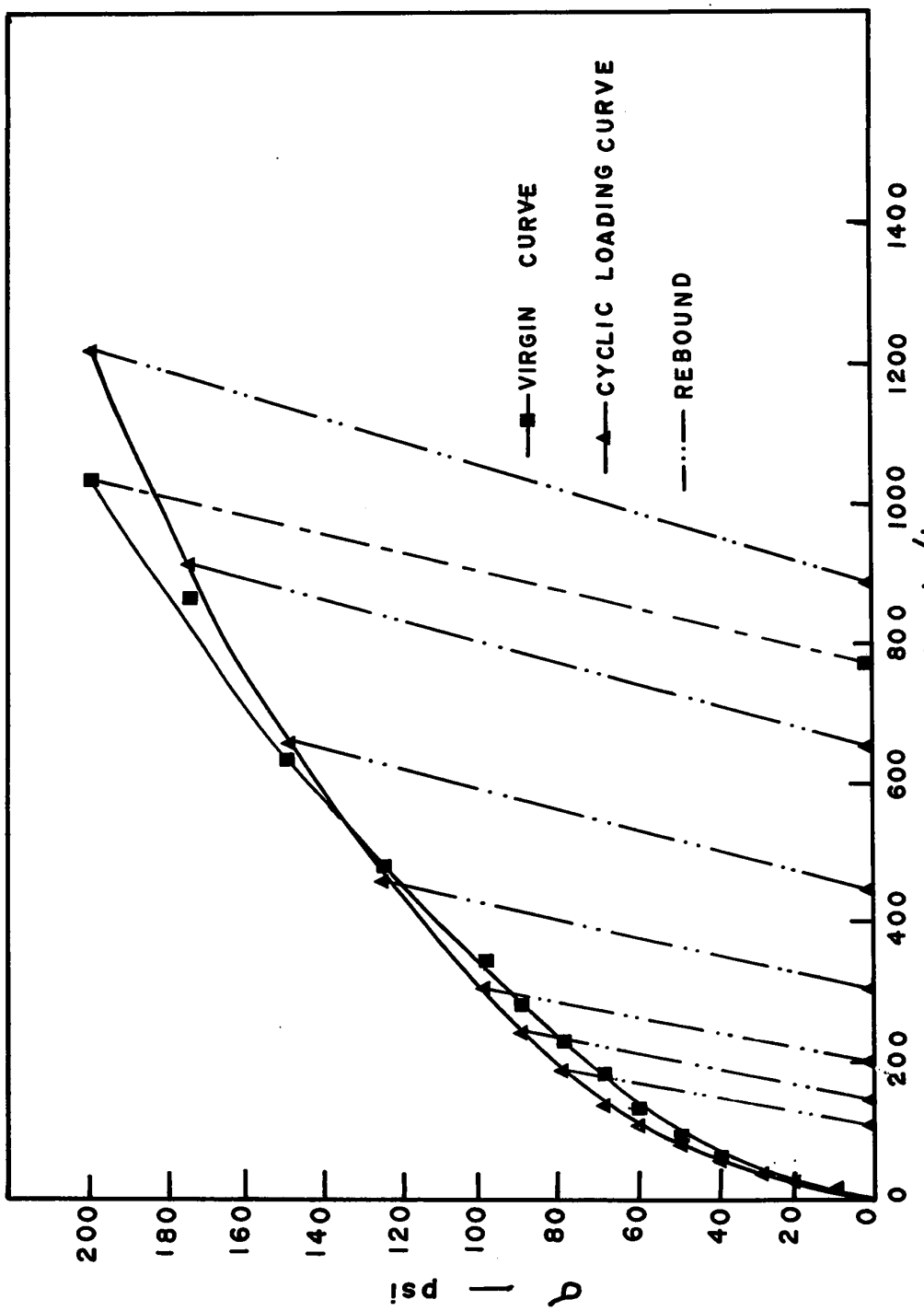

FIG. 17. - Comparison of Cyclic Loading Curve with Virgin Curve

CHAPTER IV

DISCUSSION OF TEST RESULTS

a) Tests with Various Loading Rates

The graphs for the first set of tests appear in Appendix B, Fig. 24 to Fig. 39. When these results were plotted it was possible to fit a smooth curve through all the points for a particular test with almost no points lying off the line. They seemed to be a family of parabolic curves.

It was found that when these curves were plotted on log-log paper they transformed into straight lines. The equations calculated for each of the curves were all of the form,

$$\sigma = A\varepsilon^{m} \tag{8}$$

with $m < 1$, as predicted by Vialov[9].

The various values for 'A' and 'm' were tabulated and can be found in Appendix C, Tables I, II and III.

However, when an attempt was made to obtain one general equation there was not enough correlation. When values of 'A' or 'm' were plotted against time, temperature or saturation, the points were too scattered to formulate any type of relationship. Nevertheless, general conclusions can be drawn from these tests.

First of all, the stress-strain behaviour of the frozen sand was a function of the temperature at which the test was taken. High temperatures resulted in greater strains. Also, the strain varied with the ice saturation of the sample. Low saturations produced high stresses. Finally, these tests showed the time dependency of the stress-strain relation.

There were some uncontrollable factors which might have caused the results to be not so reliable. One phenomenon which was difficult to control was the manner in which the sample froze. At times, ice would bulge up at the surface. This resulted in some reduction of ice content of the sample. Unfortunately, this action was not consistent. The intensity seemed to vary arbitrarily. However, it was probably also affected by the temperature at which the freezing took place and by the ice saturation of the sample. All the samples could not be frozen in an identical manner since the temperature to be attained varied from sample to sample.

b) Tests Separating the Elastic and Plastic Components

The graphs for the second series of tests appear in Appendix D, Fig. 41 to Fig. 52. The plots of the total strain curves were similar to the curves in the first series, that is, parabolic. When separated into elastic and plastic components, the elastic curve could be approximated by a straight line and a modulus of elasticity could be obtained.

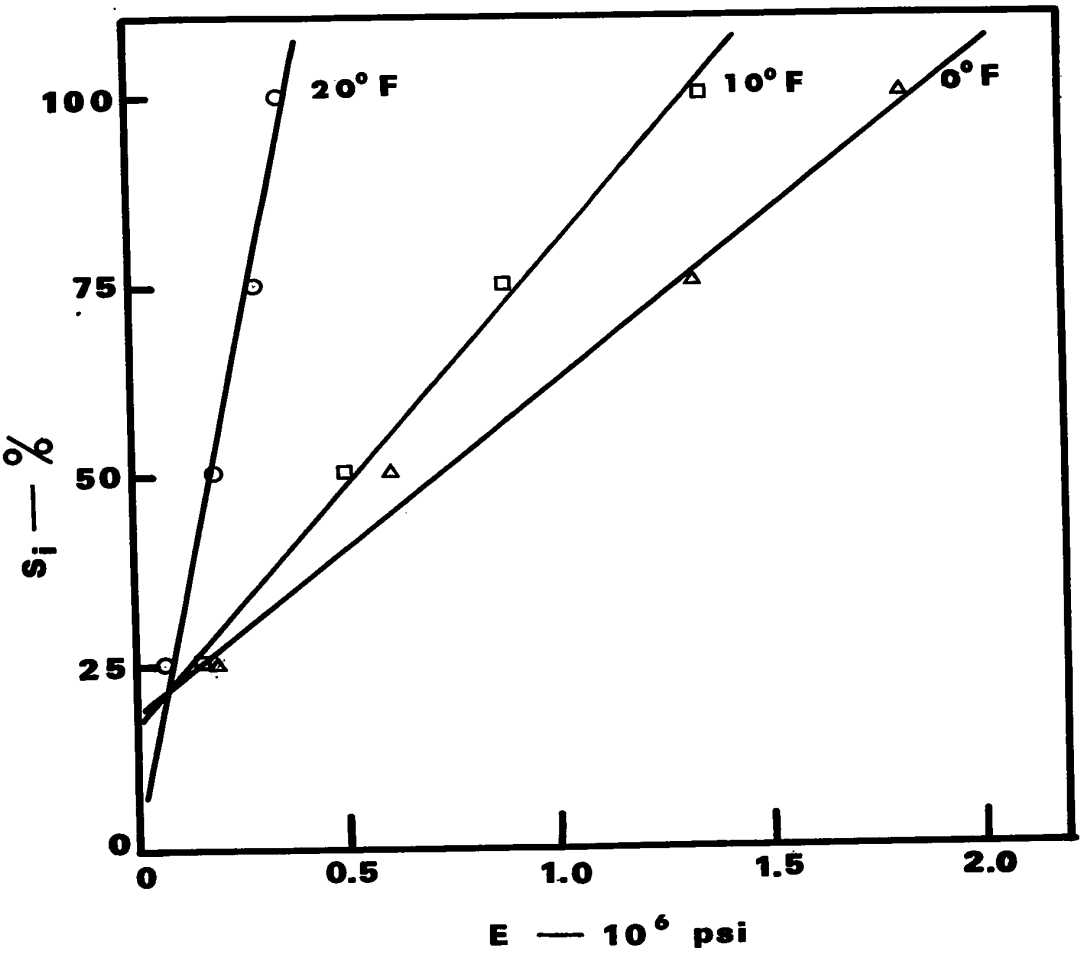

FIG. 18. - Modulus of Elasticity vs. Ice Saturation

These values of the modulus of elasticity were then plotted against ice saturation (S_i) for each of the temperatures at which tests were performed (Fig. 18). The straight lines which resulted indicated a linear relationship between the modulus of elasticity (E) and ice saturation (S_i). By interpolating, Fig. 18 can be used to determine the modulus of elasticity for any given ice saturation and temperature.

The curve obtained for the plastic component of the strain seemed to remain parabolic in shape as was the total strain curve. To obtain a formula for this curve the same procedure was used as in the first series of tests.

c) Derivation of Formula for Plastic Component

A parabolic equation assumed was of the form -

$$\sigma = A\varepsilon_{PL}^{m} \tag{9}$$

The curves were plotted on log-log paper and as illustrated in Fig. 19 straight lines resulted. From these plots, values of 'A' and 'm' were found for each test and these were tabulated in Appendix E, Table IV according to temperature and ice saturation.

1) Determination of 'm'

The value of 'm' varied only slightly with temperature and was therefore assumed not to vary with temperature. Therefore, an average 'm' was calculated for each ice saturation and plotted as shown in Fig. 20.

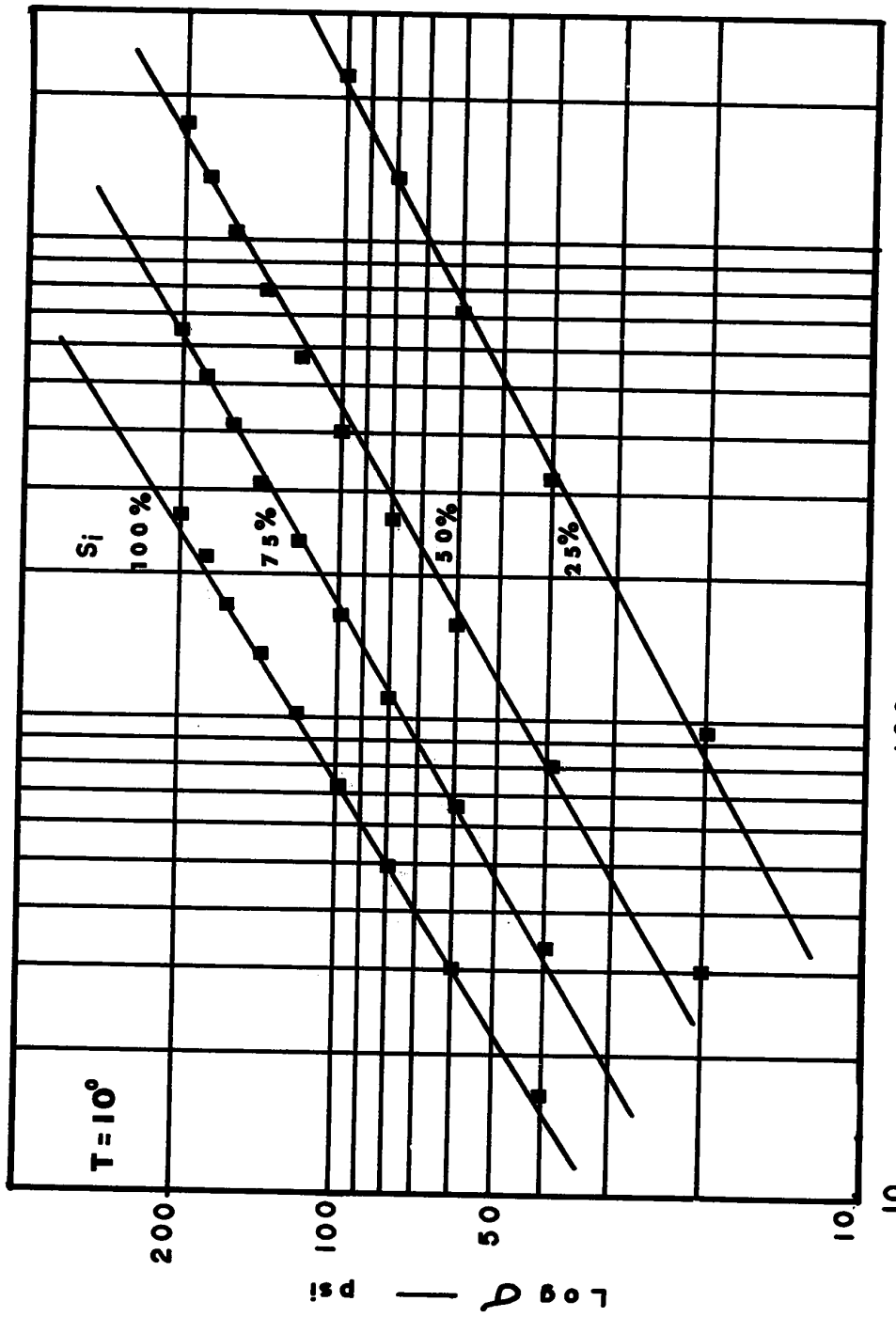

FIG. 19. - Typical Log-Log Plots of Plastic Stress-Strain Curves

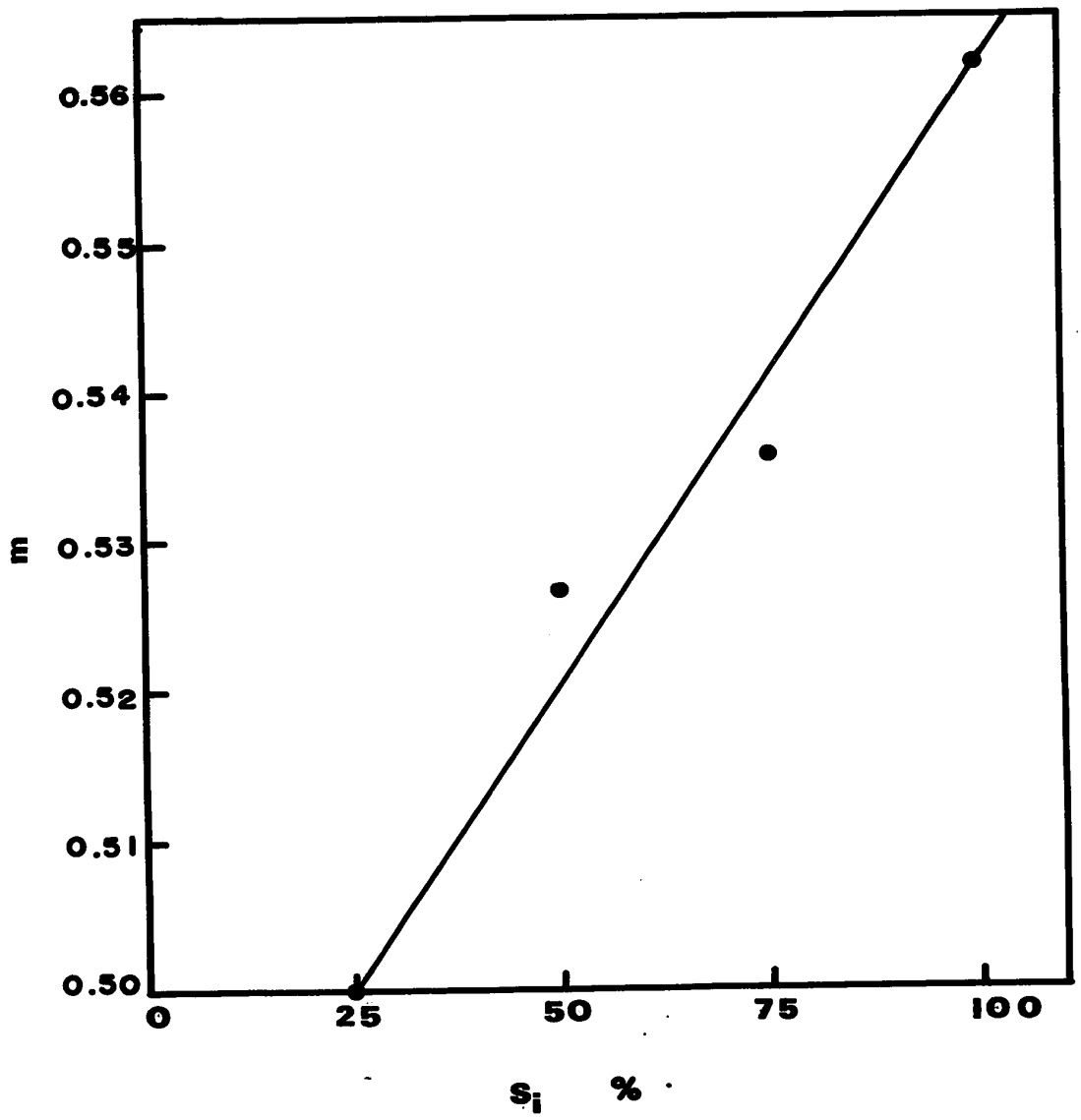

FIG. 20. - Determination of 'm' as a Function of the Ice Saturation

This resulted in a linear relationship of the form,

$$m = 0.000827S_i + 0.479 \quad (10)$$

2) Determination of 'A'

The values of 'A' were plotted against ice saturation (S_i) for each of the test temperatures (Fig. 21). This resulted in three straight lines, one for each temperature, of the form,

$$A = nS_i + C \quad (11)$$

Values for 'n' and 'C' are tabulated in Appendix E, Table V.

The values of 'C' were then plotted against temperature and a curve resulted as shown in Fig. 22. However, when C^2 was plotted against temperature, a linear relationship resulted. From this an equation for 'C' was calculated,

$$C = [|0.02T - 0.25|^{\frac{1}{2}}] \quad (12)$$

Similarily, 'n' was plotted against temperature (Fig. 23). A cosine function was assumed to describe this curve and was approximated to be

$$n = 0.10 \cos \frac{\pi T}{52} \quad (13)$$

Therefore, by substituting Equation 12 and Equation 13 into Equation 12,

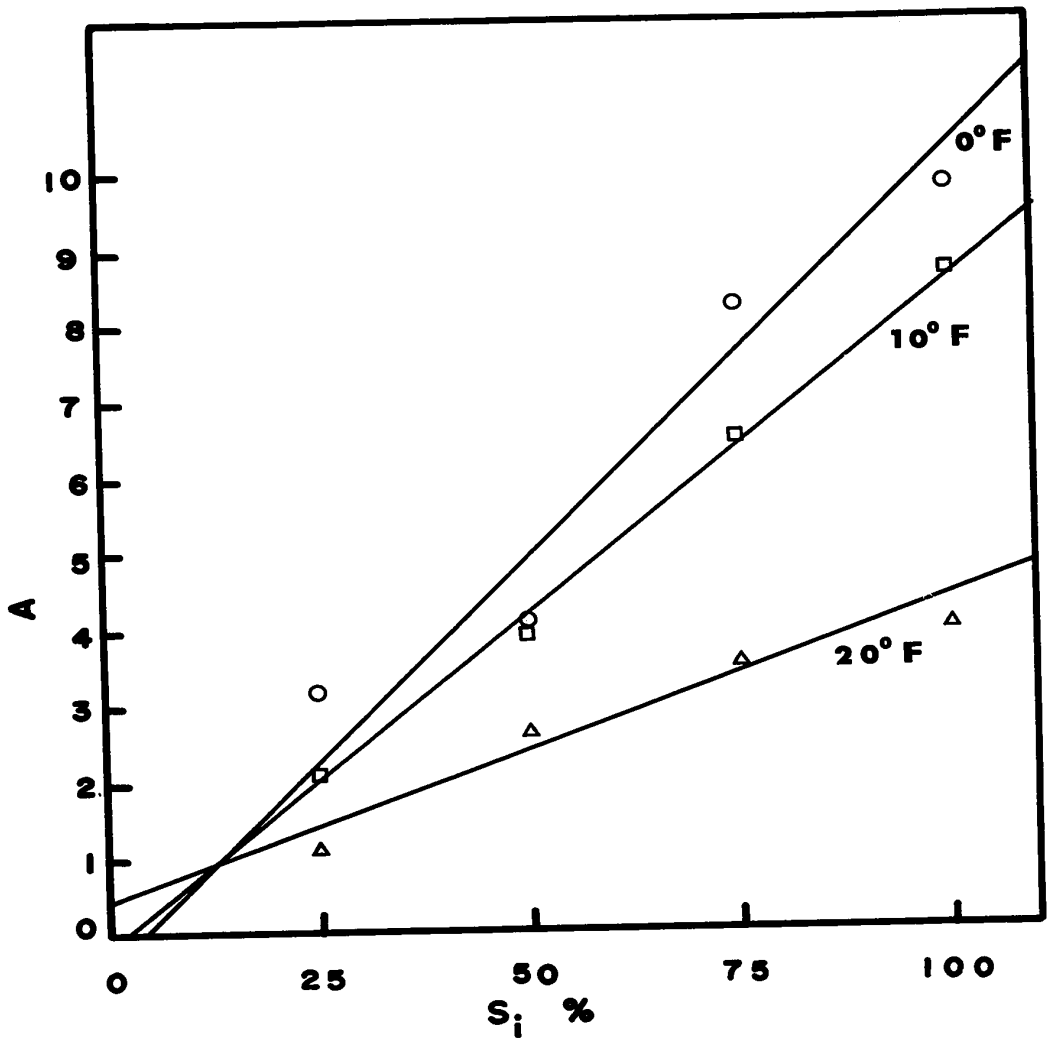

FIG. 21. - Determination of 'A' as a Function of the Ice Saturation

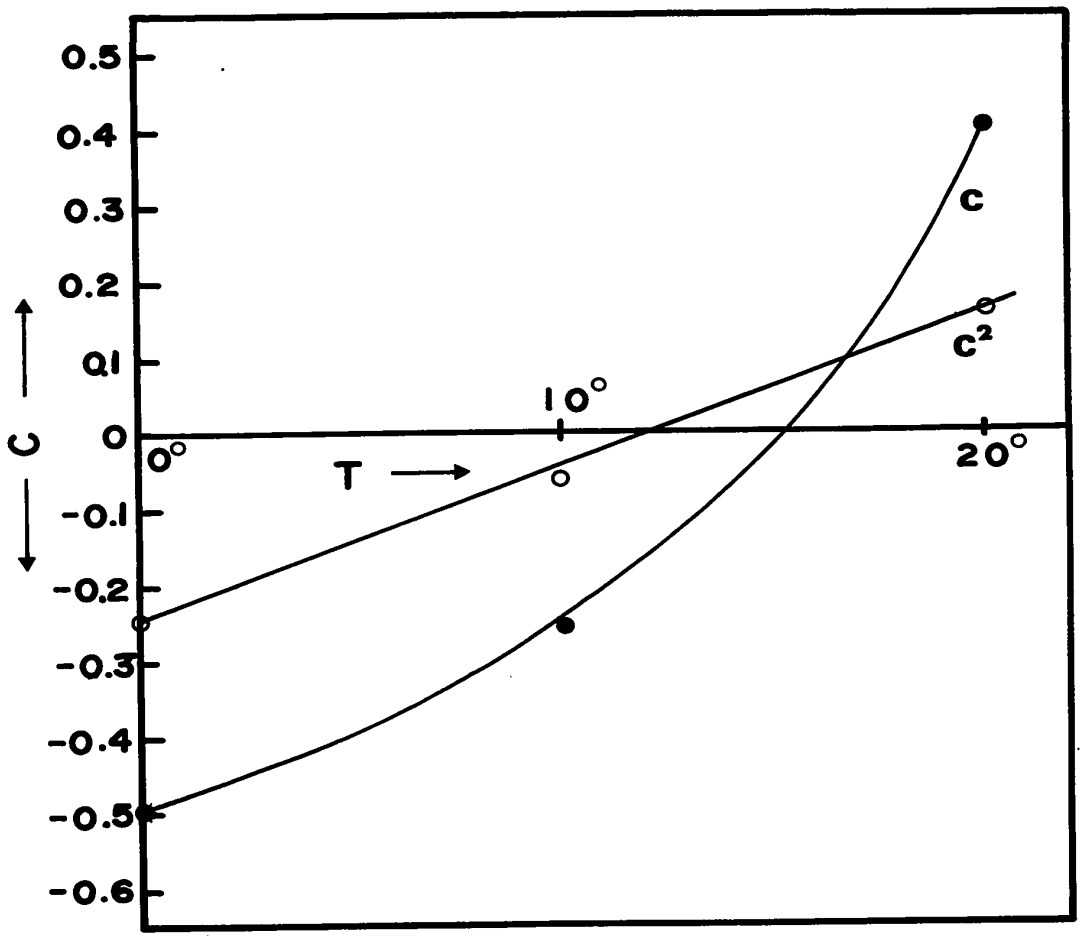

FIG. 22. - Determination of 'C' as a Function of Temperature

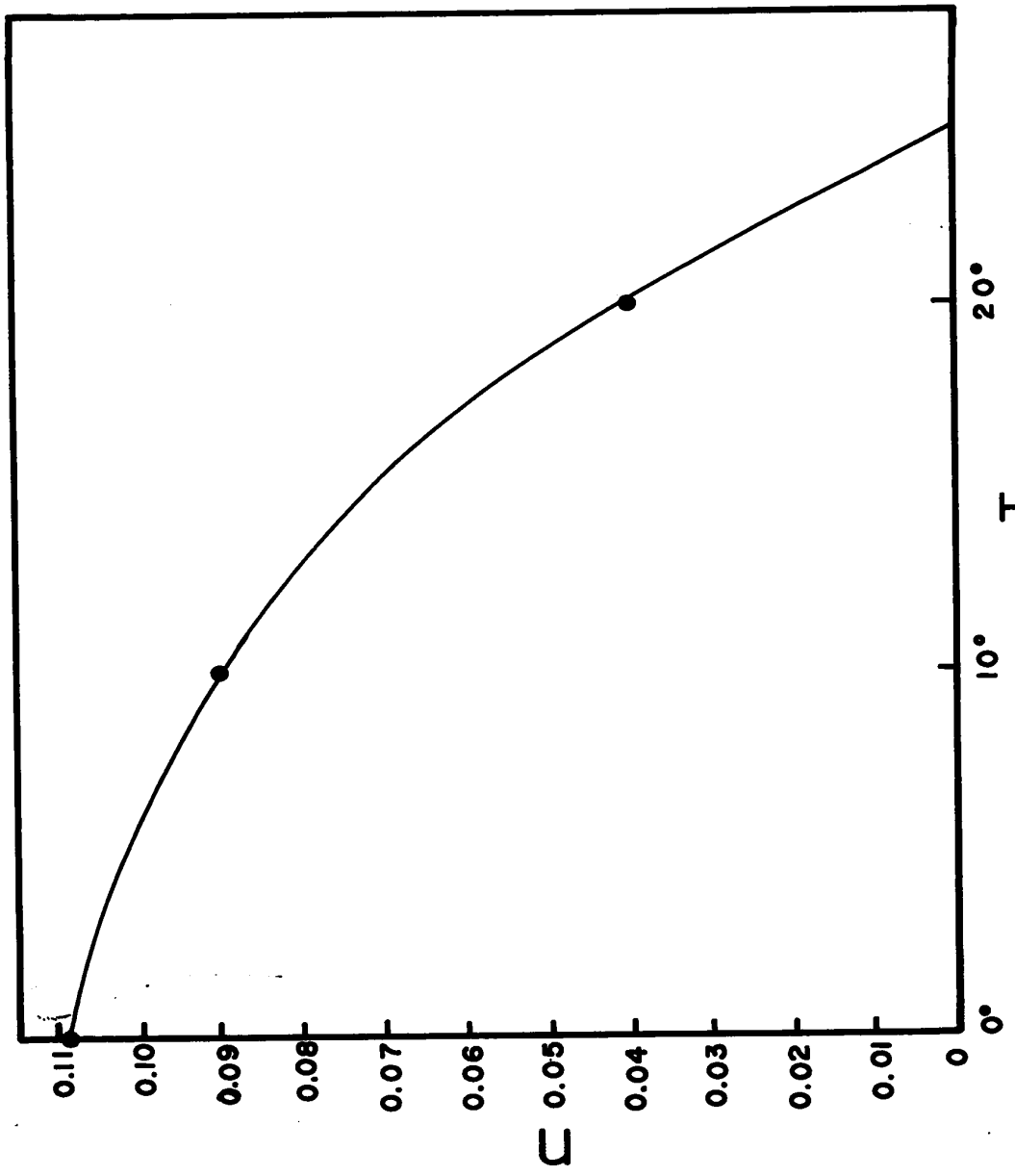

FIG. 23. - Determination of 'n' as a Function of Temperature

$$A = (0.10 \cos\tfrac{T}{52})S_i + |0.02T - 0.25|^{\frac{1}{2}} \quad (14)$$

Then by substituting equation 14 and 10 into equation 9,

$$\sigma = \left[(0.10 \cos\tfrac{T}{52})S_i + |0.02T - 0.25|^{\frac{1}{2}}\right] \varepsilon_{PL}[0.000827S_i + 0.479] \quad (15)$$

The elastic equation is,

$$\sigma = \varepsilon_{EP}E \quad (16)$$

Rewriting equations 15 and 16,

$$\varepsilon_{PL} = \left[\frac{\sigma}{\left[(0.10 \cos\tfrac{T}{52})S_i + |0.02T - 0.25|^{\frac{1}{2}}\right]}\right] \frac{1}{0.000827S_i + 0.479} \quad (17)$$

$$\varepsilon_{EL} = \frac{\sigma}{E} \quad (18)$$

Since,

$$\varepsilon_T = \varepsilon_{EL} + \varepsilon_{PL} \quad (19)$$

adding equations 17 and 18,

$$\varepsilon_T = \frac{\sigma}{E} + \left[\frac{\sigma}{\left[(0.10 \cos\tfrac{T}{52})S_i + |0.02T - 0.25|^{\frac{1}{2}}\right]}\right] \frac{1}{0.000827S_i + 0.479} \quad (20)$$

where E = modulus of elasticity from Fig.

T = temperature in F^{o}

S_i = ice saturation in %

σ = stress in p.s.i.

ε_T = total strain in microns/in.

Equation 15 agrees very well with Vialov's[9] theory. As he predicted, 'm' the strengthening factor is less than unity and is also independent of temperature.

Using Equation 15, curves were produced for the various conditions at which experiments had been performed. These represented the plastic portion of the stress-strain curves. The experimental data was also plotted on the sheet with corresponding conditions (ice saturation, temperature). As can be seen from Fig. 56 to 64 (Appendix F) there was a good fit. In most curves, the experimental points lie on the curve obtained from the equation.

CHAPTER V

CONCLUSIONS AND RECOMMENDATIONS

a) Conclusions

Test with Various Loading Rates

These tests in which the strain was considered integrated (not resolved into plastic and elastic components) resulted in curves, each of which were definitely of the form of the parabolic Equation 8. But, since no correlation could be found between the curves and no general equation describing the curves could be derived, it seems that perhaps the plastic strain and elastic strain should be considered separately. Treating them as one entity makes analysis difficult if not impossible. However, these tests do illustrate the dependence of the soil behaviour upon temperature, ice saturation and time. That is,

1) as temperature increases, strain increases
2) as ice saturation decreases, strain increases
3) as the time of application of the load increment increases, the strain increases.

Tests on the Elastic and Plastic Components

These tests proved very successful. As in the former series of tests, the curves were also parabolic for

those describing the plastic behaviour. On the other hand, the elastic curves approximated a linear reltionship whose slope was the modulus of elasticity. Therefore, these tests gave a value for a modulus of elasticity independent of the plastic component. This is much more reliable than trying to estimate an initial tangent modulus or using other more vague moduli such as a secant modulus. This elastic modulus is also a function of ice saturation and temperature as is the parabolic equation for the plastic component of strain.

In summary,

1) an elastic modulus (E) was determined and was a function of ice saturation and temperature
2) a general equation was found for the plastic component
3) using the above conclusions, a parabolic equation was derived to describe the general stress-strain behaviour of the frozen sand (Equation 20).

b) Recommendations for Further Work

1) Time Dependency

Tests of the type which separated the elastic and plastic components should be repeated at different loading rates.

2) Other Soils

It would be of interest to do similar tests with other sands or perhaps even clays if reproducibility is possible.

3) Manner of Freezing

A more uniform and consistent method of freezing the samples should be developed. Perhaps freezing large specimens and then cutting the samples from the same large piece would be an improvement.

4) Low Stresses

A more accurate apparatus should be developed to study the behaviour at lower stresses.

APPENDIX A

NOMENCLATURE

NOMENCLATURE

ε = strain

ε_T = total strain

ε_{EL} = elastic strain

ε_{PL} = plastic strain

σ = stress

σ_1 = major principal stress

σ_3 = confining stress

$(\sigma_1-\sigma_3)$ = deviator stress or stress difference

S_i = ice saturation

T = temperature

E = modulus of elasticity

E_t = tangent modulus

E_s = secant modulus

E_f = final modulus after unloading

A = modulus of deformation

A_t = modulus of total deformation

m = strengthening factor

n = slope of A vs S_i plot

c = intercept of A vs S_i plot

a = reciprocal of initial tangent modulus

b = reciprocal of asymptotic value of stress difference

σ_k = proof stress in pseudo-instantaneous stress-strain equation

k = exponent in stress-strain equation

t = time of duration of load increment

t_r = time of relaxation

APPENDIX B

TOTAL STRESS-STRAIN CURVES FOR VARIOUS S_i, T and t

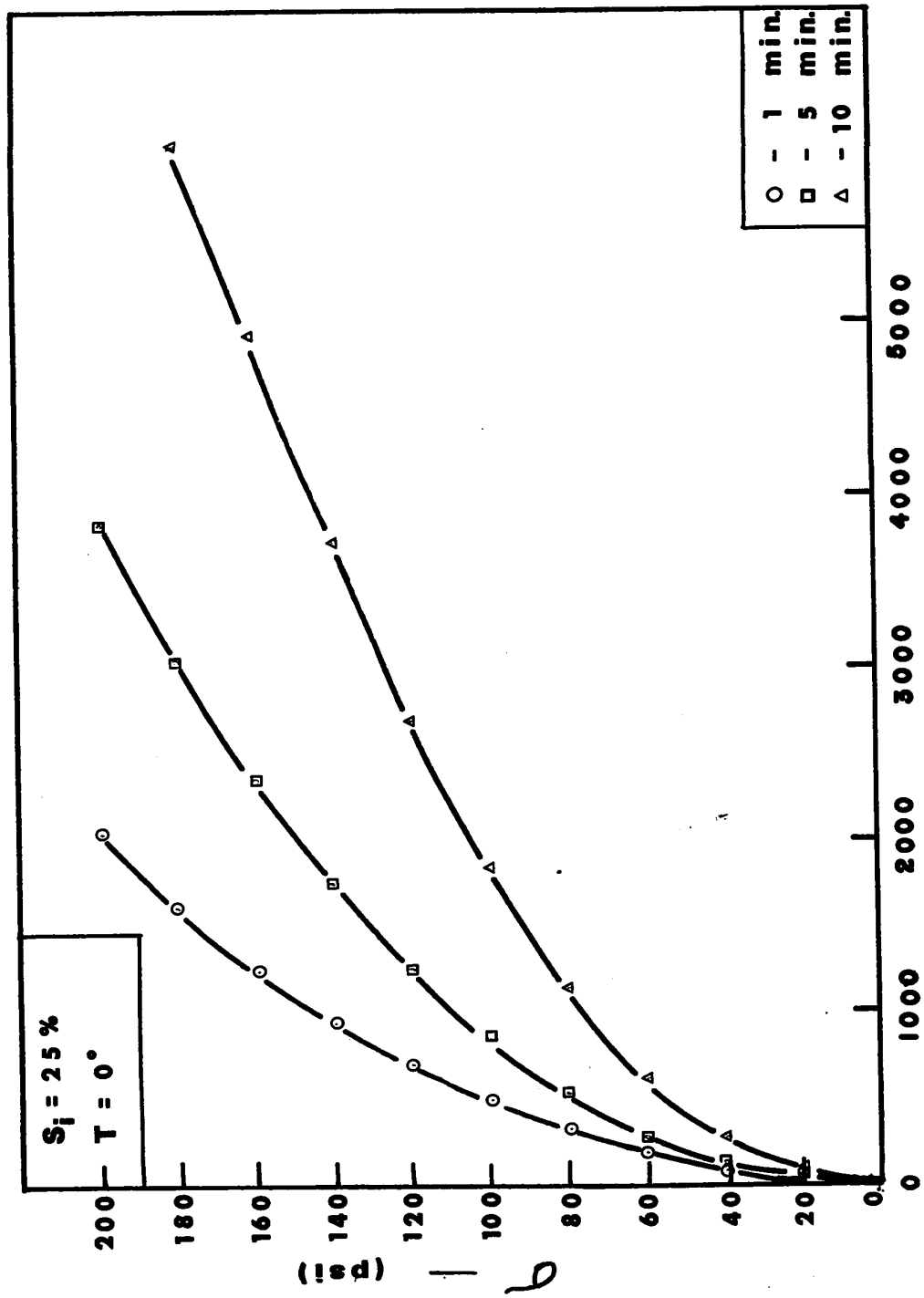
S_i = 25 %
T = 0°
○ - 1 min.
□ - 5 min.
△ - 10 min.
σ — (psi)
0
20
40
60
80
100
120
140
160
180
200
0
1000
2000
3000
4000
5000
ϵ - (microin./in.)

FIG. 24

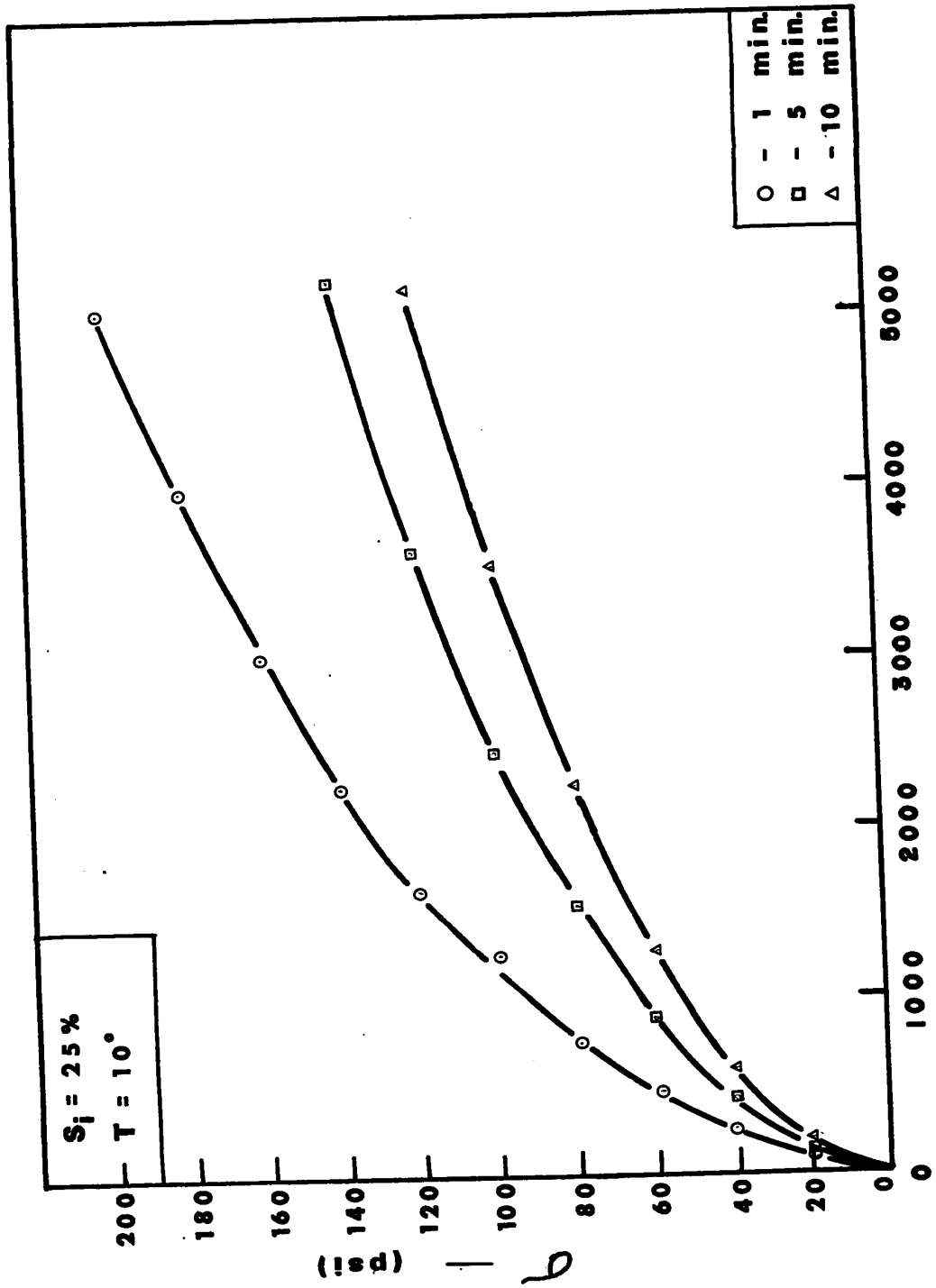
S_i = 25 %
T = 10°
○ - 1 min.
□ - 5 min.
△ - 10 min.
σ — (psi)
ϵ - (microin./in.)
0
20
40
60
80
100
120
140
160
180
200
1000
2000
3000
4000
5000

FIG. 25

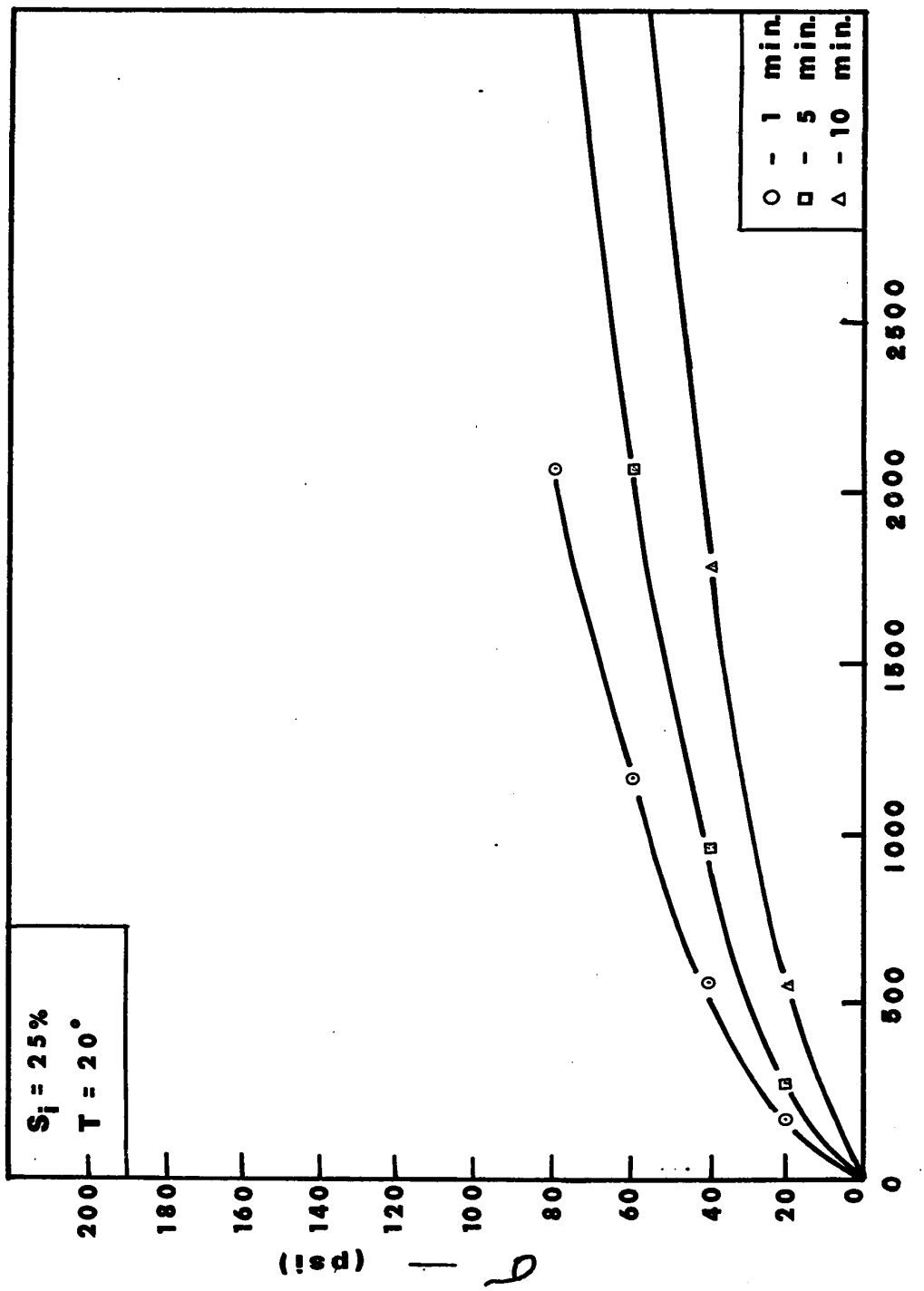
S_i = 25%
T = 20°
○ - 1 min.
□ - 5 min.
△ - 10 min.
σ — (psi)
0
20
40
60
80
100
120
140
160
180
200
500
1000
1500
2000
2500
ϵ - (microin./in.)

FIG. 26

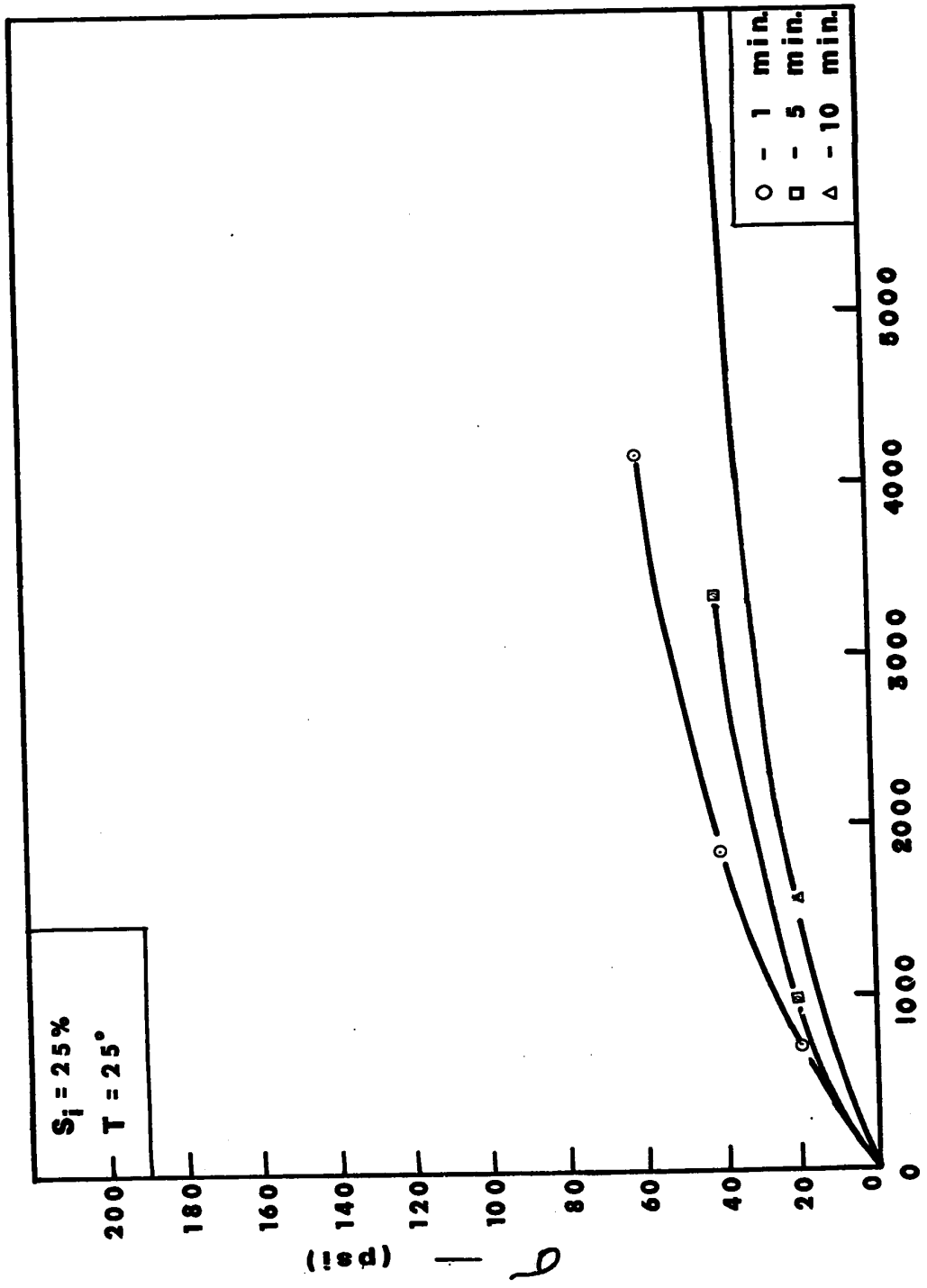
S_i = 25 %
T = 25°
○ - 1 min.
□ - 5 min.
△ - 10 min.
σ — (psi)
200
180
160
140
120
100
80
60
40
20
0
0
1000
2000
3000
4000
5000
ϵ - (microin./in.)

FIG.27

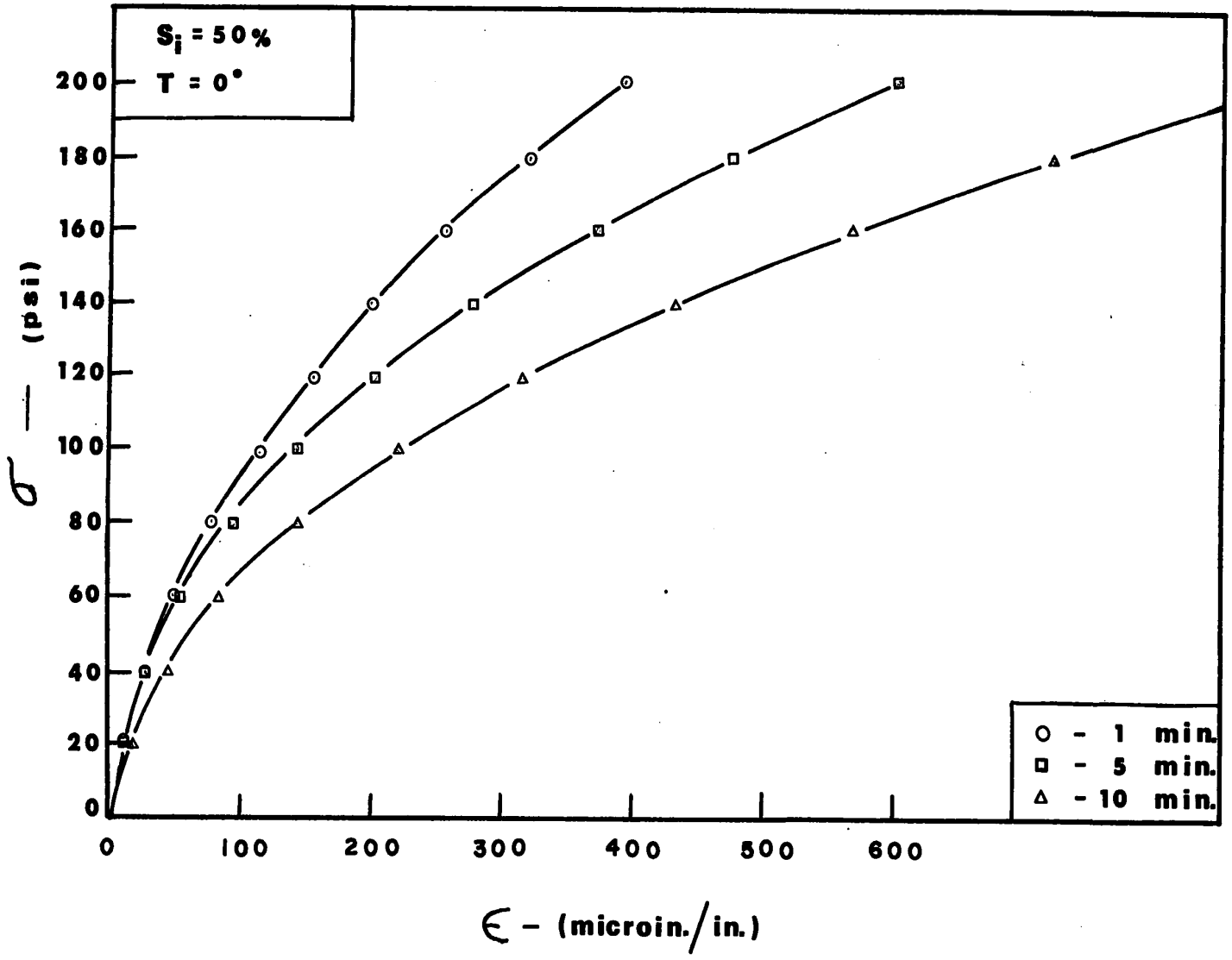
S_i = 50%
T = 0°
200
180
160
140
120
100
80
60
40
20
0
σ — (psi)
0
100
200
300
400
500
600
∈ – (microin./in.)
○ – 1 min.
□ – 5 min.
△ – 10 min.

FIG. 28

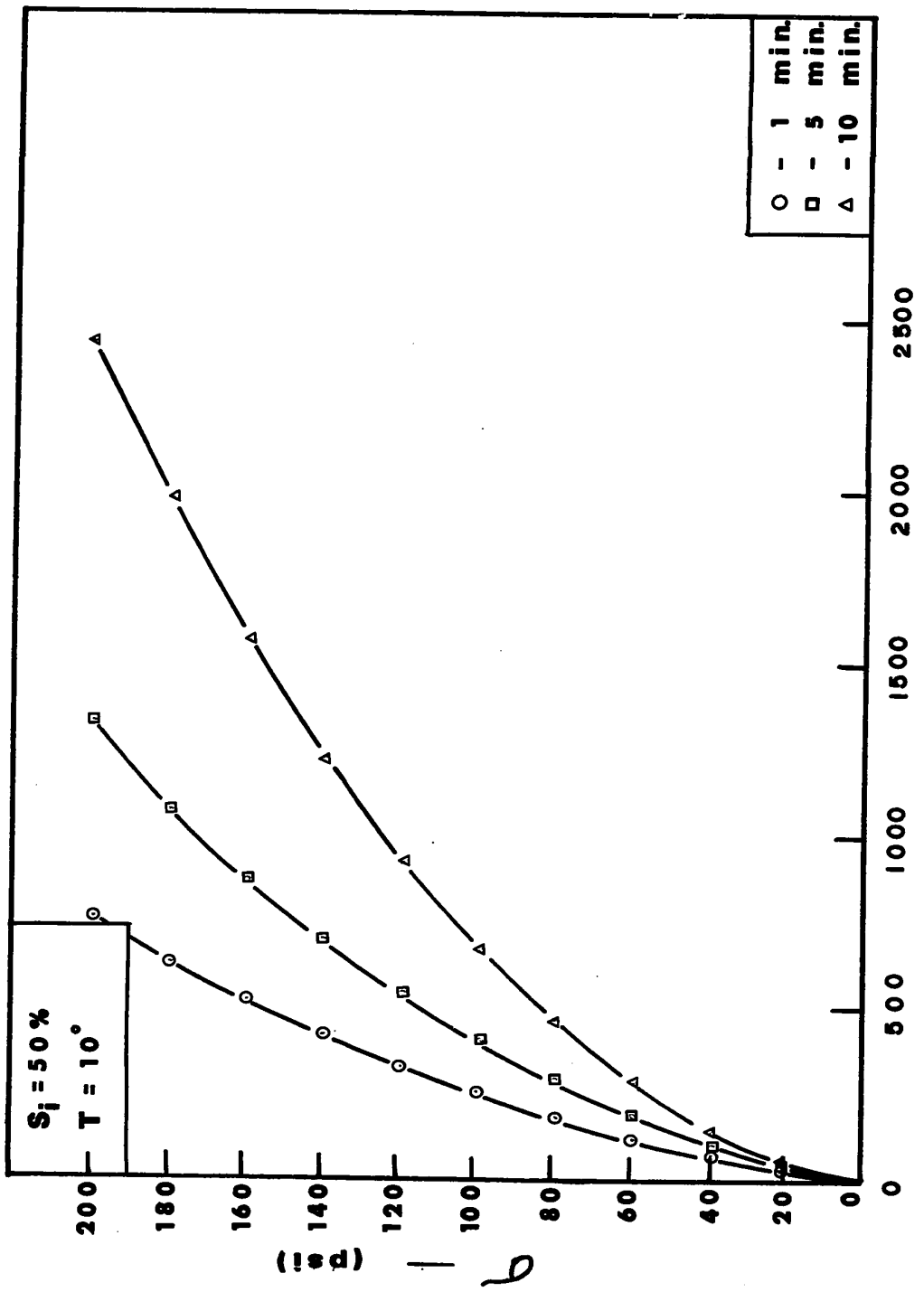
○ - 1 min.
□ - 5 min.
△ - 10 min.
S_i = 50 %
T = 10°
σ — (psi)
200
180
160
140
120
100
80
60
40
20
0
0
500
1000
1500
2000
2500
ϵ - (microin./in.)

FIG. 29

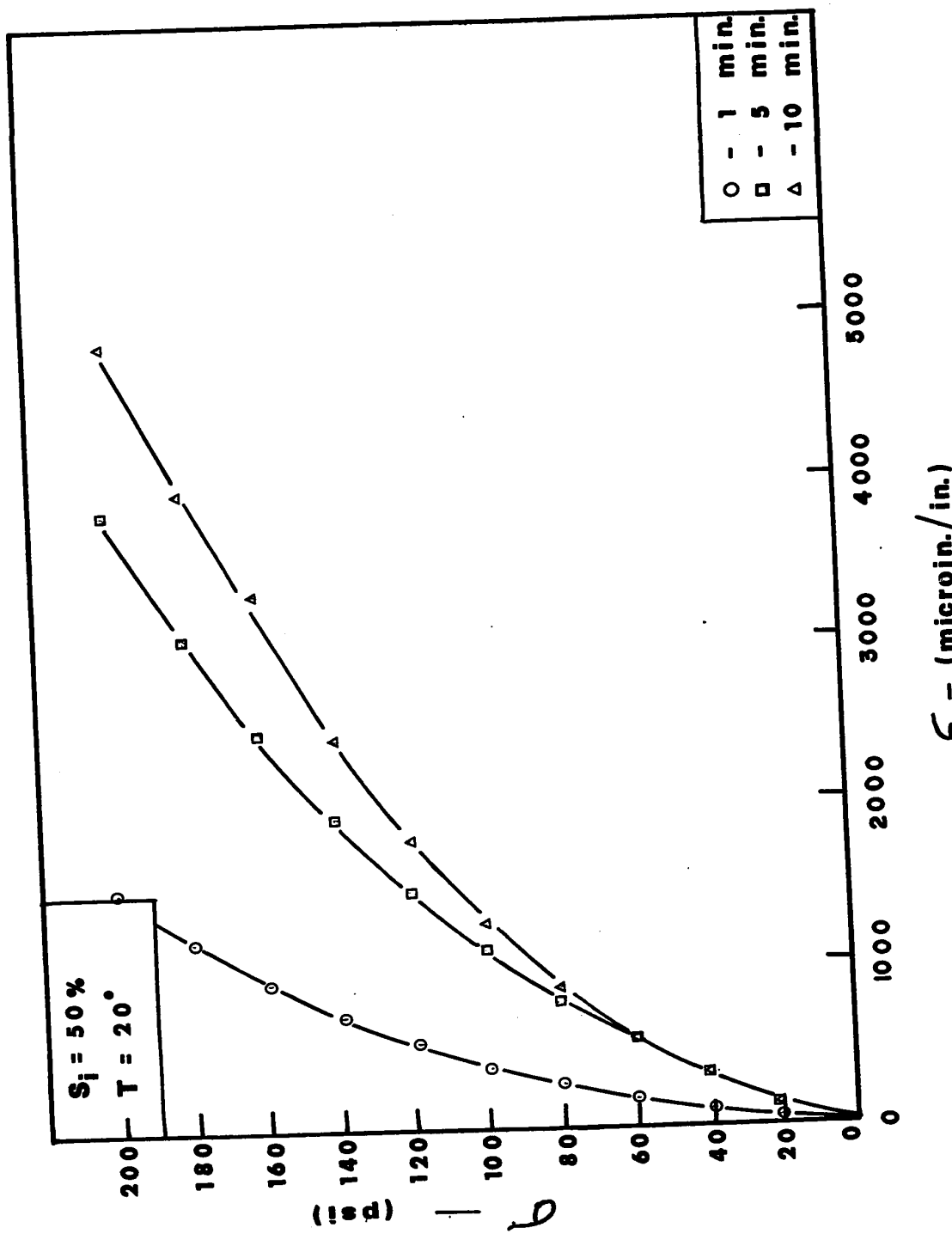
S_i = 50 %
T = 20°
○ - 1 min.
□ - 5 min.
△ - 10 min.
σ — (psi)
0
20
40
60
80
100
120
140
160
180
200
1000
2000
3000
4000
5000
ϵ - (microin./in.)

FIG. 30

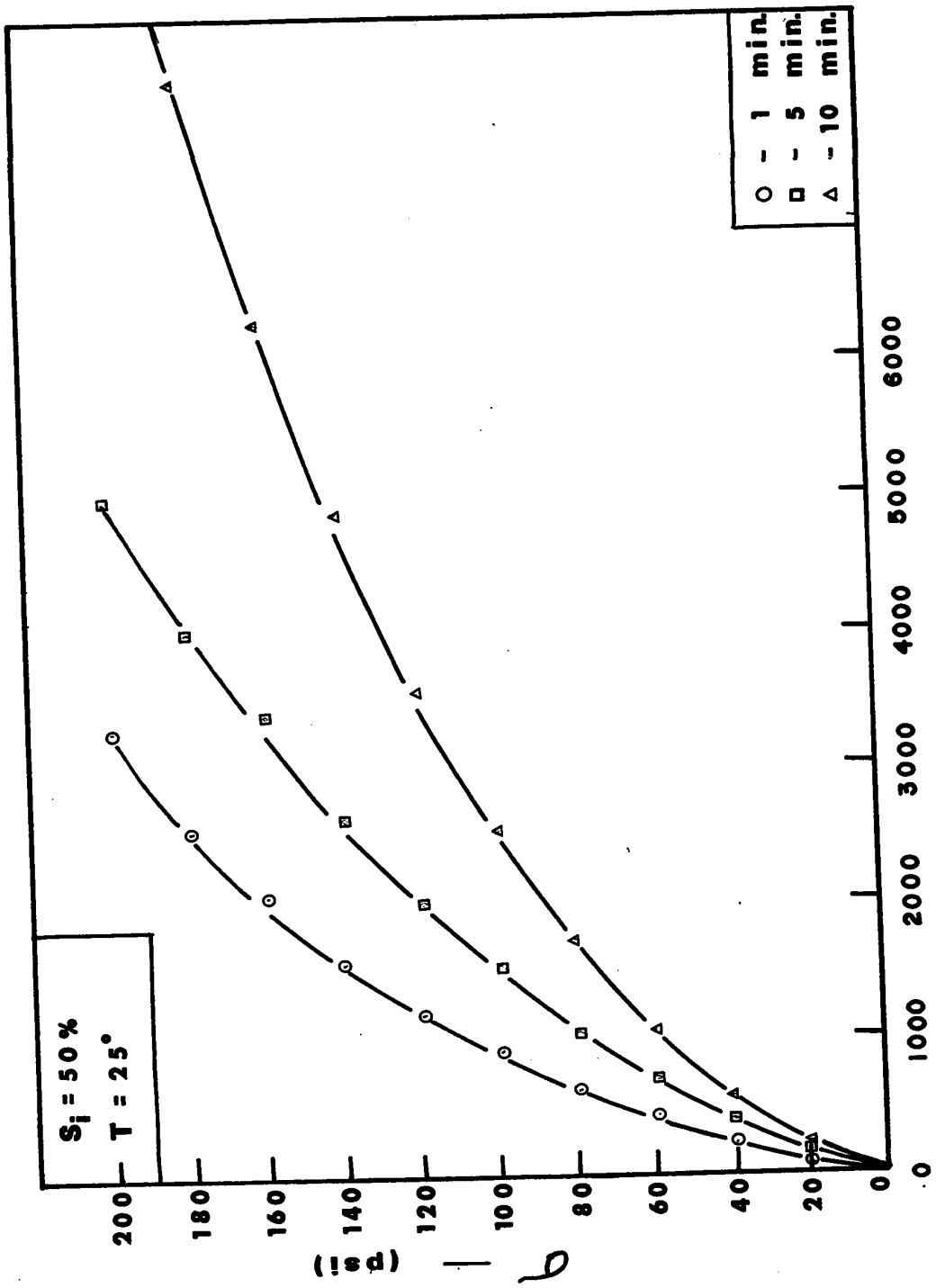
S_i = 50 %
T = 25°
1 min.
5 min.
10 min.
σ — (psi)
ε — (microin./in.)
0
20
40
60
80
100
120
140
160
180
200
1000
2000
3000
4000
5000
6000

FIG. 31

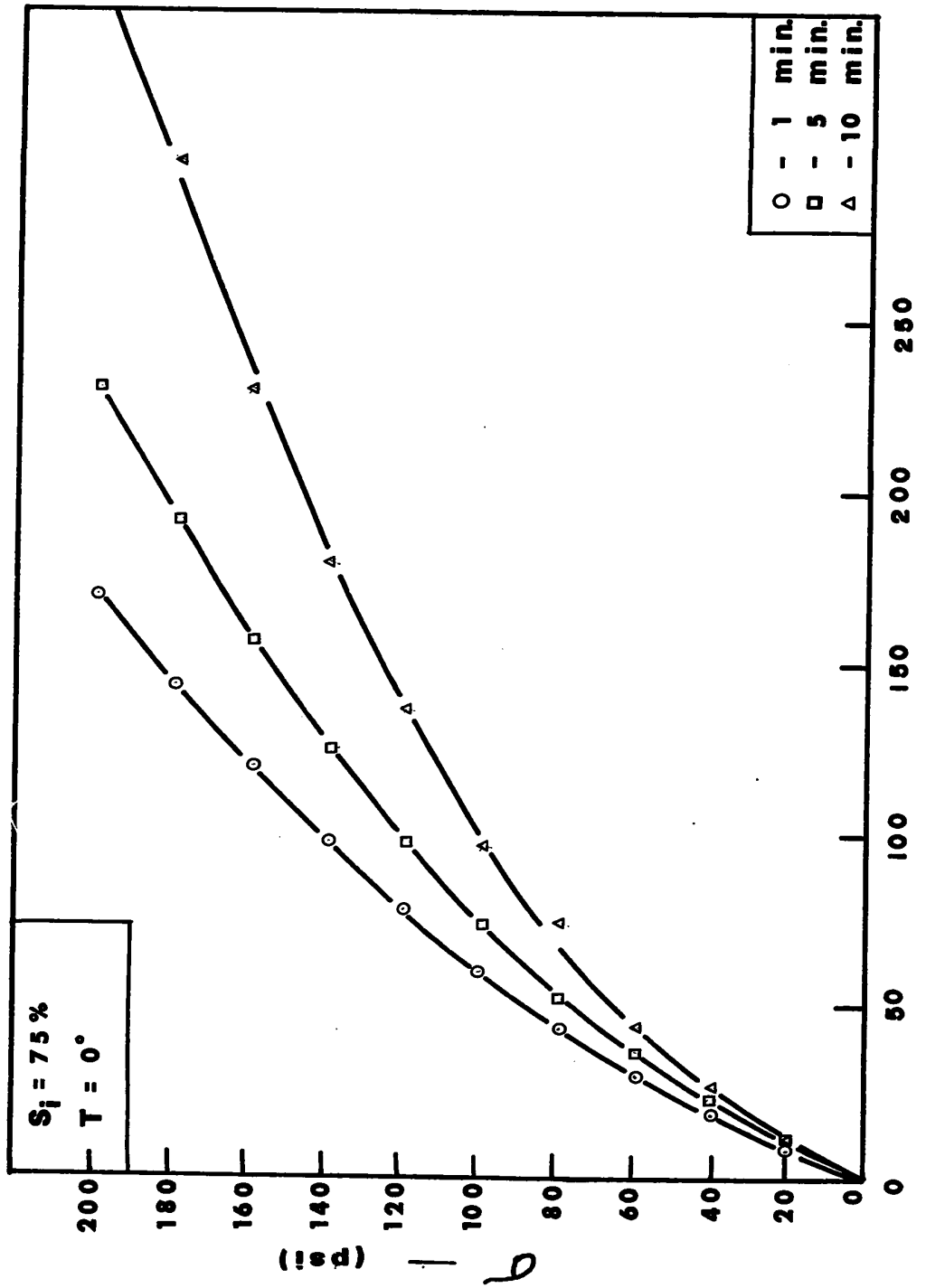
S_i = 75 %
T = 0°
○ - 1 min.
□ - 5 min.
△ - 10 min.
σ — (psi)
0
20
40
60
80
100
120
140
160
180
200
0
50
100
150
200
250
ϵ - (microin./in.)

FIG. 32

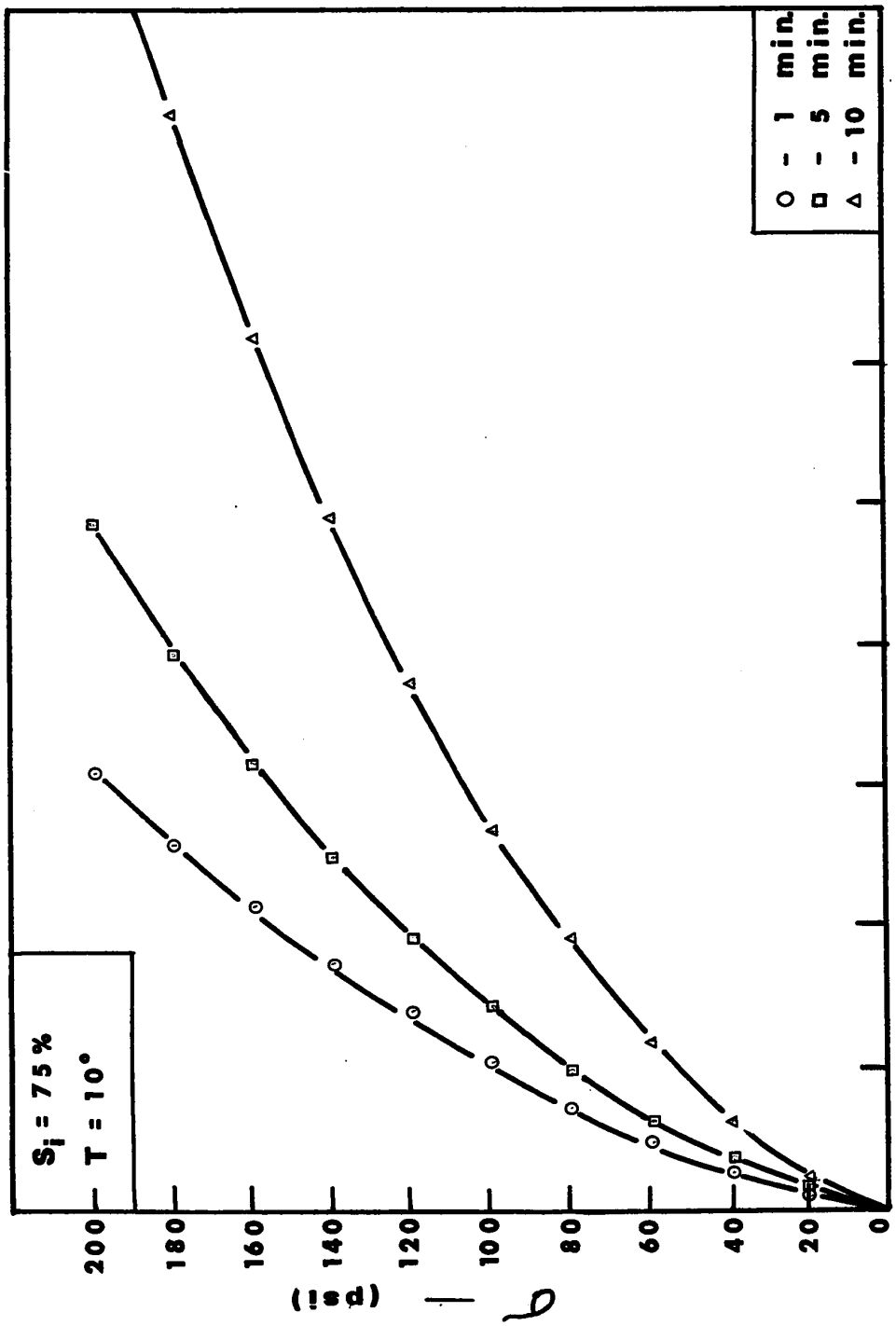
S_i = 75 %
T = 10°
○ - 1 min.
□ - 5 min.
△ - 10 min.
σ — (psi)
0
20
40
60
80
100
120
140
160
180
200
0
100
200
300
400
500
600
ϵ - (microin./in.)

FIG. 33

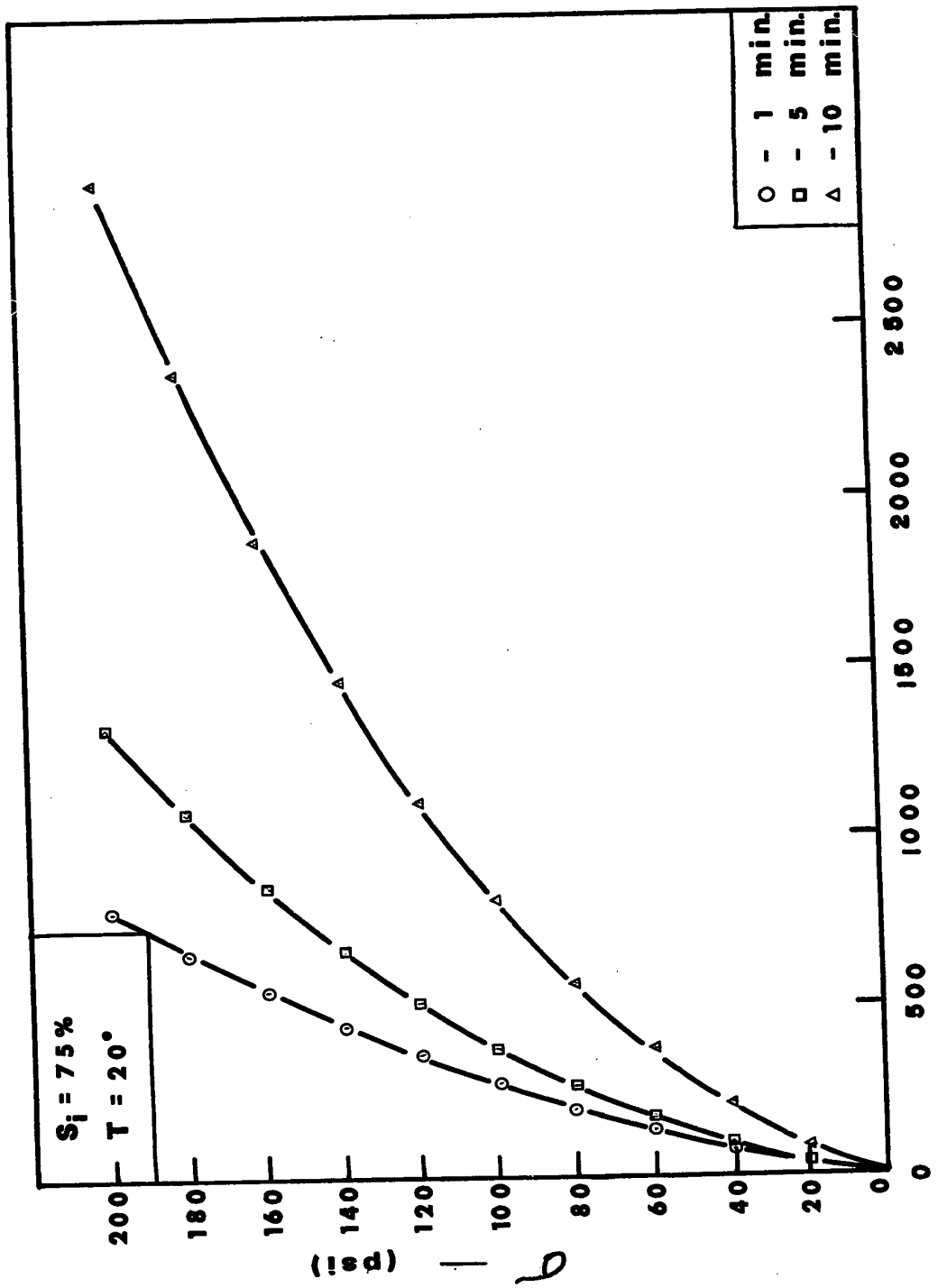
S_i = 75 %
T = 20°
○ - 1 min.
□ - 5 min.
△ - 10 min.
σ — (psi)
0
20
40
60
80
100
120
140
160
180
200
0
500
1000
1500
2000
2500
ϵ - (microin./in.)

FIG. 34

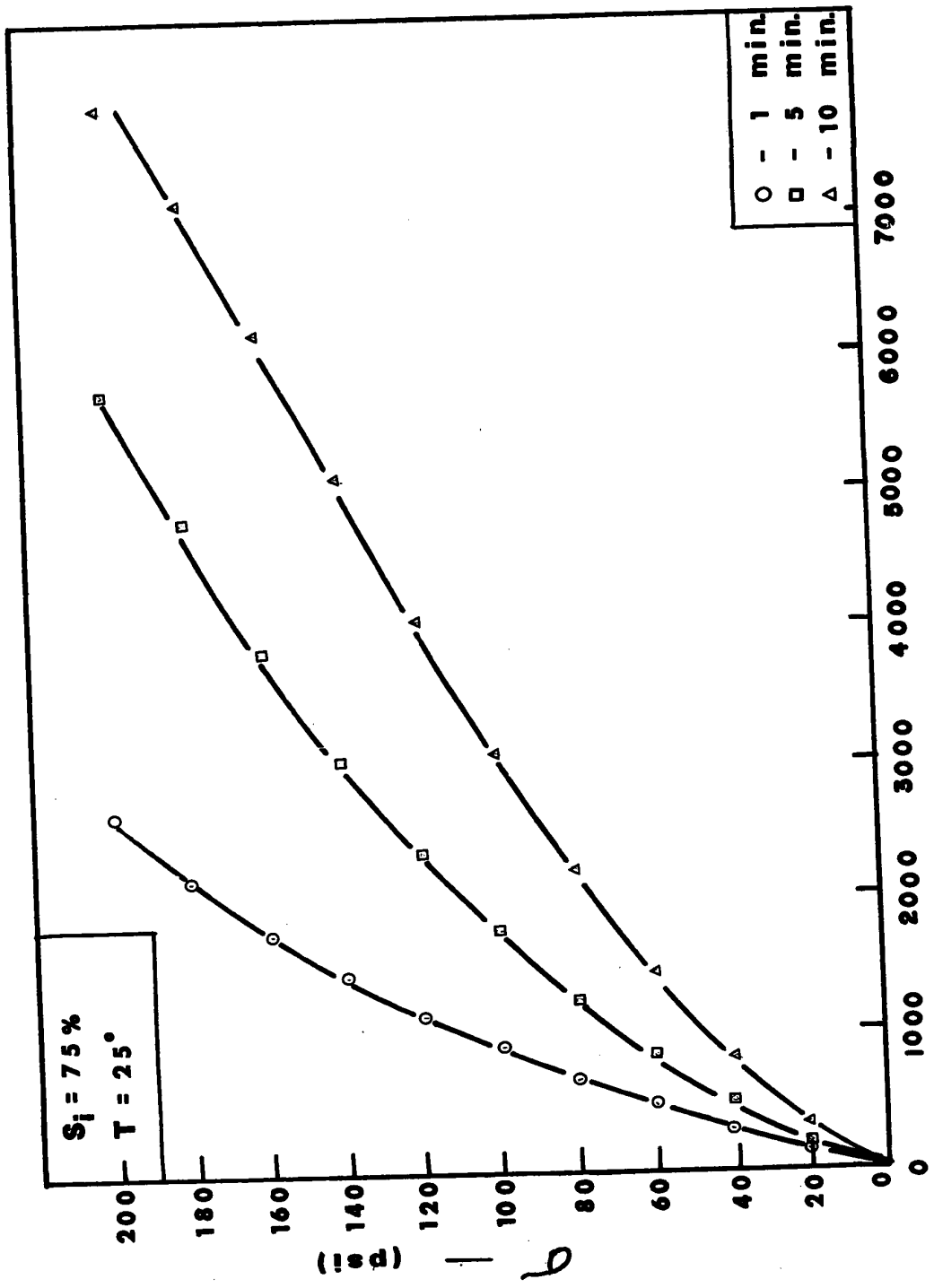
S_i = 75 %
T = 25°
○ - 1 min.
□ - 5 min.
△ - 10 min.
σ — (psi)
0
20
40
60
80
100
120
140
160
180
200
0
1000
2000
3000
4000
5000
6000
7000
ϵ - (microin./in.)

FIG. 35

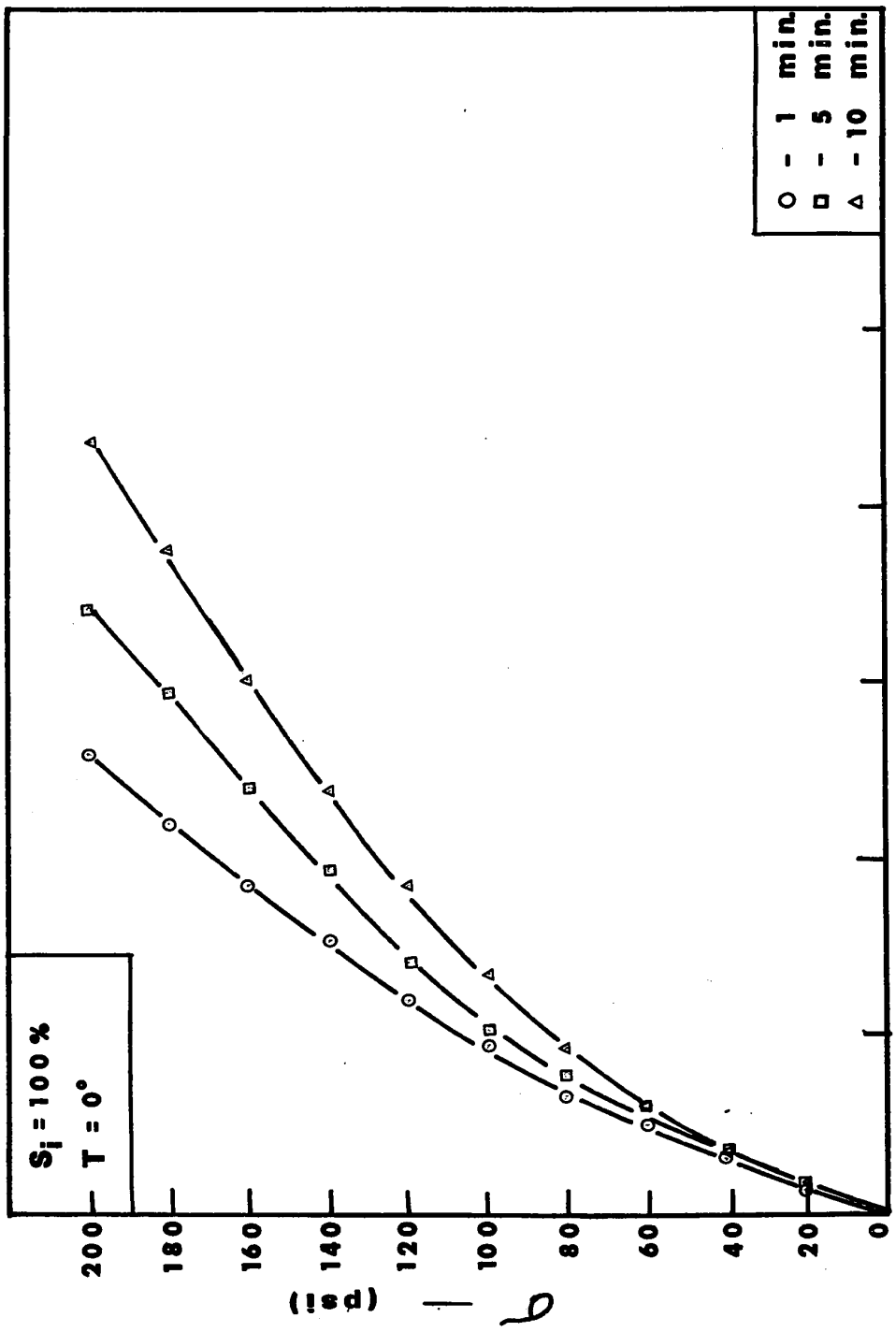
S_i = 100 %
T = 0°
○ - 1 min.
□ - 5 min.
△ - 10 min.
σ — (psi)
0
20
40
60
80
100
120
140
160
180
200
0
50
100
150
200
250
ϵ - (microin./in.)

FIG. 36

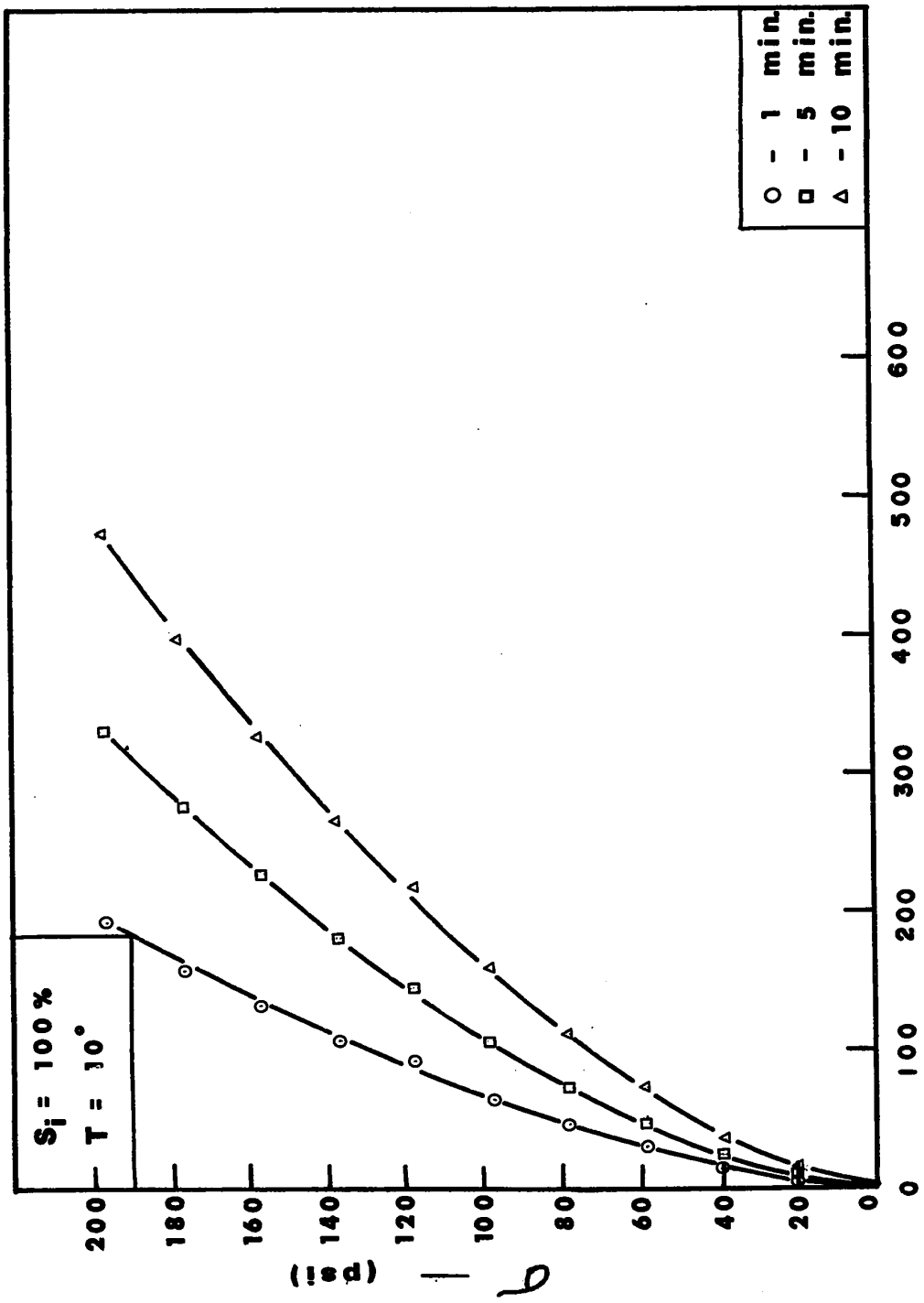
S_i = 100 %
T = 10°
○ - 1 min.
□ - 5 min.
△ - 10 min.
σ — (psi)
0
20
40
60
80
100
120
140
160
180
200
0
100
200
300
400
500
600
ϵ - (microin./in.)

FIG. 37

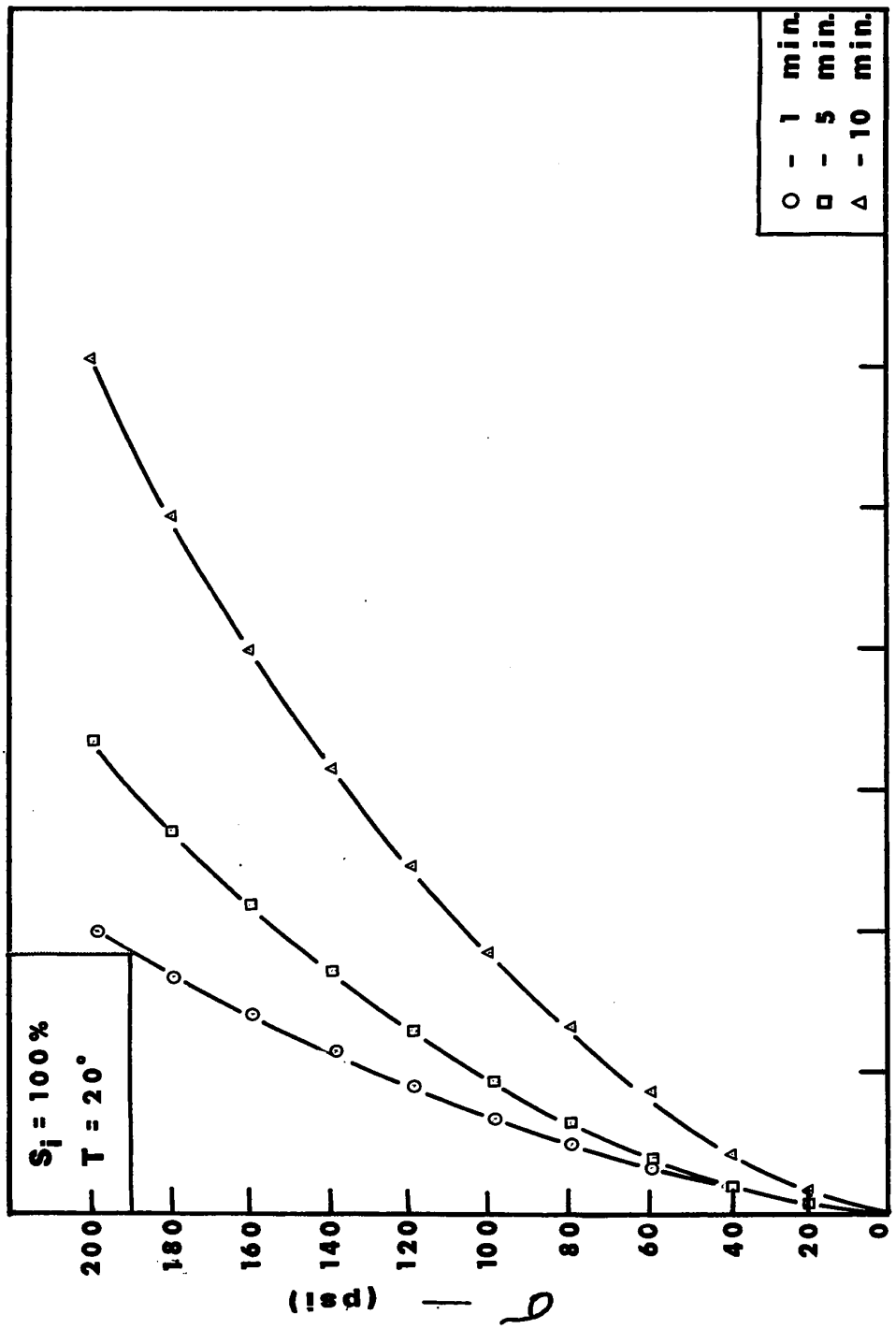
S_i = 100 %
T = 20°
○ - 1 min.
□ - 5 min.
△ - 10 min.
σ — (psi)
ϵ - (microin./in.)
0
20
40
60
80
100
120
140
160
180
200
200
400
600
800
1000
1200

FIG. 38

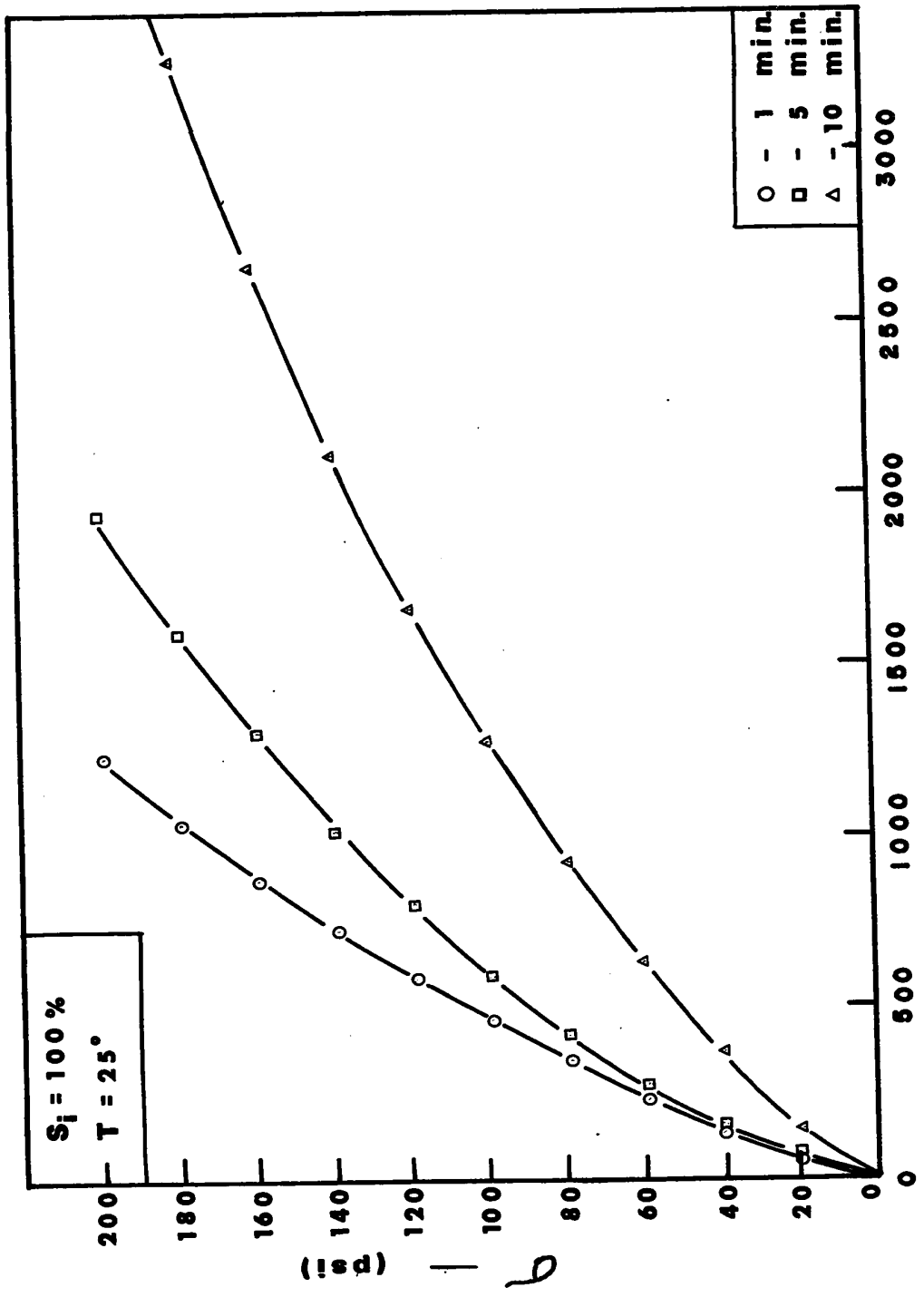
S_i = 100 %
T = 25°
○ - 1 min.
□ - 5 min.
△ - 10 min.
σ — (psi)
ε - (microin./in.)
0
20
40
60
80
100
120
140
160
180
200
500
1000
1500
2000
2500
3000

FIG. 39

FIG 40

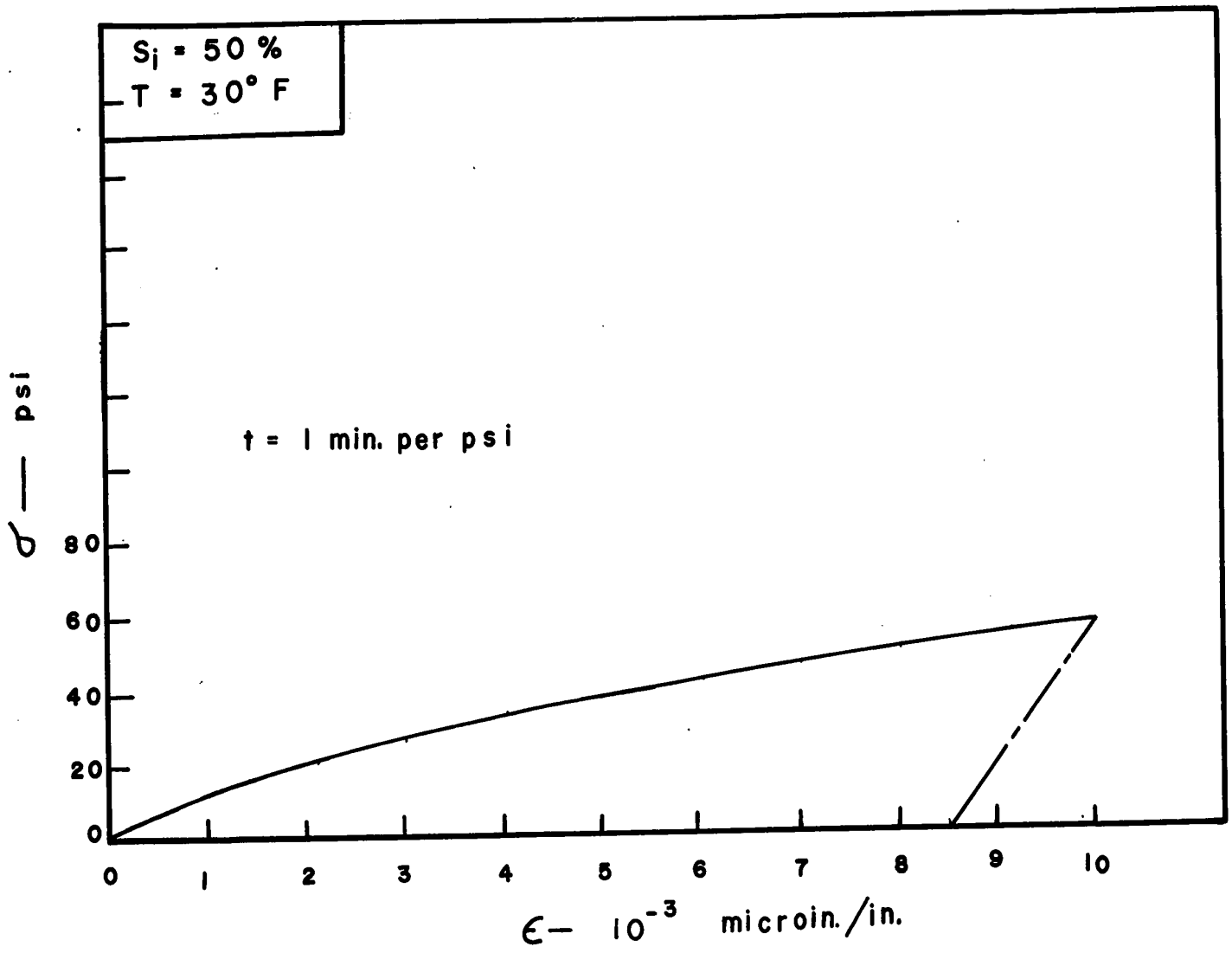

FIG. 40.- Special Case at 30°F

APPENDIX C

TABLES OF 'A' AND 'm' FOR VARIOUS t

$\frac{A}{m}$ $t = 1$ min.

S_i / T	25 %	50 %	75 %	100 %
0°	3.631 / 0.531	7.278 / 0.552	5.598 / 0.699	7.482 / 0.674
10°	2.280 / 0.530	6.761 / 0.638	3.758 / 0.696	7.709 / 0.625
20°	1.028 / 0.572	3.532 / 0.560	2.028 / 0.693	3.251 / 0.680
25°	2.270 / 0.350	1.439 / 0.616	0.510 / 0.768	1.016 / 0.745

TABLE I

$\frac{A}{m}$

t = 5 min.

T \ S_i	25 %	50 %	75 %	100%
0°	3.908 / 0.480	6.383 / 0.548	5.333 / 0.673	8.356 / 0.625
10°	1.914 / 0.507	1.977 / 0.650	3.573 / 0.665	6.310 / 0.598
20°	0.969 / 0.540	1.279 / 0.621	1.932 / 0.660	4.634 / 0.580
25°	0.380 / 0.572	0.953 / 0.631	0.447 / 0.715	1.503 / 0.650

TABLE II

$\frac{A}{m}$

t = 10 min.

T \ S_i	25 %	50 %	75 %	100 %
0°	2.455 / 0.494	5.309 / 0.534	5.176 / 0.635	7.656 / 0.605
10°	1.581 / 0.500	2.606 / 0.560	3.365 / 0.594	4.315 / 0.620
20°	0.537 / 0.575	1.262 / 0.605	1.256 / 0.645	2.198 / 0.637
25°	0.616 / 0.471	0.825 / 0.606	0.438 / 0.660	0.646 / 0.700

TABLE III

APPENDIX D

TOTAL, ELASTIC, AND PLASTIC STRAINS VS. STRESS

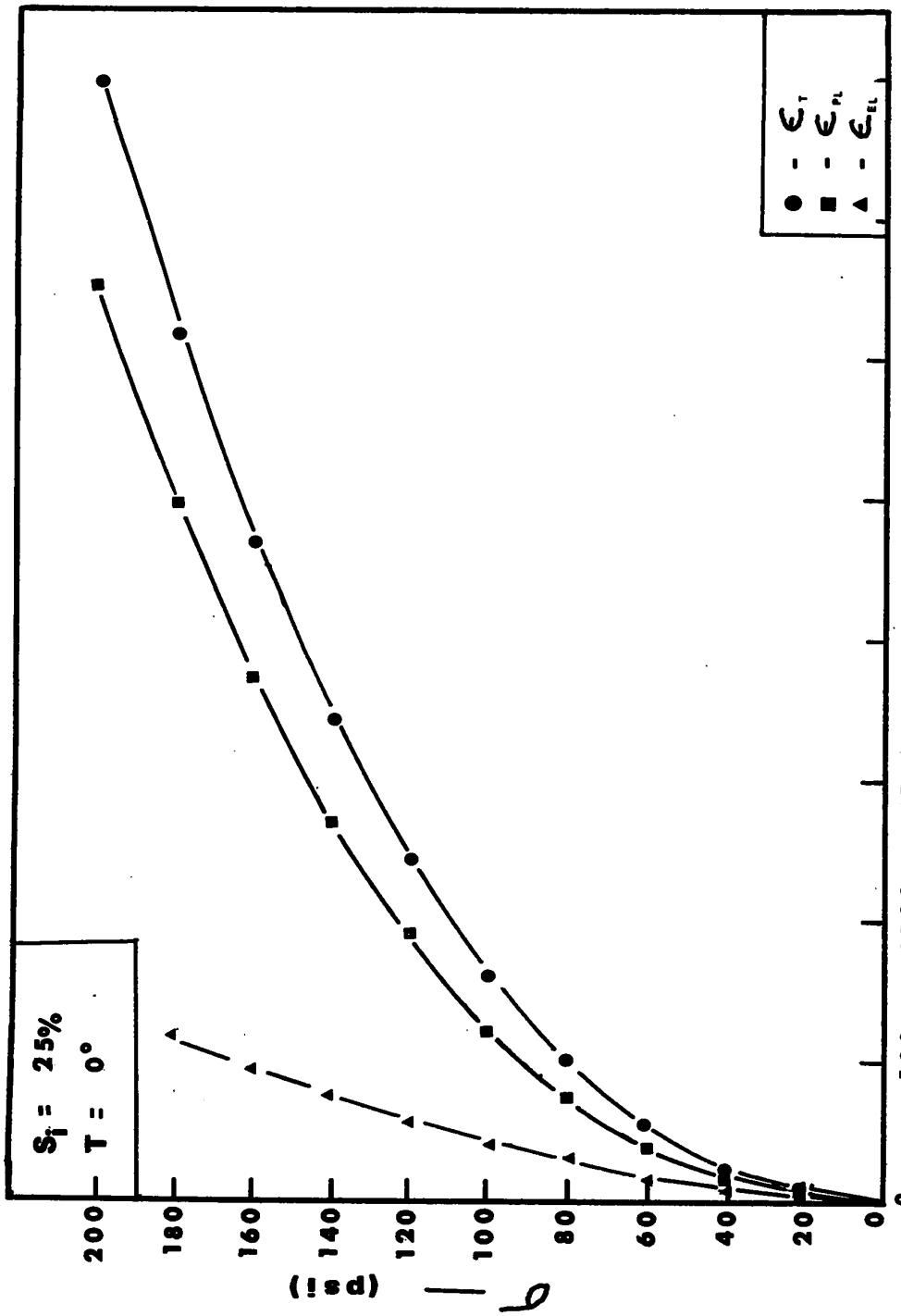
S_f = 25%
T = 0°
● - ϵ_T
■ - ϵ_{PL}
▲ - ϵ_{EL}
σ — (psi)
0
20
40
60
80
100
120
140
160
180
200
0
500
1000
1500
2000
2500
3000
ϵ — (microin./in.)

FIG. 41

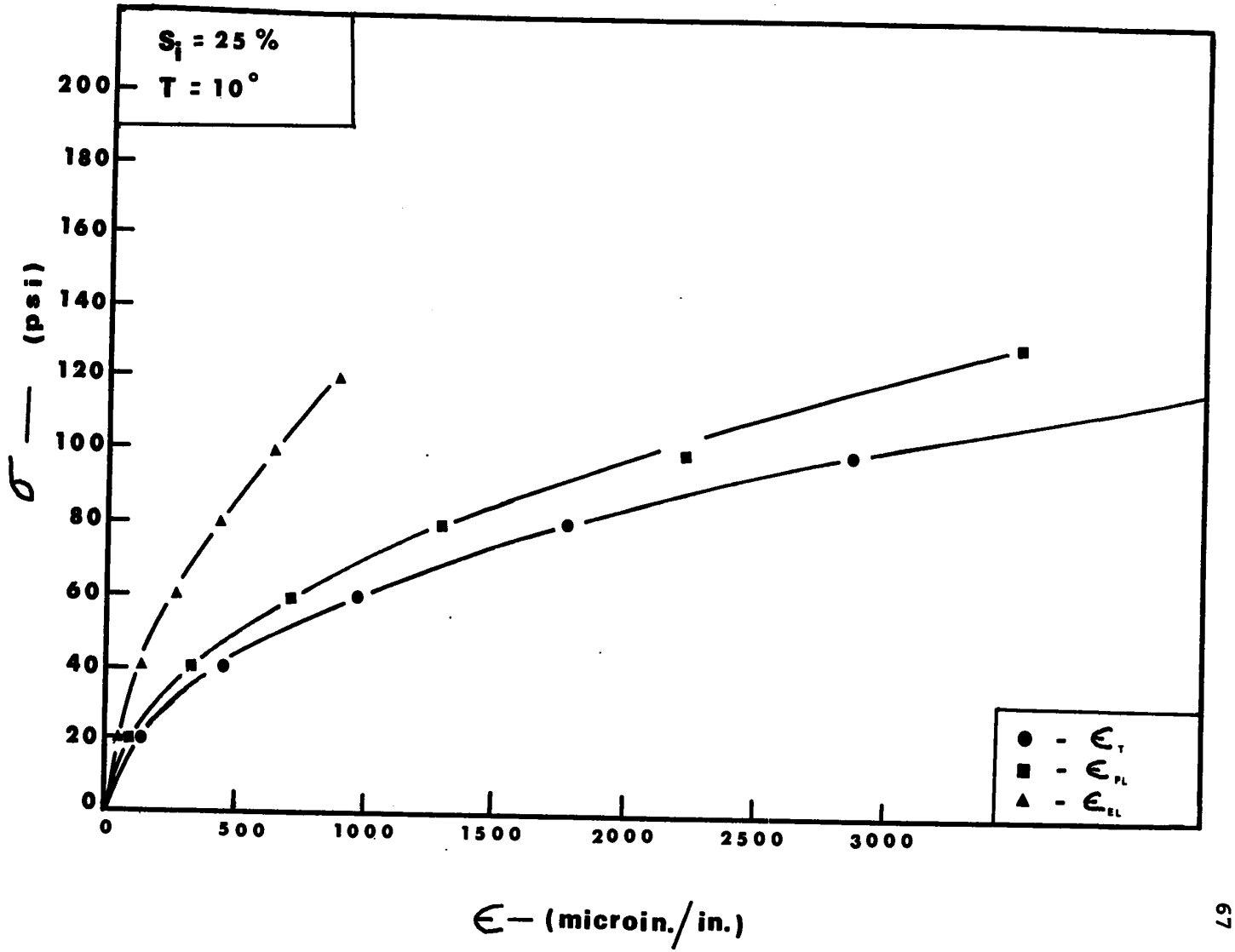
S_i = 25 %
T = 10°
200
180
160
140
120
100
80
60
40
20
0
σ — (psi)
0
500
1000
1500
2000
2500
3000
● - ϵ_T
■ - ϵ_{PL}
▲ - ϵ_{EL}
ϵ — (microin./in.)

FIG. 42

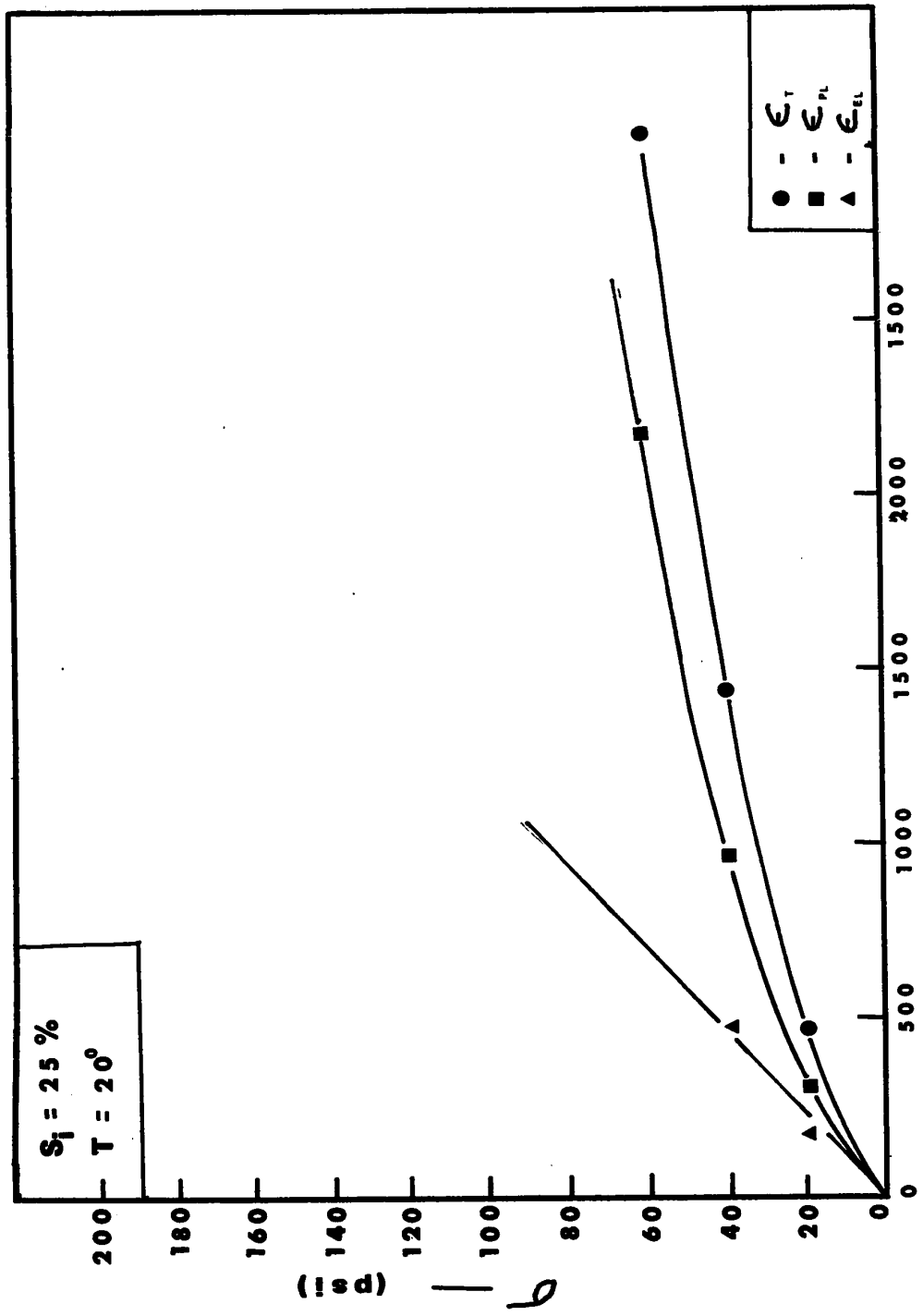
S_i = 25 %
T = 20°
σ — (psi)
200
180
160
140
120
100
80
60
40
20
0
0
500
1000
1500
2000
1500
ϵ — (microin./in.)
- ϵ_T
- ϵ_{PL}
- ϵ_{EL}

FIG. 43

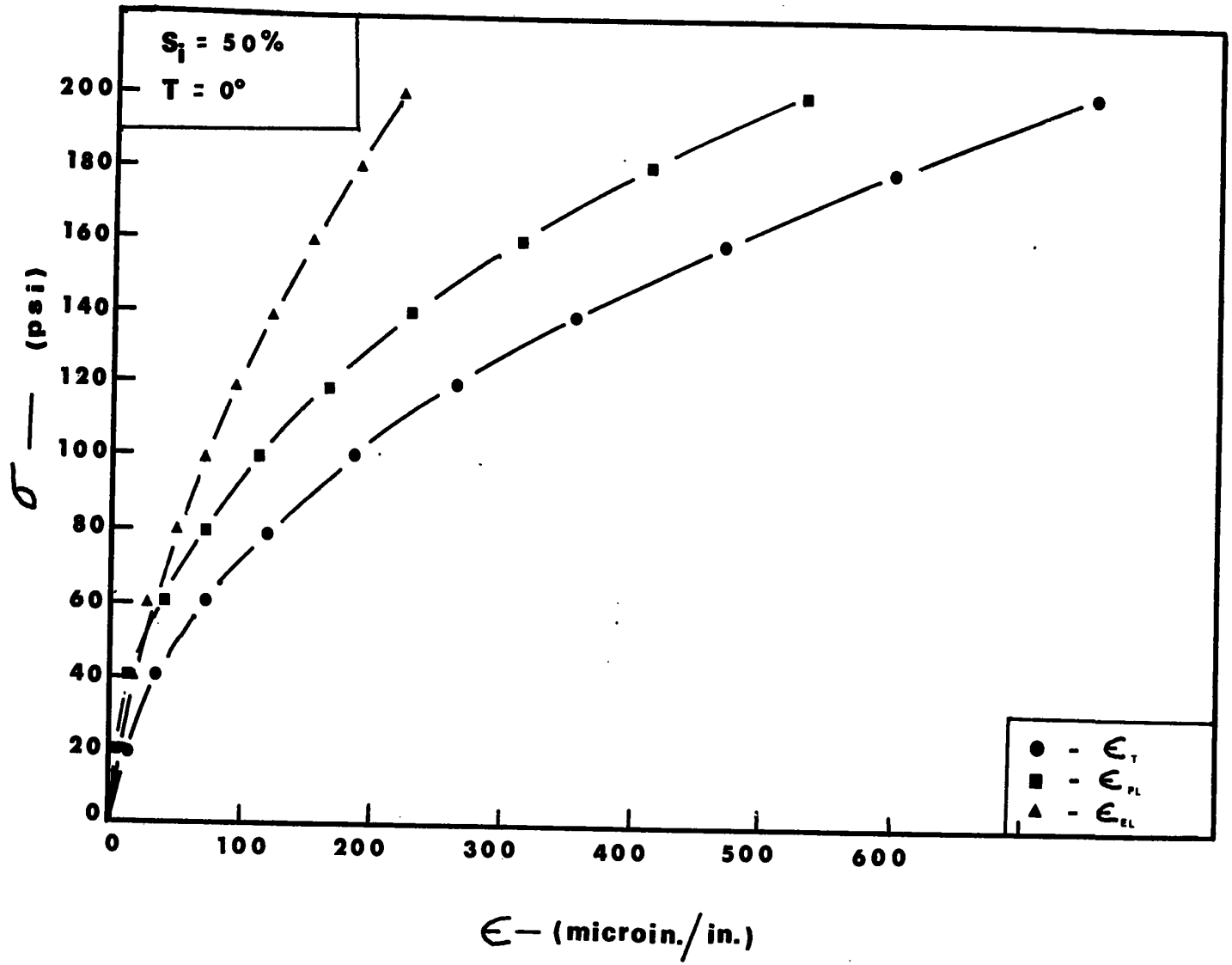
S_i = 50%
T = 0°
200
180
160
140
120
100
80
60
40
20
0
σ — (psi)
0
100
200
300
400
500
600
∈— (microin./in.)
● - ϵ_T
■ - ϵ_{PL}
▲ - ϵ_{EL}

FIG. 44

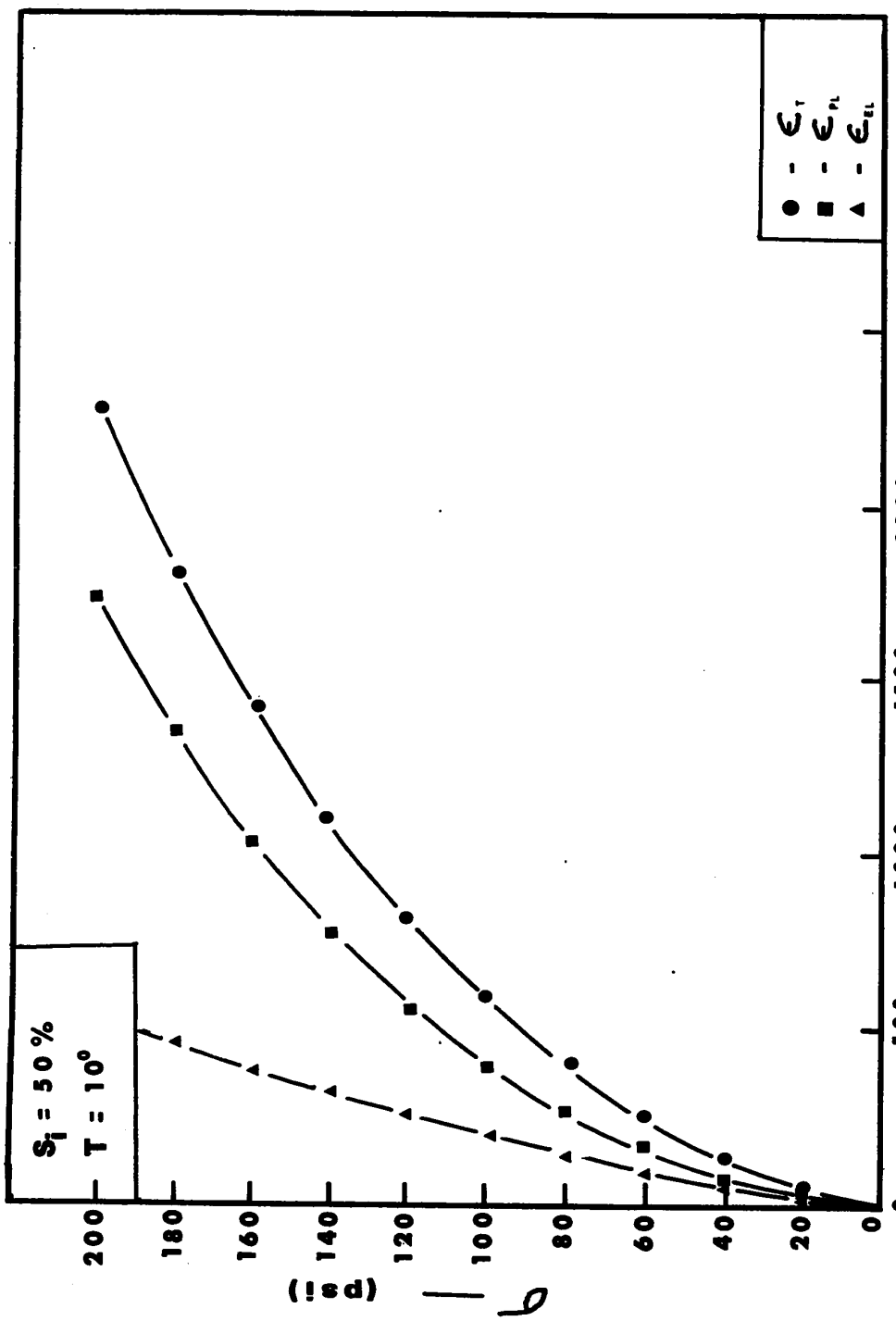
S_i = 50 %
T = 10°
● - ϵ_T
■ - ϵ_{PL}
▲ - ϵ_{EL}
σ — (psi)
0
20
40
60
80
100
120
140
160
180
200
0
500
1000
1500
2000
2500
ϵ — (microin./in.)

FIG. 45

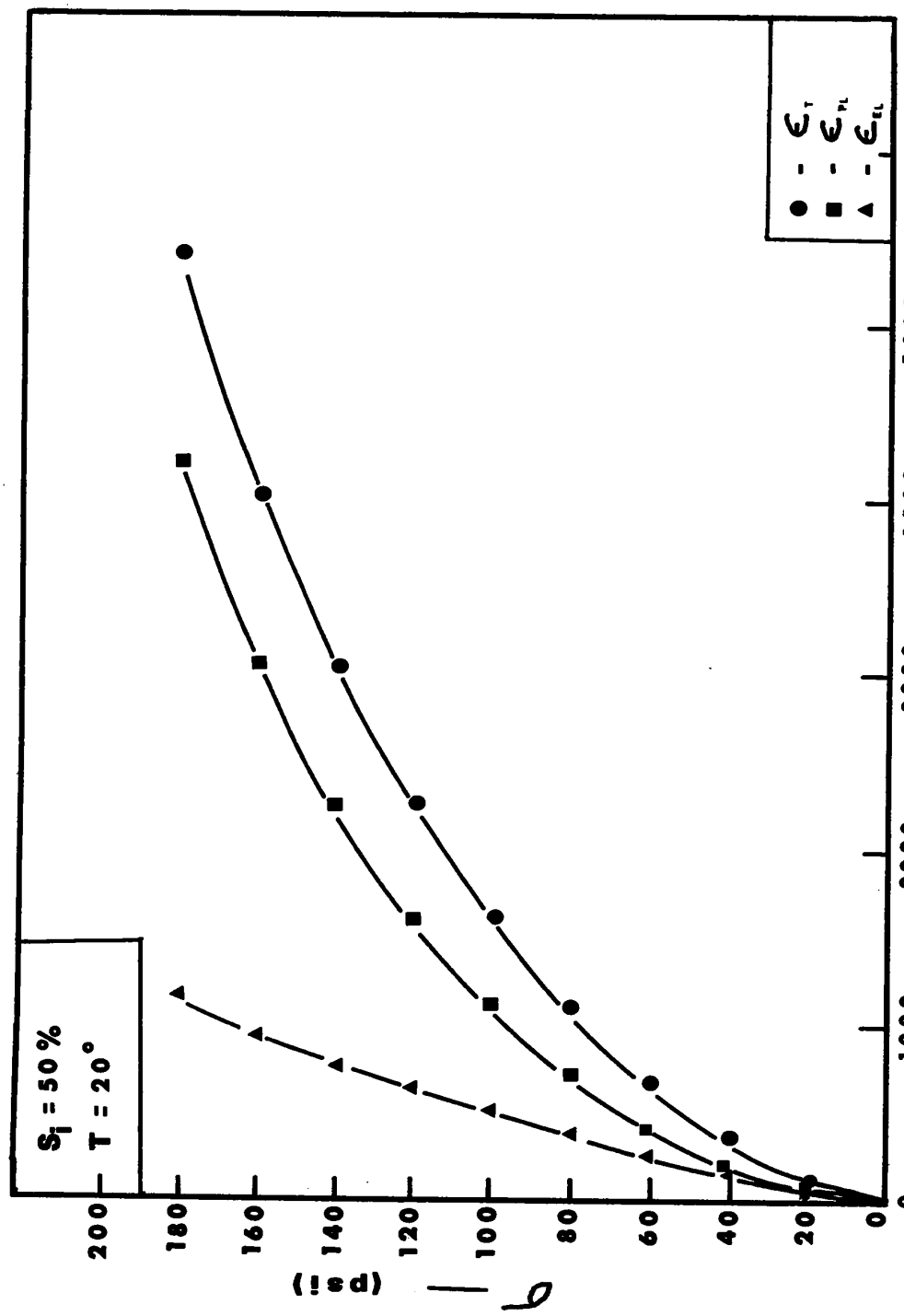
S_i = 50 %
T = 20°
ϵ_T
ϵ_{TL}
ϵ_{tL}
σ — (psi)
0
20
40
60
80
100
120
140
160
180
200
1000
2000
3000
4000
5000
ϵ — (microin./in.)

FIG. 46

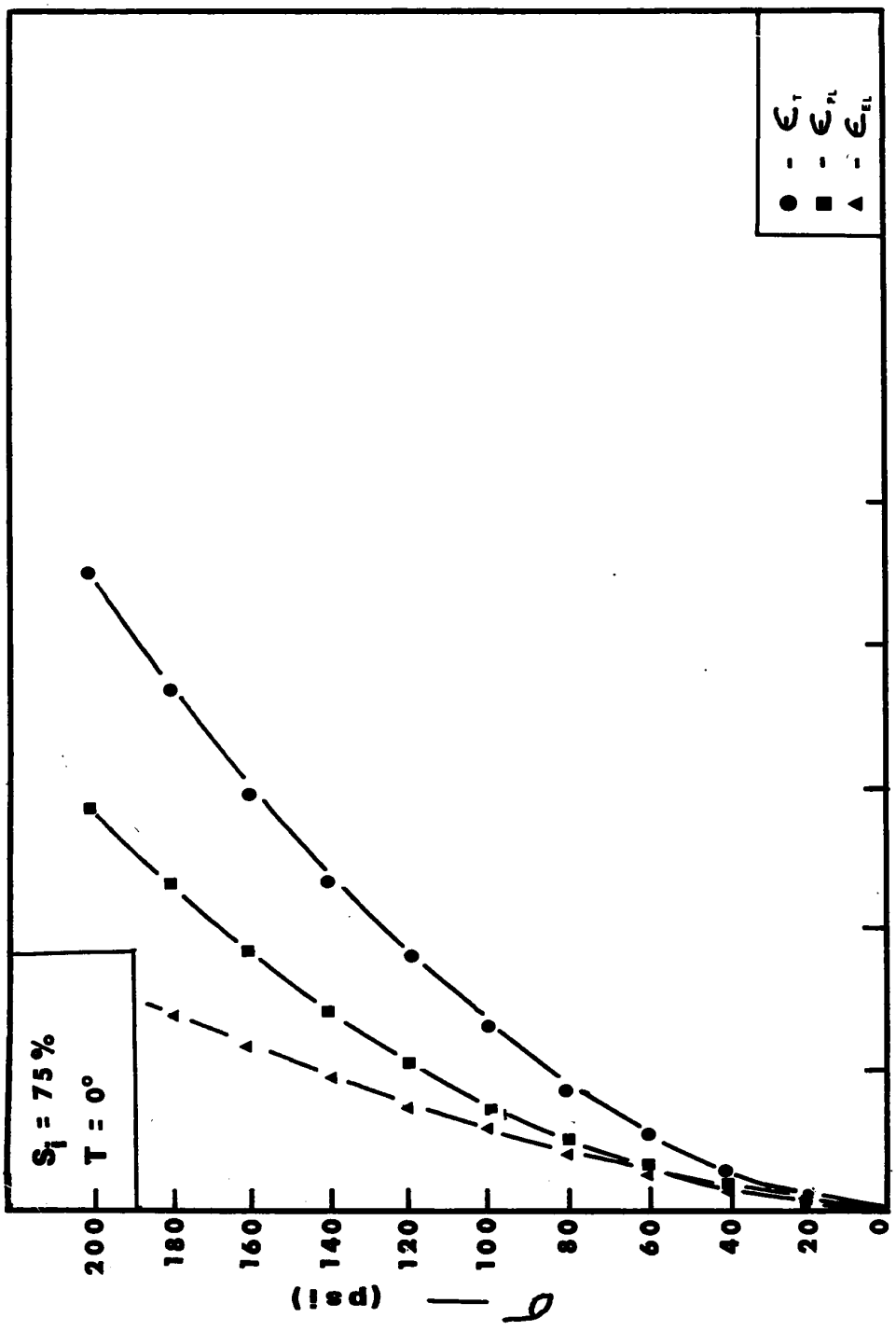
S_i = 75 %
T = 0°
ϵ_T
ϵ_{PL}
ϵ_{EL}
σ — (psi)
200
180
160
140
120
100
80
60
40
20
0
0
100
200
300
400
500
ϵ — (microin./in.)

FIG.47

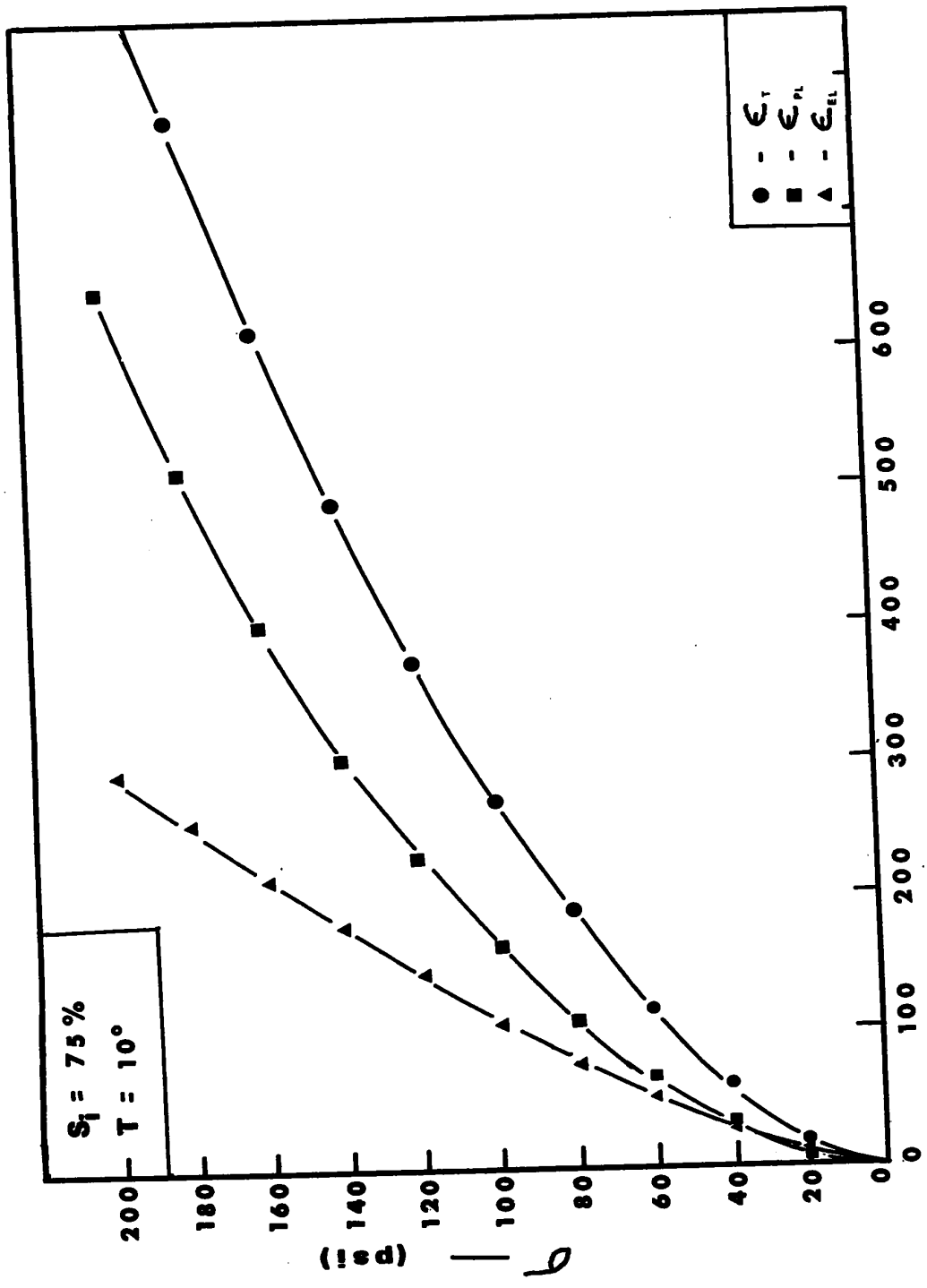
S_i = 75 %
T = 10°
● - ϵ_T
■ - ϵ_{PL}
▲ - ϵ_{EL}
σ — (psi)
200
180
160
140
120
100
80
60
40
20
0
0
100
200
300
400
500
600
ϵ — (microin./in.)

FIG. 48

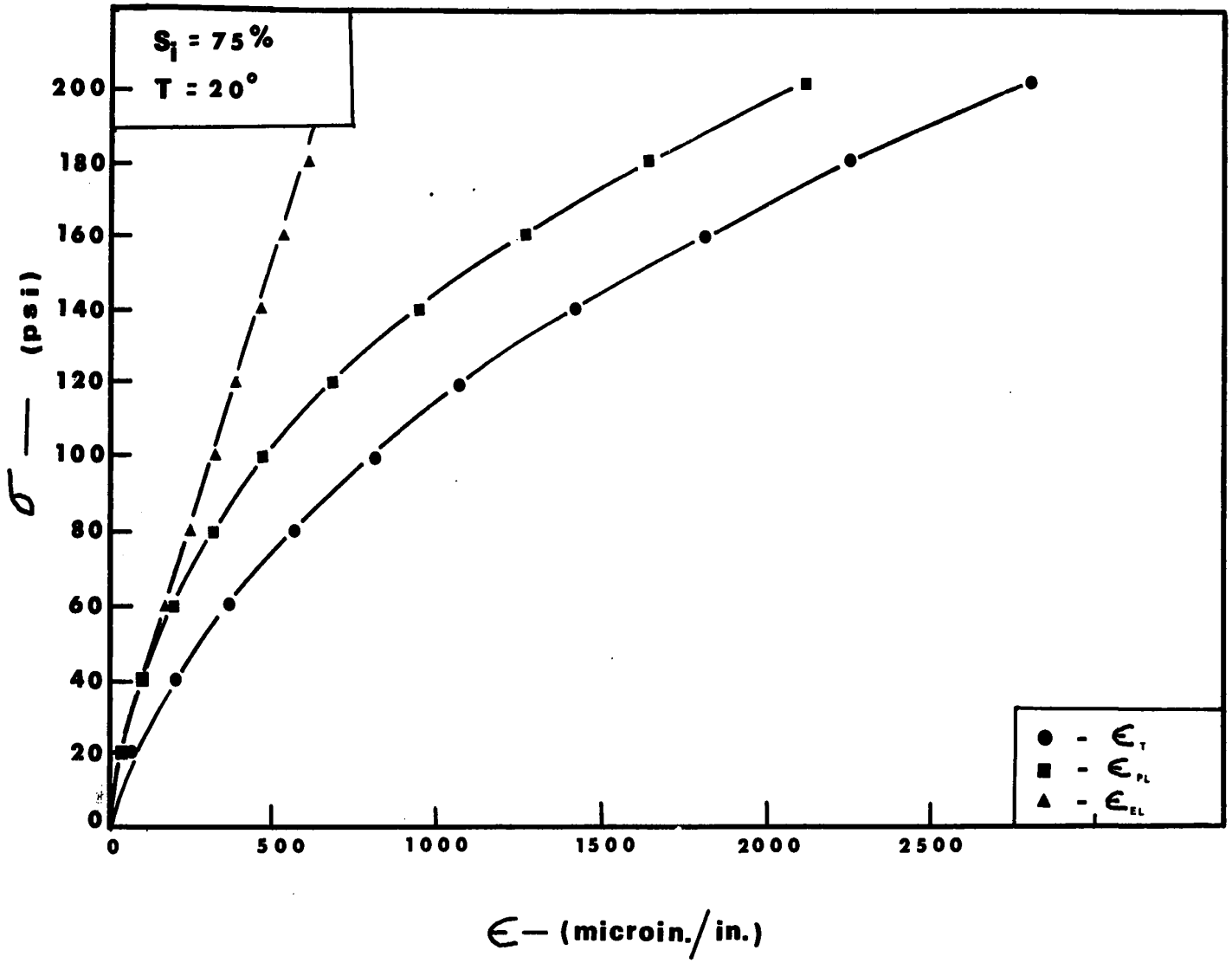
S_1 = 75%
T = 20°
σ — (psi)
200
180
160
140
120
100
80
60
40
20
0
0
500
1000
1500
2000
2500
● - ϵ_T
■ - ϵ_{PL}
▲ - ϵ_{EL}
ϵ— (microin./in.)

FIG. 49

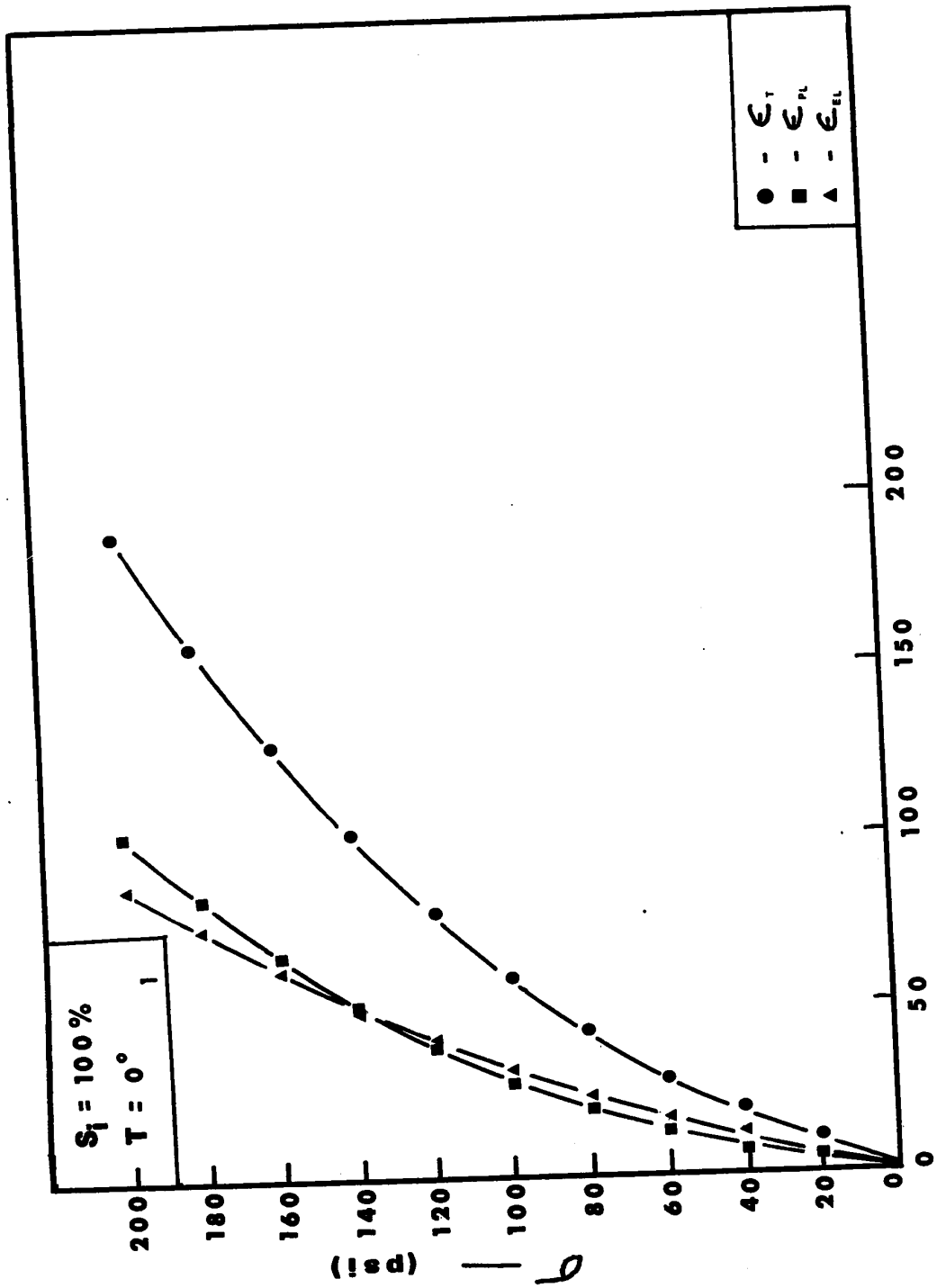
S_l = 100%
T = 0°
ϵ_T
ϵ_{PL}
ϵ_{EL}
σ — (psi)
200
180
160
140
120
100
80
60
40
20
0
50
100
150
200
ϵ — (microin./in.)

FIG. 50

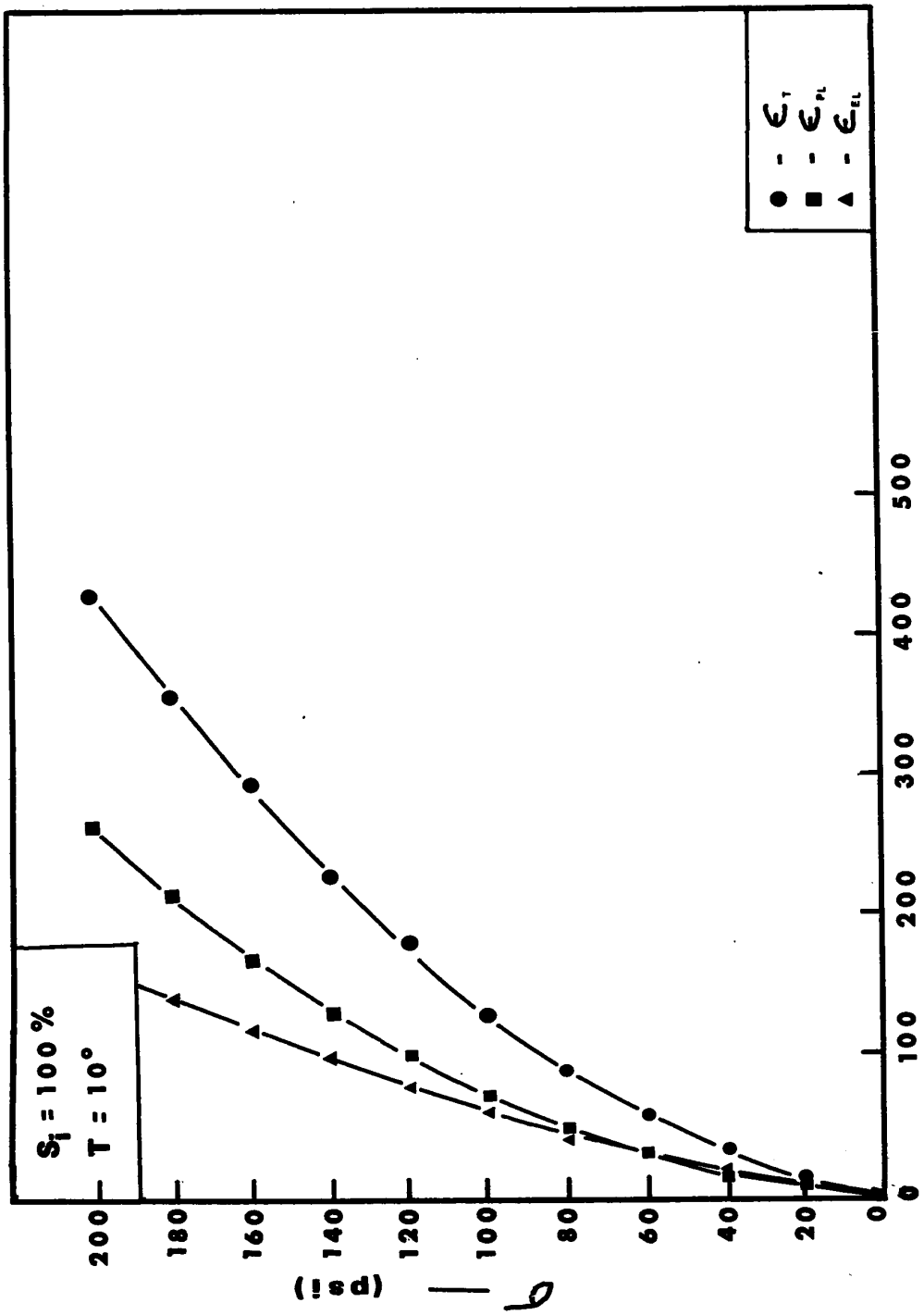
S_j = 100 %
T = 10°
ϵ_T
ϵ_{PL}
ϵ_{EL}
σ — (psi)
0
20
40
60
80
100
120
140
160
180
200
0
100
200
300
400
500
ϵ — (microin./in.)

FIG. 51

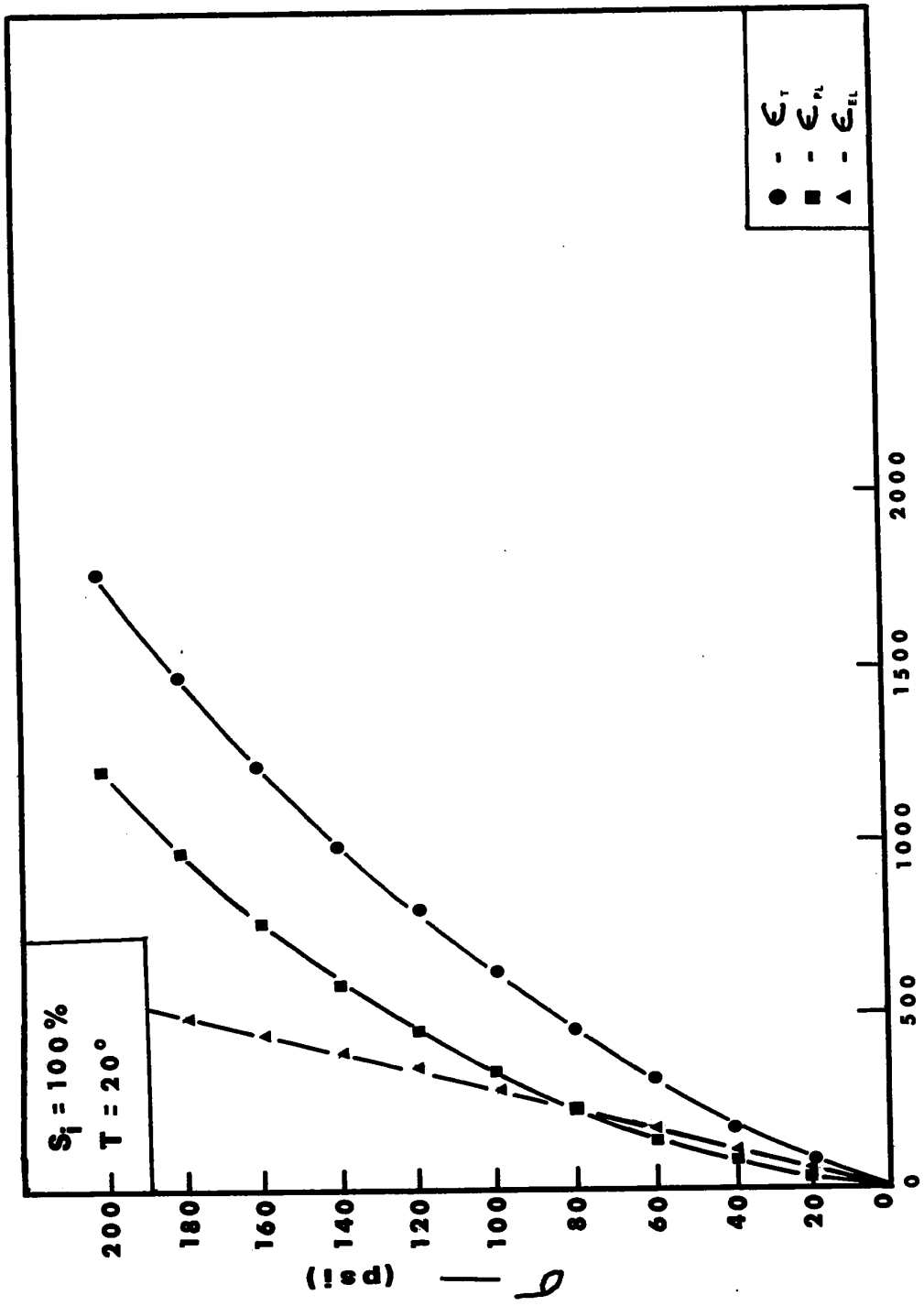
S_i = 100 %
T = 20°
ϵ_T
ϵ_{PL}
ϵ_{EL}
σ — (psi)
200
180
160
140
120
100
80
60
40
20
0
0
500
1000
1500
2000
ϵ — (microin./in.)

FIG. 52

APPENDIX E

$\frac{A}{m}$

T \ Si	25 %	50%	75 %	100 %
0°	3.221 / 0.466	4.131 / 0.537	8.260 / 0.537	9.773 / 0.570
10°	2.138 / 0.502	3.899 / 0.537	6.471 / 0.535	8.715 / 0.567
20°	1.169 / 0.512	2.742 / 0.508	3.597 / 0.535	3.954 / 0.550
Avg. m =	0.500	0.527	0.536	0.562

TABLE IV

$$A = nS_i + C$$

T	n	C
0°	0.108	-0.50
10°	0.090	-0.25
20°	0.040	+0.40

TABLE V

APPENDIX F

COMPARISON OF EXPERIMENTAL DATA TO THE EMPIRICAL EQUATION

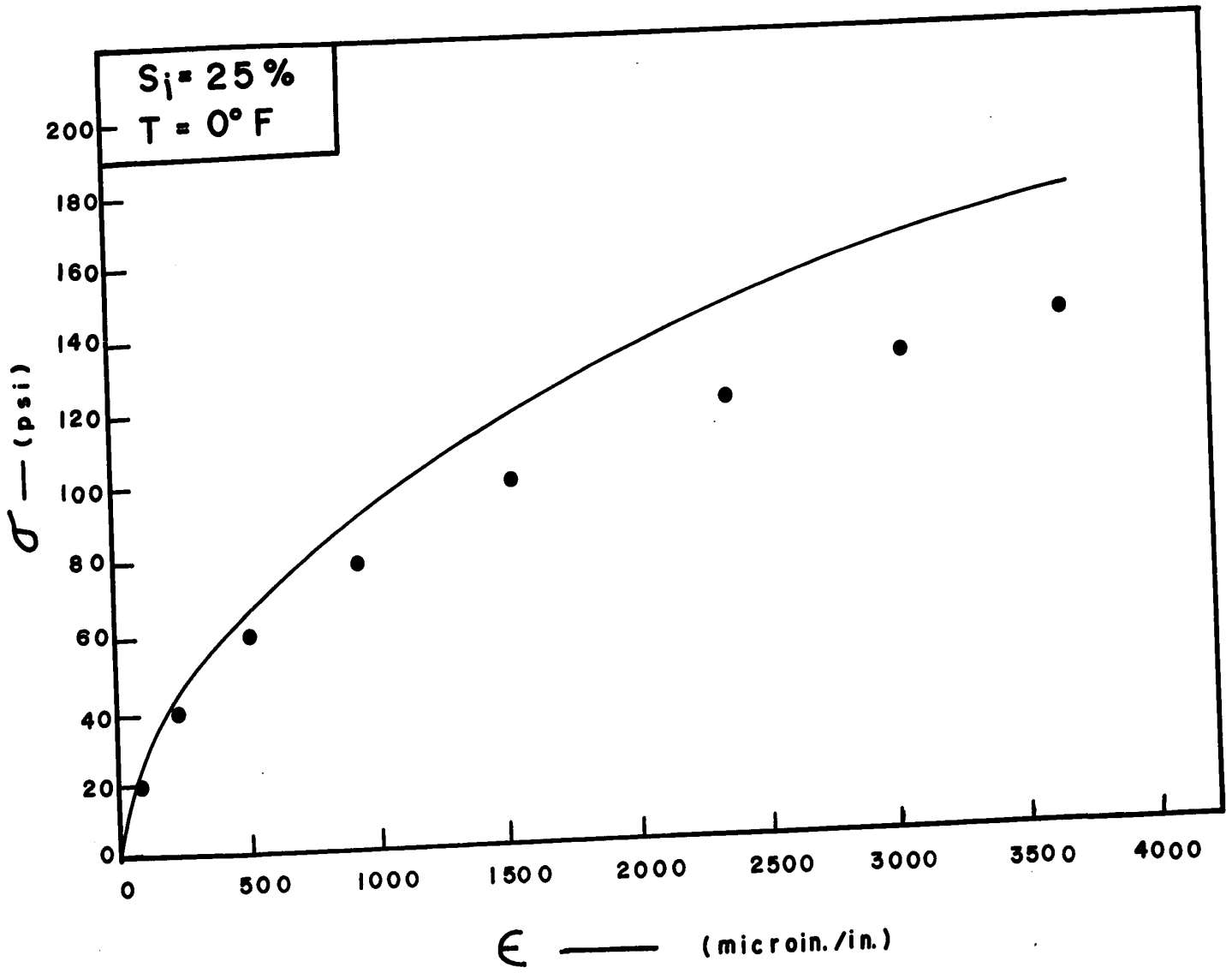
Si = 25 %
T = 0° F
σ — (psi)
200
180
160
140
120
100
80
60
40
20
0
0
500
1000
1500
2000
2500
3000
3500
4000
ε —— (microin./in.)

FIG. 53

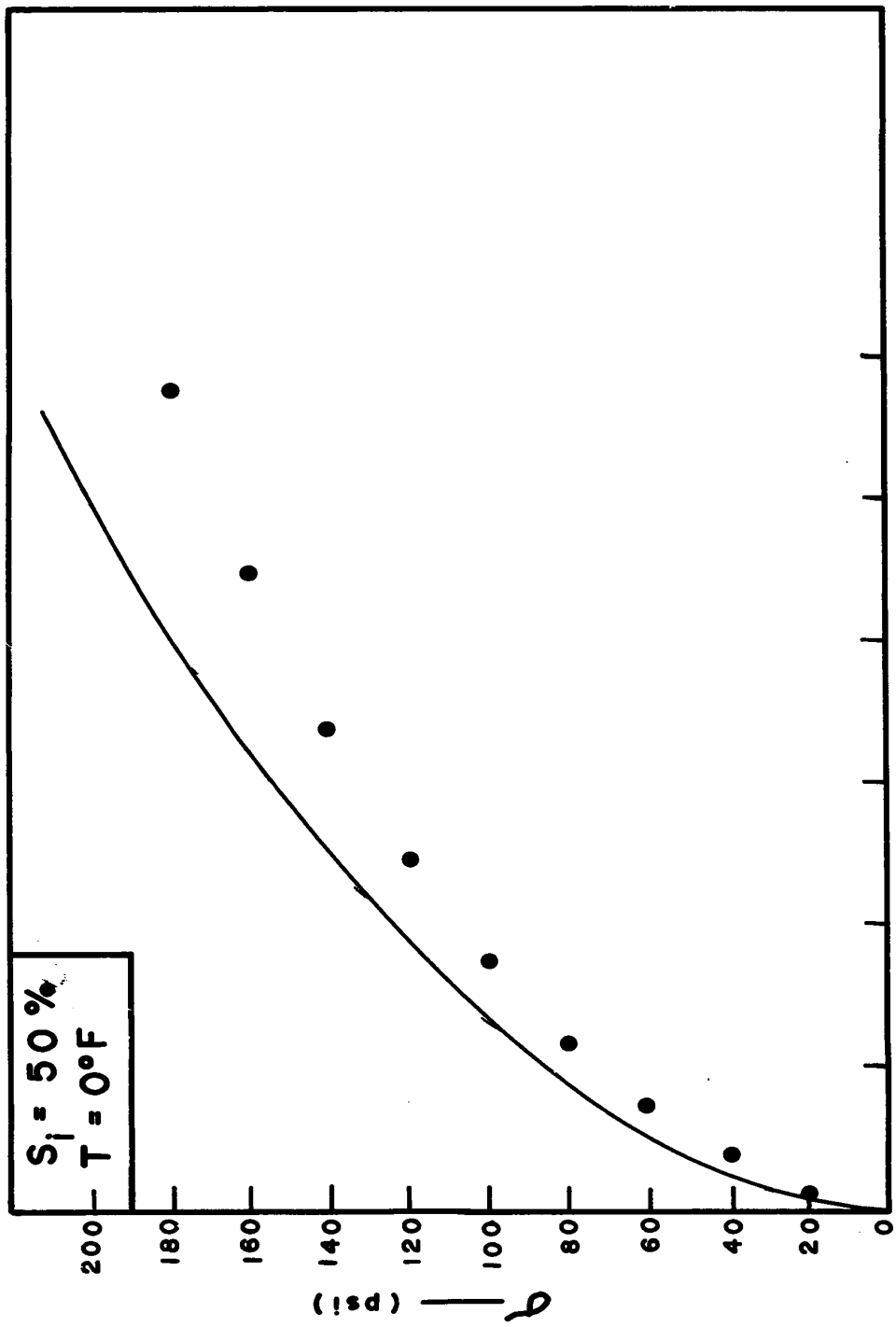
S_i = 50 %
T = 0°F
σ —— (psi)
0
20
40
60
80
100
120
140
160
180
200
0
200
400
600
800
1000
1200
ε —— (microin./in.)

FIG. 54

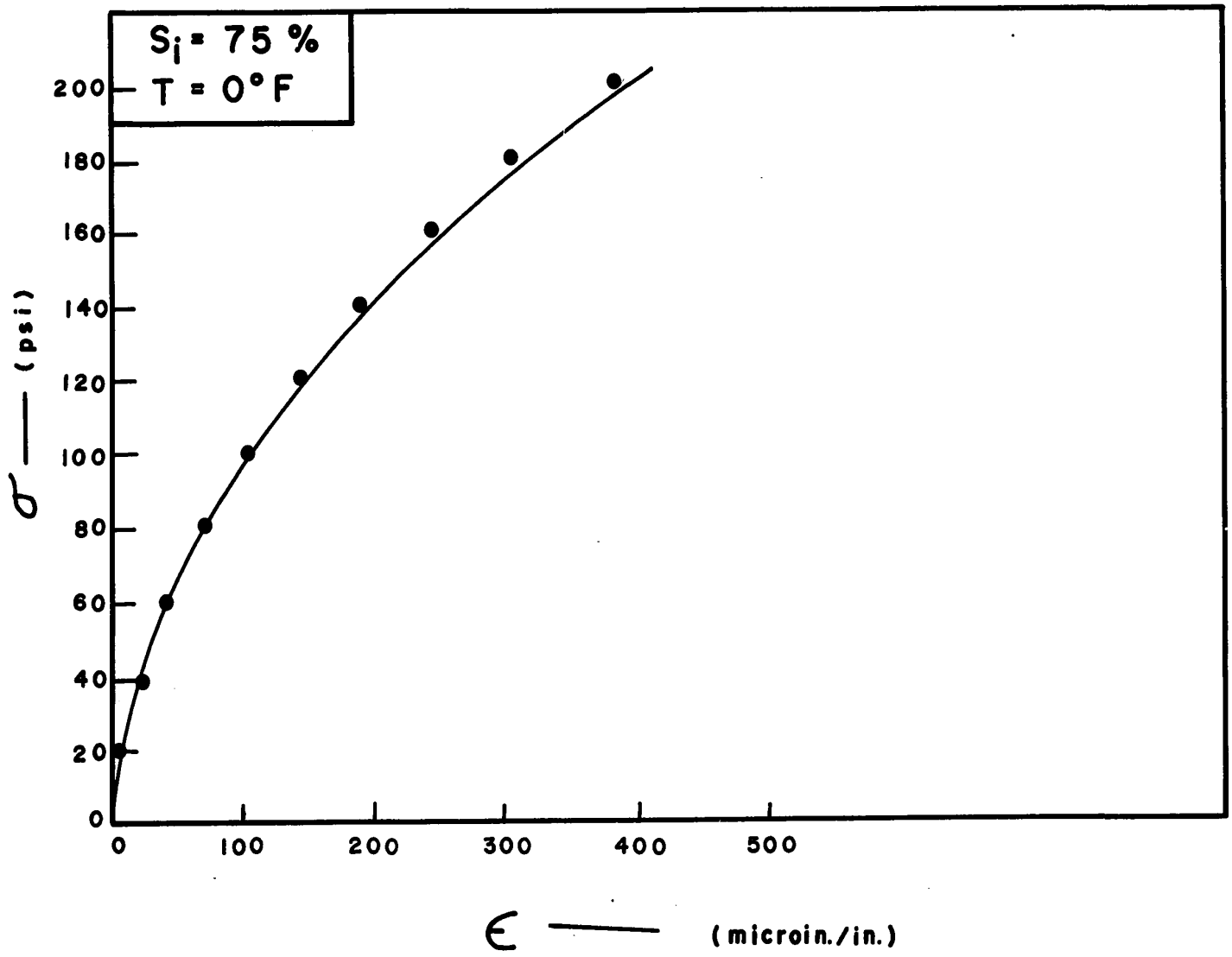
S_i = 75 %
T = 0° F
σ — (psi)
0
20
40
60
80
100
120
140
160
180
200
0
100
200
300
400
500
ϵ — (microin./in.)

FIG. 55

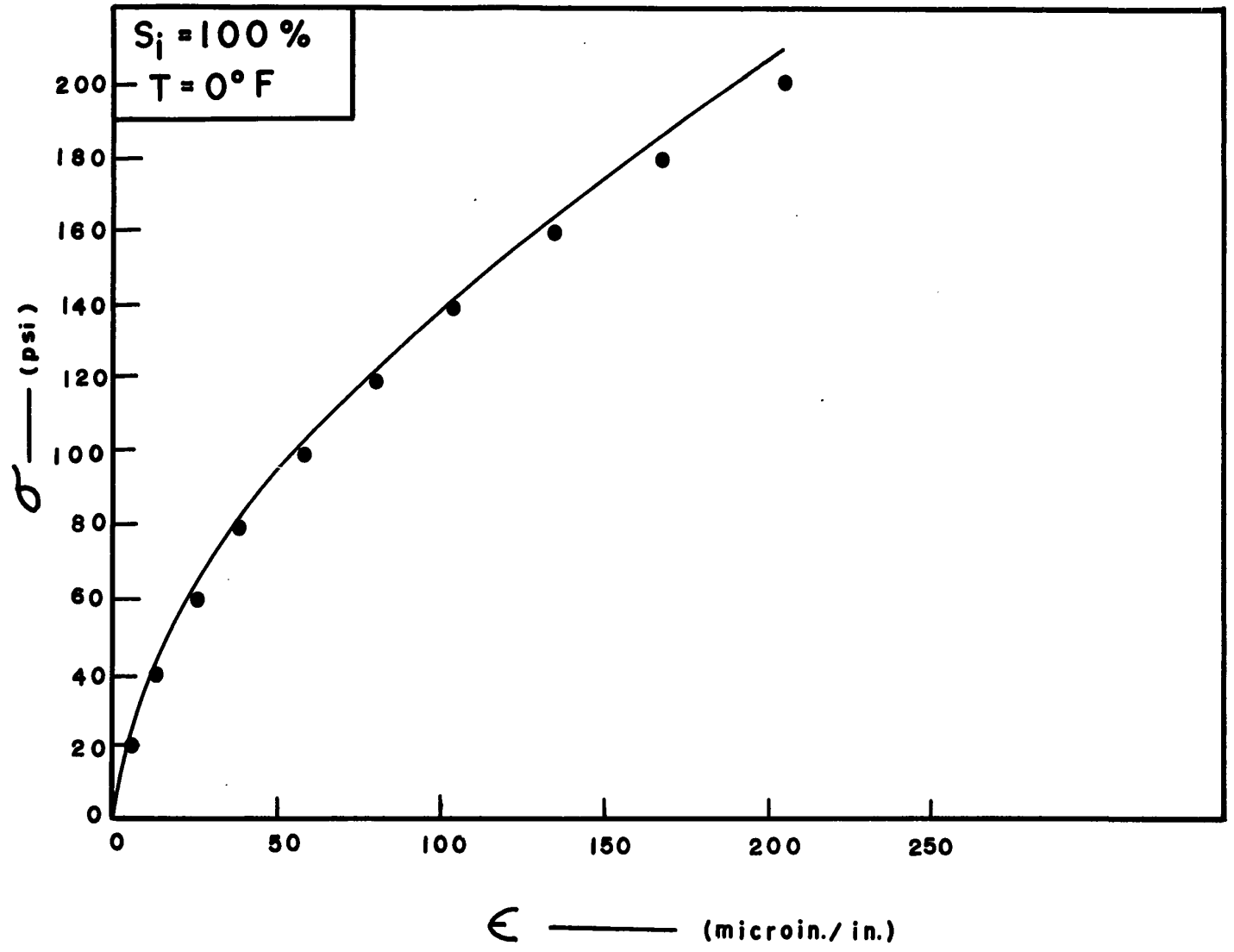
S_i = 100 %
T = 0° F
σ —— (psi)
0
20
40
60
80
100
120
140
160
180
200
0
50
100
150
200
250
ε —— (microin./ in.)

FIG. 56

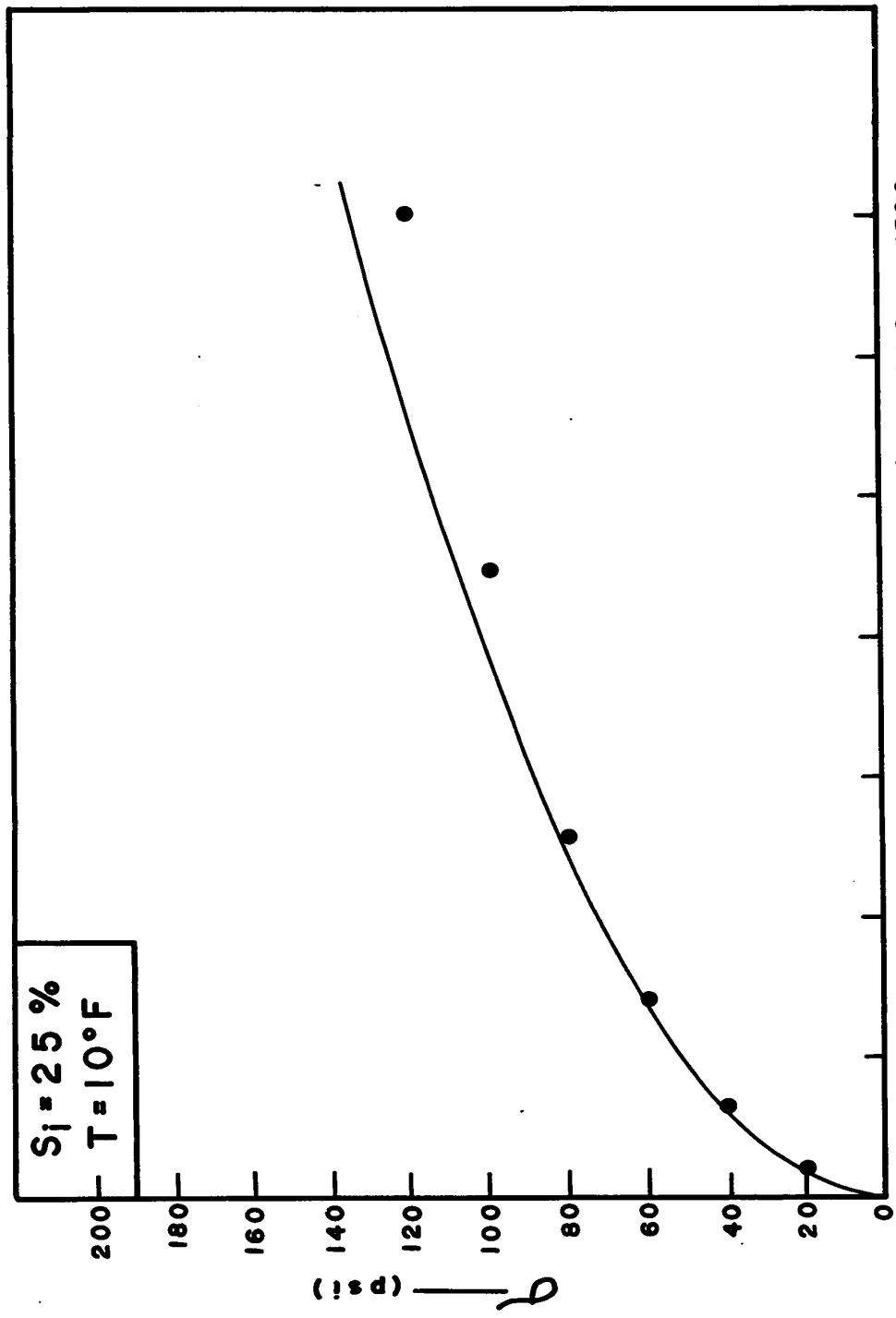
S_j = 25 %
T = 10°F
σ —— (psi)
ε —— (microin./in.)
0
20
40
60
80
100
120
140
160
180
200
500
1000
1500
2000
2500
3000
3500

FIG. 57

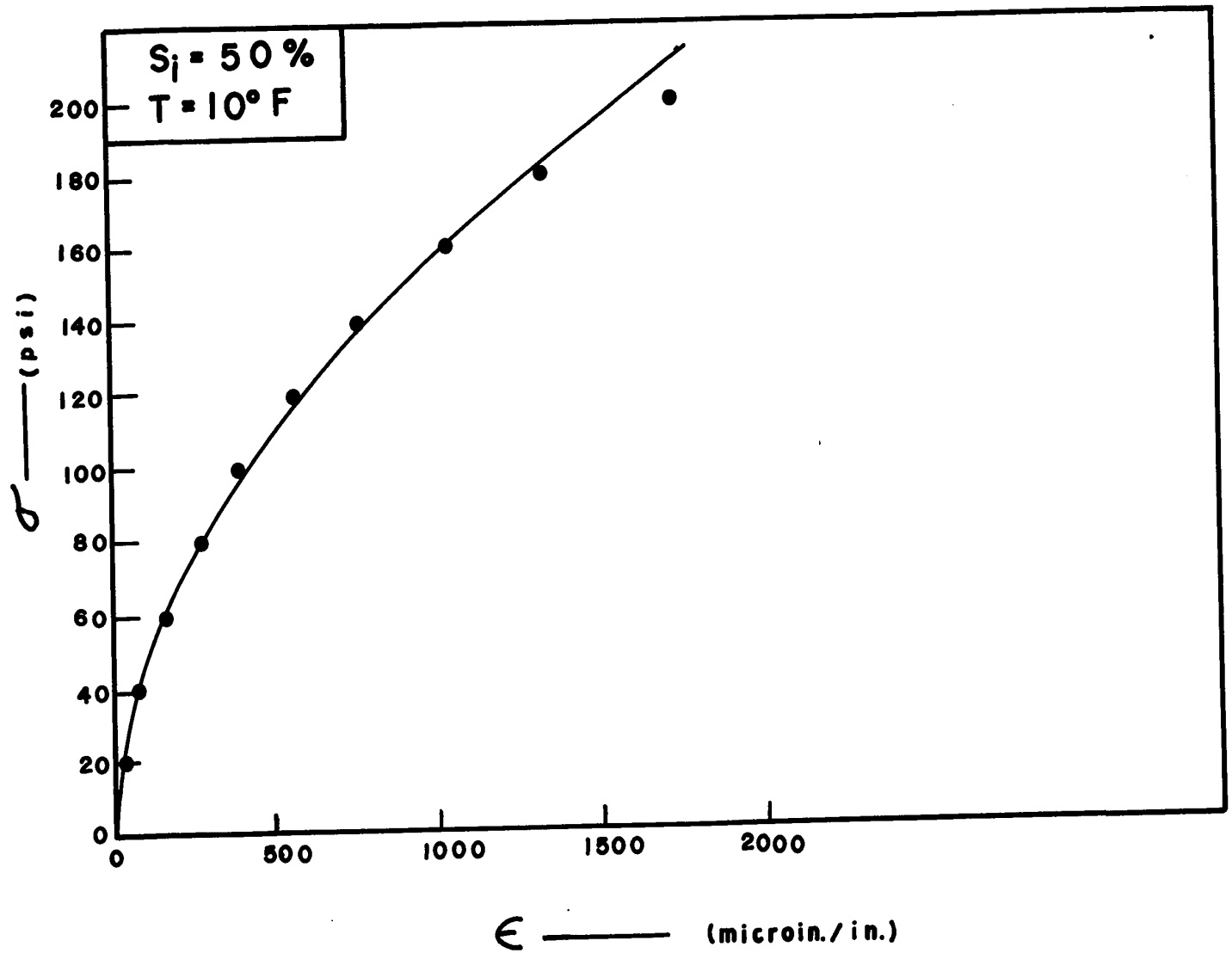
S_i = 50 %
T = 10° F
σ —— (psi)
200
180
160
140
120
100
80
60
40
20
0
0
500
1000
1500
2000
ϵ —— (microin./in.)

FIG. 58

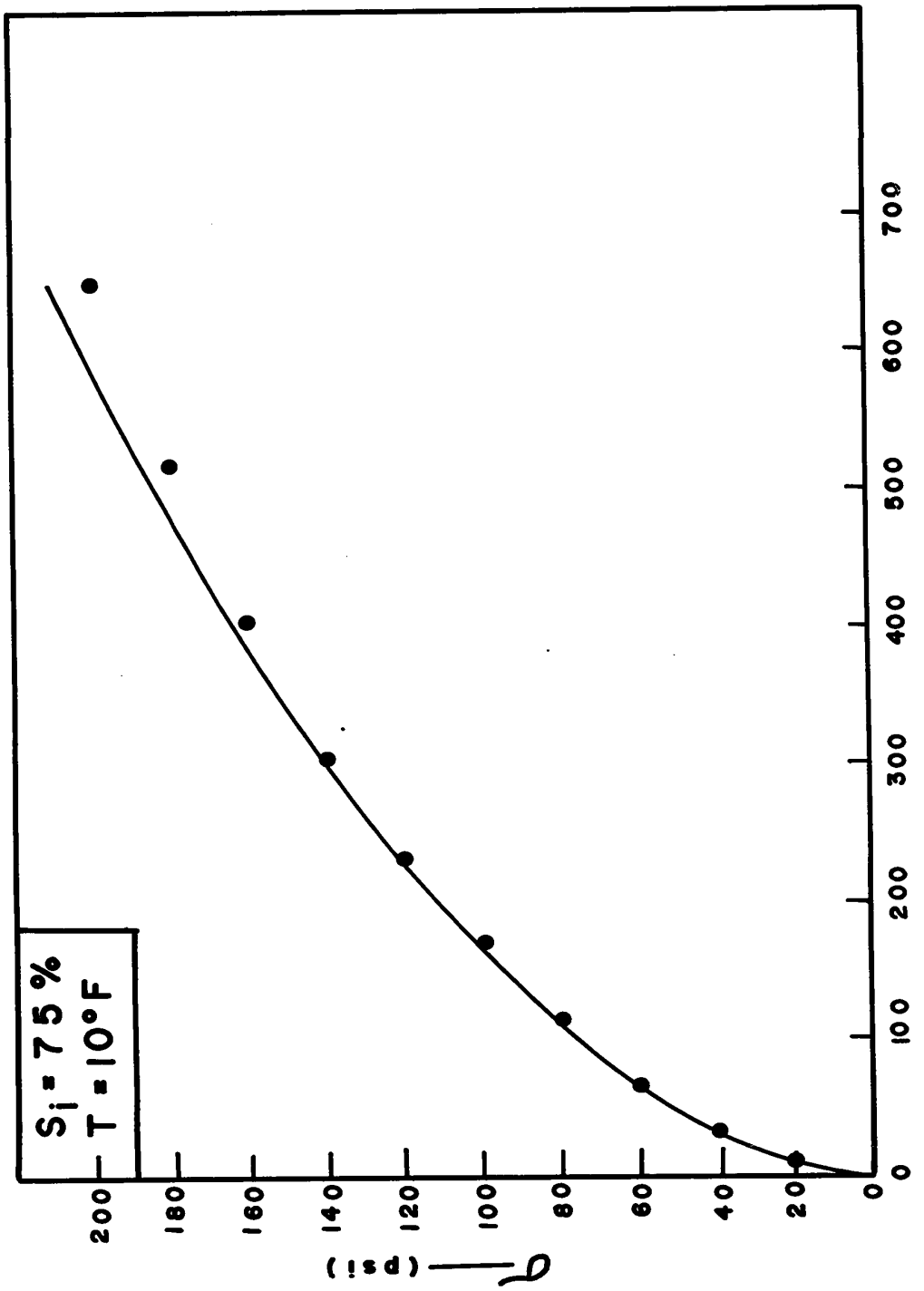
S_i = 75 %
T = 10°F
σ —— (psi)
ε —— (microin./in.)
0
20
40
60
80
100
120
140
160
180
200
100
200
300
400
500
600
700

FIG. 59

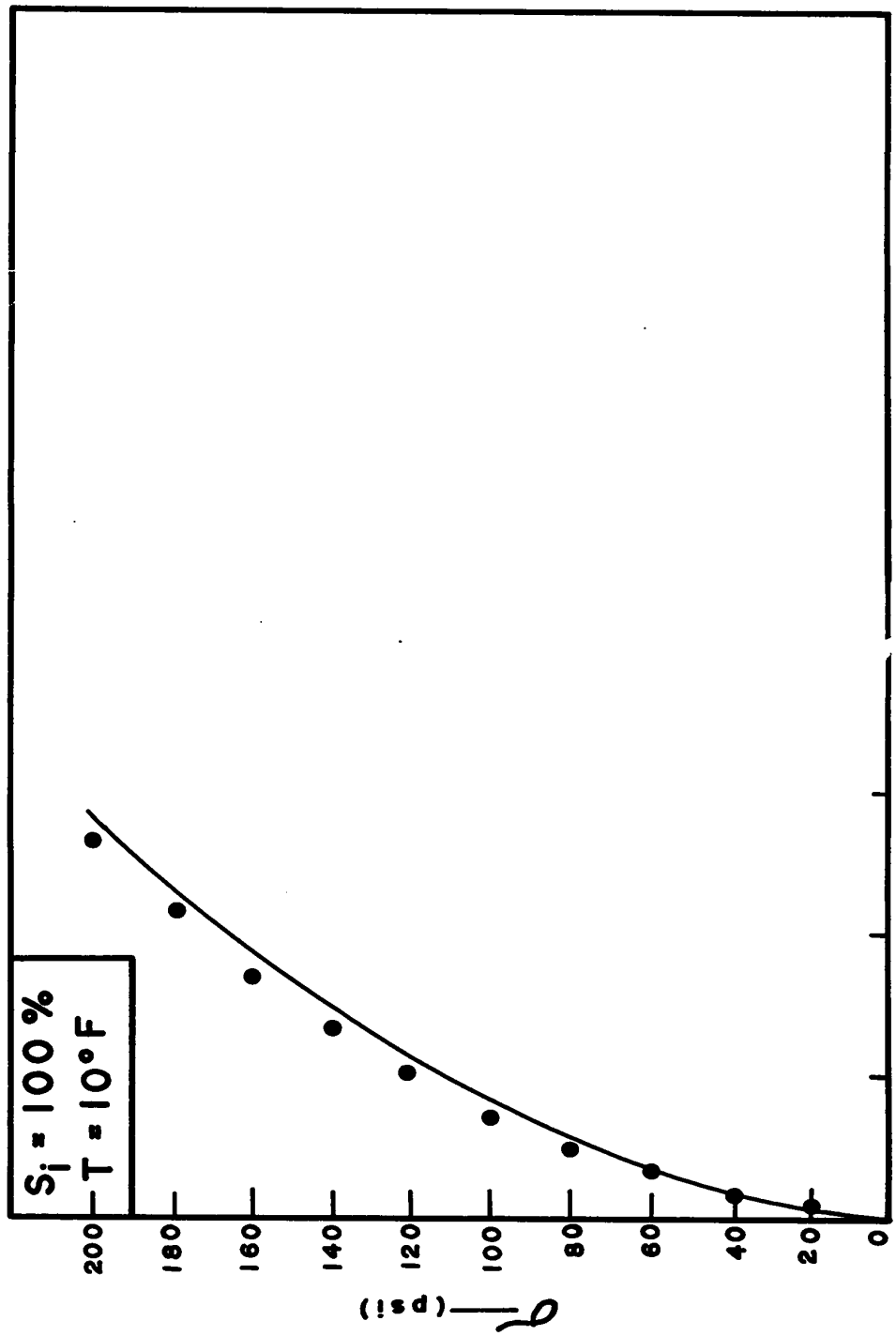
S_i = 100 %
T = 10°F
σ (psi)
ε (microin./in.)
0
20
40
60
80
100
120
140
160
180
200
100
200
300

FIG. 60

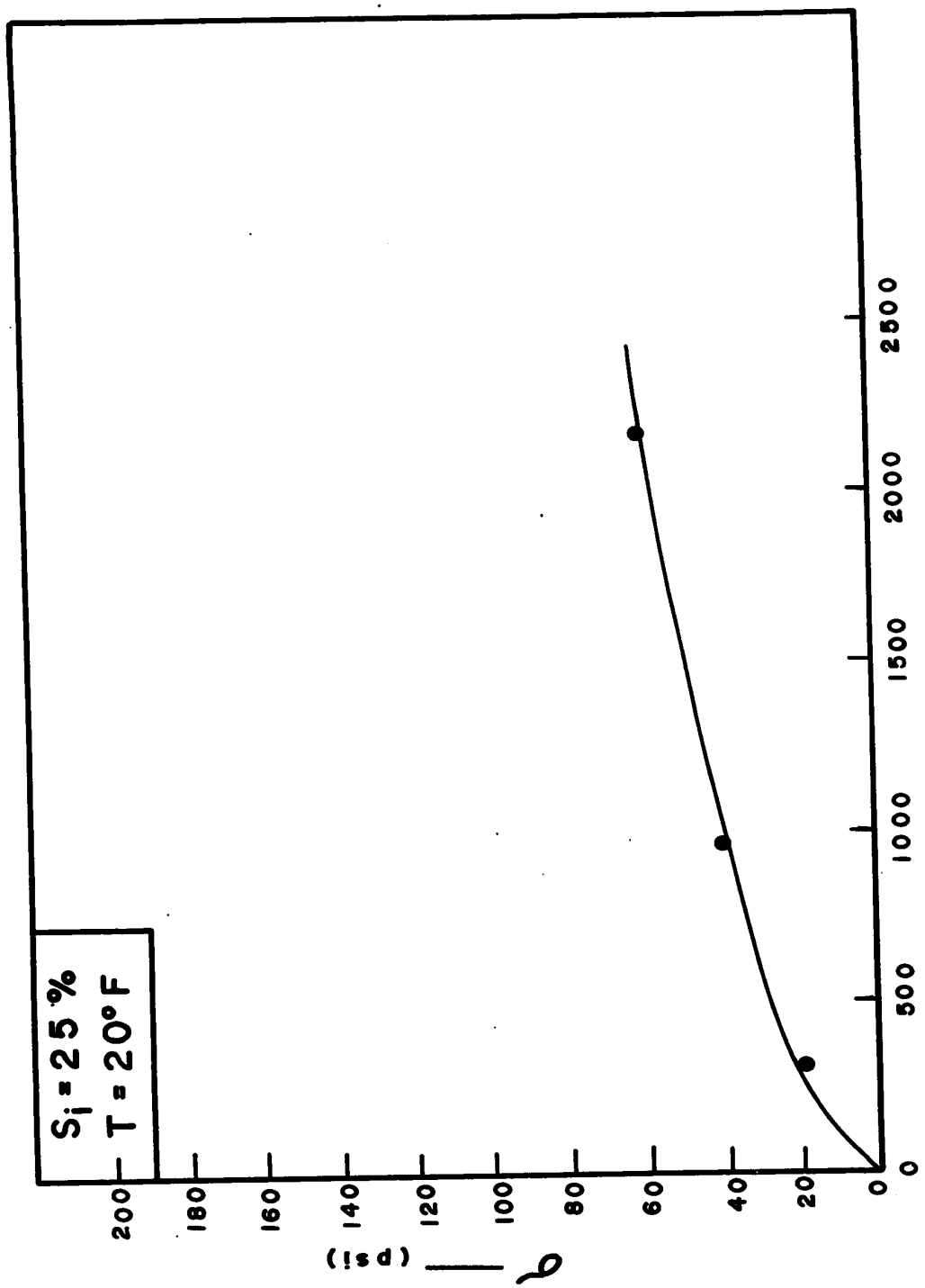
S_i = 25 %
T = 20°F
σ —— (psi)
200
180
160
140
120
100
80
60
40
20
0
0
500
1000
1500
2000
2500
ε —— (microin./in.)

FIG. 61

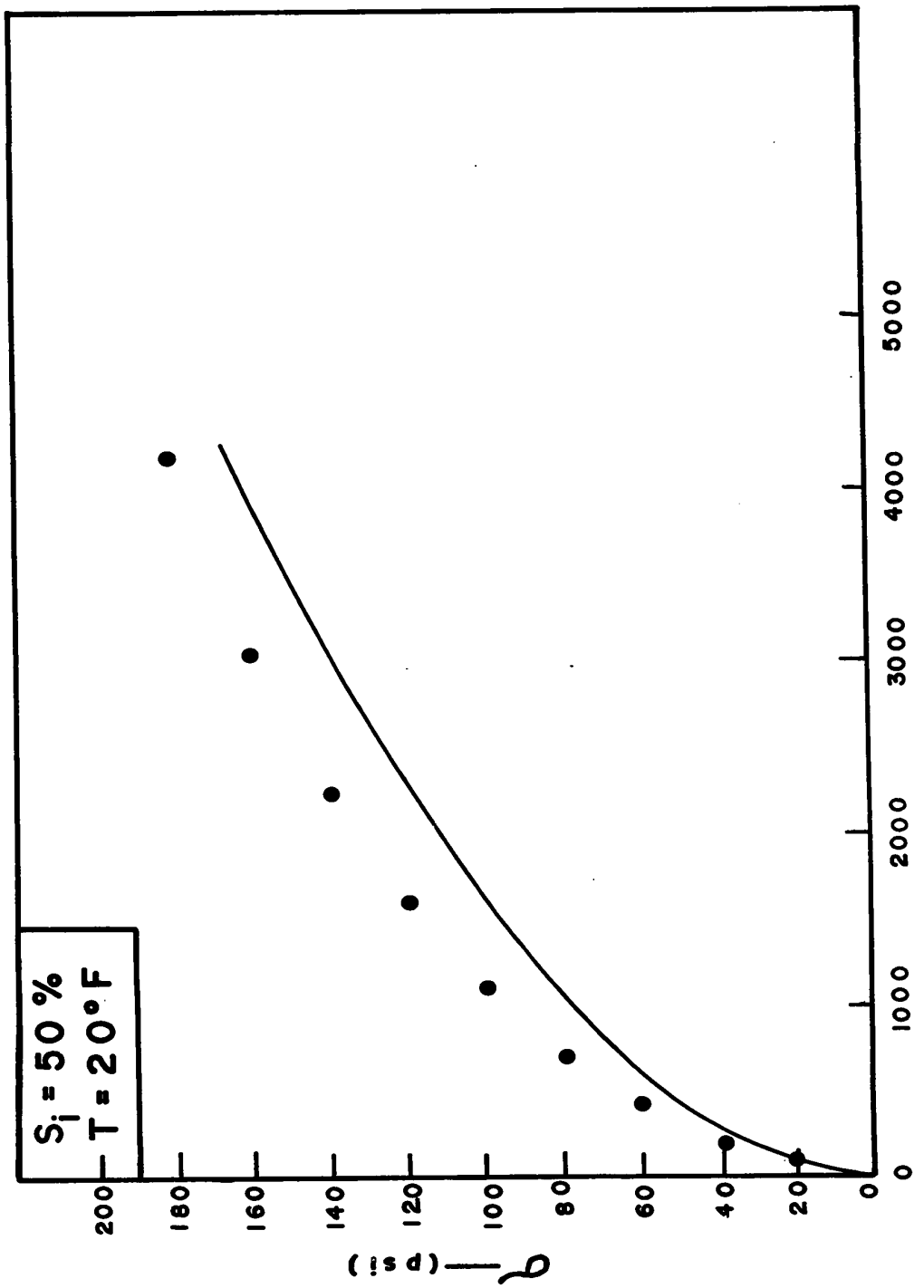
S_i = 50 %
T = 20°F
200
180
160
140
120
100
80
60
40
20
0
q — (psi)
0
1000
2000
3000
4000
5000
ε — (microin./in.)

FIG. 62

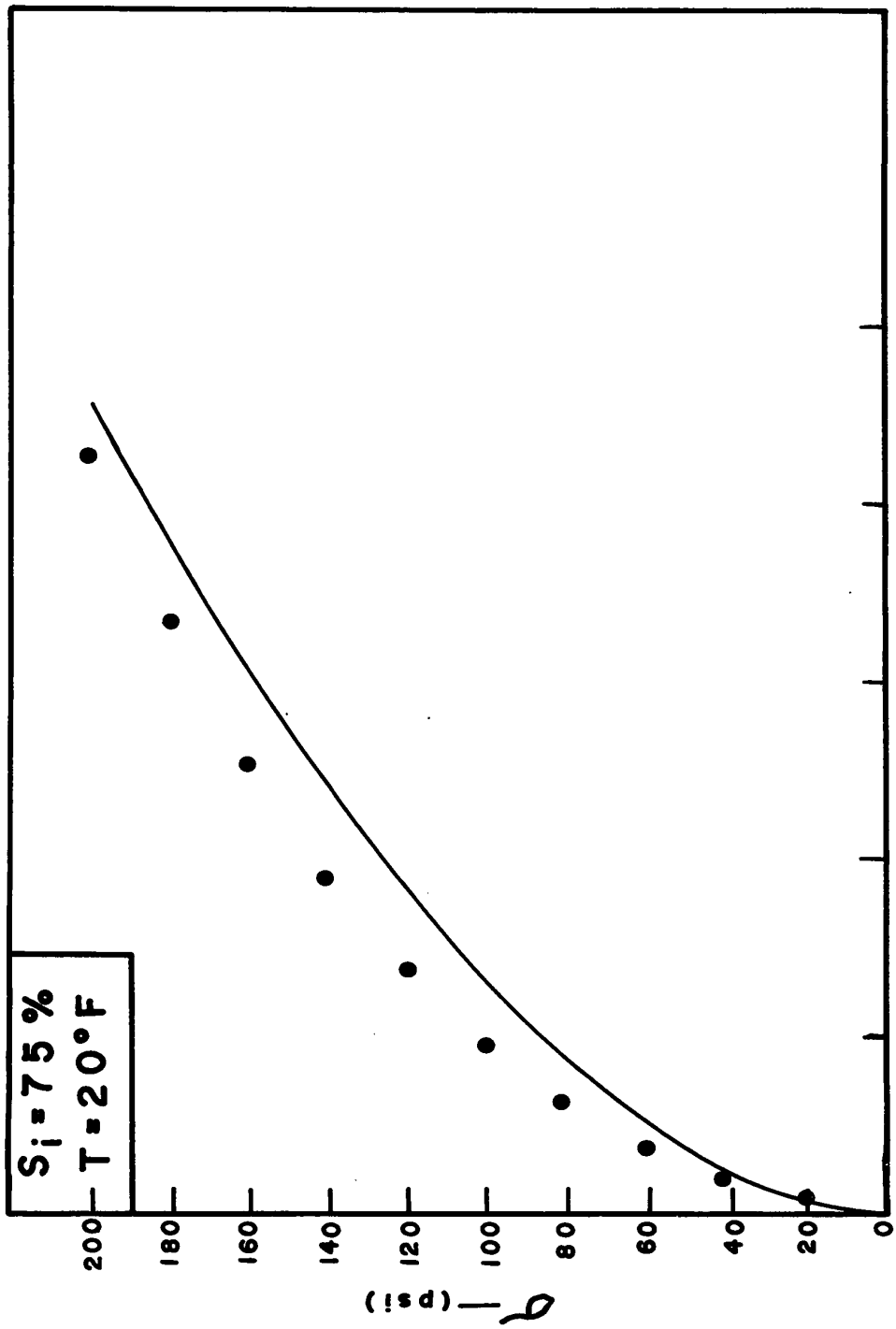
S_i = 75 %
T = 20°F
σ — (psi)
ε — (microin./in.)
0
20
40
60
80
100
120
140
160
180
200
500
1000
1500
2000
2500

FIG. 63

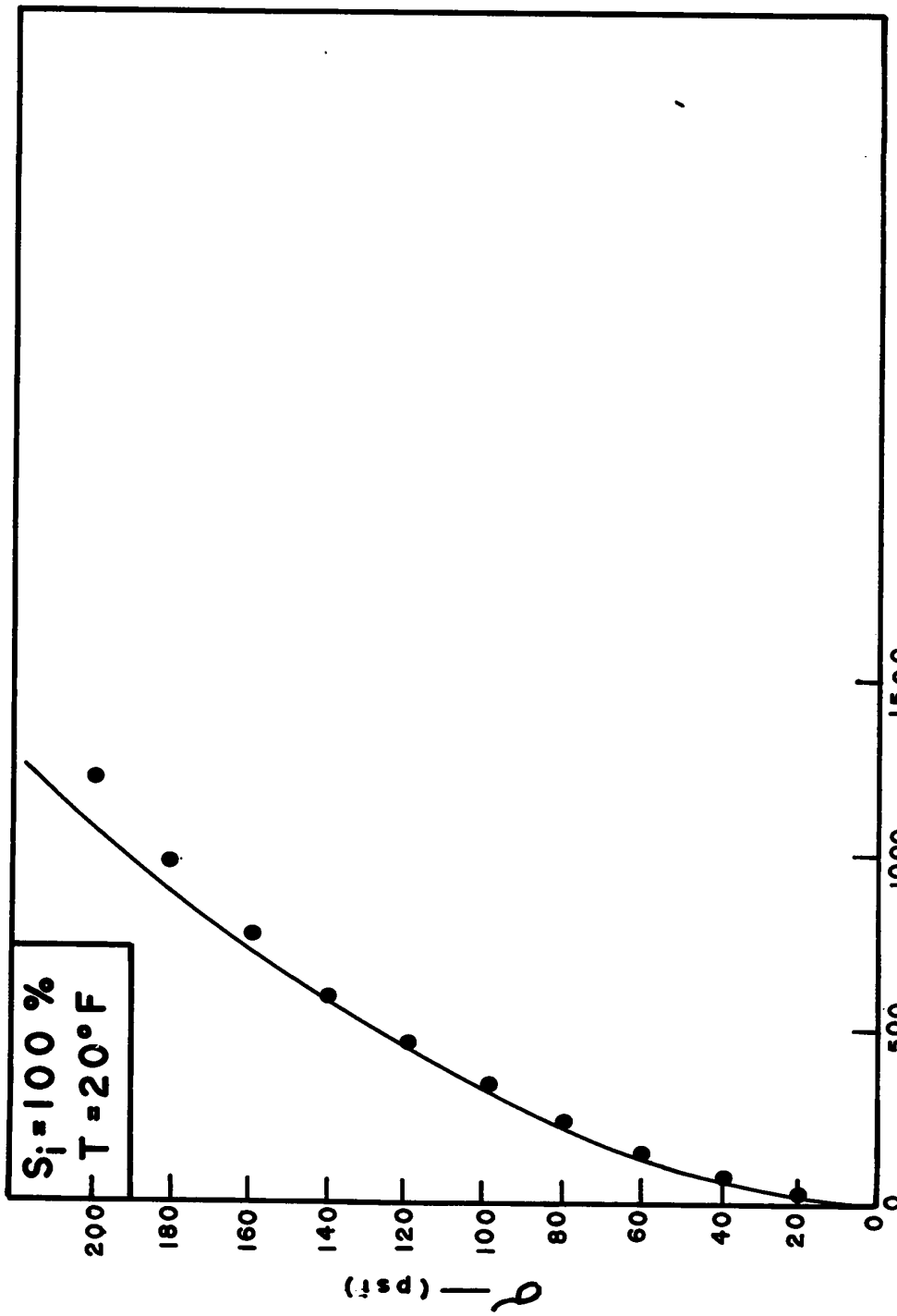
S_i=100 %
T=20°F
200
180
160
140
120
100
80
60
40
20
0
σ — (psi)
0
500
1000
1500
ε — (microin./in.)

FIG. 64

REFERENCES

1. DUNCAN, J.M. and CHANG, CHIN-YUNG, "Nonlinear Analysis of Stress and Strain in Soils", Journal of the Soil Mechanics and Foundations Division, ASCE, Vol. 96, No. SM5, Proc. Paper 7513, September, 1970, pp. 1629-1653.

2. ANDERSLAND, O.B. and ALNOURI, I, "Time-Dependent Strength Behaviour of Frozen Soil", Journal of Soil Mechanics and Foundations Division, ASCE, Vol. 96, No. S.M.4, 1970, pp. 1249-1265.

3. KONDNER, R.L., "Hyperbolic Stress-Strain Response: Cohesive Soils", Journal of S.M.&F. Division, ASCE, Vol. 89, S.M.1, 1963, pp. 115-143.

4. KONDNER, R.L. and ZELASKO, V.S., "A Hypervolic Stress-Strain Formulation for Sands", 2nd Pan-American Conference on Soil Mechanics and Formations, Vol. 1, 1963, pp. 289-324.

5. MAKHLOUF, H.M. and STEWART, J.J., "Factors Influencing the Modulus of Elasticity of Dry Sand", Proceedings 6th International Conference on S.M.&F. Engineering, Montreal, Vol. 1, 1965, pp. 298-302.

6. GOUGHOUR, R.R. and ANDERSLAND, O.B., "Mechanical Properties of Sand-Ice Systems:, Journal of S.M.&F. Division, ASCE, Vol. 94, No. S.M.4, 1968, pp. 923-950.

7. AKILI, W., "On the Stress-Strain Behaviour of Frozen Fine-Grained Soils", Highway Research Board, Jan. 18, 1971.

8. LADANYI, B., "An Engineering Thoery of Creep of Frozen Soils", Canadian Geotechnical Journal, Vol. 9, Feb. 1972, pp. 63-80.

9. VIALOV, S.S., "Rheology of Frozen Soils", Proceedings NAS-NRC International Permafrost Conference, 1963, Purdue University, Lafayette, Indiana, pp. 332-339.

10. LABA, J.T., "Lateral Thrust Exerted by Frozen Soil", Thesis 1970, University of Windsor, Windsor, Ontario.

VITA AUCTORIS

1947 The Author was born in Italy.

1969 He received his B.A.Sc. in Civil Engineering from the University of Windsor.

1970 He then worked in industry for one year in an engineering position, before returning to graduate studies.